FACULDADE DE ENGENHARIA DA UNIVERSIDADE DO PORTO

Study on recognition of facial expressions of affect

Beatriz Peneda Coelho

FINAL VERSION

MSC DISSERTATION

Supervisor: Hélder Filipe Pinto de Oliveira

Second Supervisor: João Pedro Silva Monteiro

January 21, 2019

Resumo

O reconhecimento de expressões faciais é uma área particularmente interessante em visão computacional, pois traz inúmeros benefícios para a nossa sociedade. Benefícios esses que podem ser traduzidos num grande número de aplicações no âmbito da neurociência, psicologia e segurança. A relevância do tema reflete-se na vasta literatura já produzida que descreve sinais notáveis de progresso. No entanto, o desenvolvimento e avanço de novas abordagens ainda enfrenta vários desafios. Esses desafios compreendem variações na posição da cabeça, variações na iluminação, oclusões e erros de registro. Um dos focos desta área é alcançar resultados semelhantes quando se passa de um ambiente controlado para um cenário mais próximo da realidade.

Embora o reconhecimento de expressões faciais tenha sido abordado em projetos consideravelmente diferentes, é exequível dar enfâse à necessidade de chamar à atenção para o design de uma interface que simula o envolvimento do paciente nos cuidados de saúde como uma aplicação futura. Uma tendência crescente tem sido observada, no entanto, ainda há algumas questões abertas que precisam de obter resposta para causar um impacto significativo no âmbito da saúde.

O objetivo deste trabalho é estudar qual seria uma boa abordagem para o reconhecimento de expressões faciais. Adicionalmente, estaria enquadrado com uma aplicação futura que permitiria ser usada no contexto da reabilitação com recurso a jogos sérios. Em outras palavras, seria uma abordagem baseada em jogos interativos que iria inferir a satisfação dos pacientes durante o jogo. Na revisão bibliográfica, serão fornecidas bases teóricas para compreender na íntegra este trabalho, bem como propostas de algoritmos anteriores para reconhecimento de expressões faciais. Além disso, esta tarefa de reconhecimento como um sistema automático será descrita passo a passo. A metodologia segue a ordem em que as etapas foram executadas. O passo inicial foi localizar os rostos nas imagens. Posteriormente, a extração de características recorrendo a dois métodos reconhecidos: Histograma de Gradientes Orientados e Padrões Binários Locais. Os resultados são apresentados para duas bases de dados, CK+ e AffectNet.

Finalmente, foi possível obter uma precisão de 96,55% para a base de dados CK+. Para uma base de dados em que os participantes estão a posar os algoritmos considerados tendem a ter bom desempenho, enquanto que uma base de dados espontânea (AffectNet) resulta num desempenho inferior. Contudo, com resultados ainda satisfatórios, uma vez que as imagens estão a ser classificadas considerando 7 expressões possíveis, mais a expressão neutra e estão a ser usadas bases de dados com um desequilíbrio no número de imagens por expressão.

Abstract

Facial expression recognition is a particularly interesting field of computer vision since it brings innumerable benefits to our society. Benefits that can be translated into a large number of applications in subjects such as, neuroscience, psychology and security. The relevance of the topic is reflected in the vast literature already produced describing notable signs of progress. However, the development and the advancement of new approaches is still facing multiple challenges. Challenges include head-pose variations, illumination variations, identity bias, occlusions, and registration errors. One of the focus in this field is to achieve similar results when moving from a controlled environment to a more naturalistic scenario.

Though facial expression recognition has been addressed in considerable different projects, it is feasible to emphasize the call for attention to the design of an interface that simulates addressing patient engagement in healthcare, as a future application. A rising tendency has been noticed, however, there are still some open questions need to be answered to make a significant impact on health care.

The goal of this work is to study what would be a good approach to perform facial expression recognition. Additionally, a framework for future application that would enable dealing with a rehabilitation context using serious games. In other words, it would be an interactive game based approach to infer the patients contentment while playing. In the literature review, theoretical basis needed to fully comprehend this work will be provided as well as the previous algorithm proposals for facial expression recognition. Furthermore, facial expression recognition as an automatic system will be described step by step. The methodology follows the order in which these steps were performed. The initial step was to locate the faces in the images. Subsequently, the extraction of features by two acknowledged methods, the Histogram of Oriented Gradients and the Local Binary Patterns. Latterly, the classification was performed using Random Forest and Support Vector Machines. The results were presented for two datasets, the CK+ and the AffectNet dataset.

Finally, it was possible to obtain 96.55% as the accuracy value for the CK+ dataset. For a posed dataset the considered algorithms tend to perform well whereas for an in-the-wild dataset (AffectNet) the outcome is a lower performance. However, the results are still satisfactory since the face images are being classified into 7 possible expressions, plus the neutral and it is been used imbalanced datasets.

Acknowledgments

I gratefully thank my supervisor Hélder Filipe Pinto de Oliveira and second supervisor João Pedro Silva Monteiro for their time, patience and knowledge. I gratefully thank my parents, sister, and grandmother as they were always there for me, giving me unconditional love and support. I gratefully thank my boyfriend that even far made himself present and supported me at all times. I gratefully thank my friends, the old ones and the new ones that I met along the way. This would not be possible to accomplish without the encouragement given by these people in my life.

Beatriz Coelho

"True worth is as inevitably discovered by the facial expression, as its opposite is sure to be clearly represented there. The human face is nature's tablet, the truth is certainly written thereon."

Johann Kaspar Lavater

Contents

List of Figures

List of Tables

Abbreviations

AdaBoost	Adaptive Boosting
AU	Action Units
BNC	Bayesan Network Classifiers
CNN	Convolutional Neural Networks
CVPR	Conference on Computer Vision and Pattern Recognition
DNN	Deep Neural Networks
DT	Decision Trees
FACS	Facial Coding Systems
FER	Facial Expression Recognition
HCI	Human–computer interaction
HMM	Hidden Markov Models
HOG	Histogram of Oriented Gradients
IJCV	International Journal of Computer Vision
IoU	Intersection Over Union
JAFFE	Japanese Female Facial Expression Database
LASSO	Least Absolute Shrinkage and Selection Operator
LDA	Linear Discriminant Analysis
MI	Mutual Information
RBF	Radial Basis Function
RF	Random Forest
RFD	Radboud Faces Database
RGB	Red, Green, Blue
SBS	Sequential Backward Selection
SFS	Sequential Forward Selection
SVM	Support Vector Machines

Chapter 1

Introduction

The development in the field of facial expression recognition is already bringing and is expected to bring even more benefits to our society due to its significant growth in the last years. A considerable amount of applications is present in subjects as neuroscience, psychology and security [14]. Notable progress has been made in the field, however, despite the development and the advancement in new approaches, there are still barriers that are not easily overcome. Moreover, it is not yet possible to draw irrefutable conclusions in the expression recognition when performed in an uncontrolled environment.

1.1 Context

In the framework of a future application to create serious games in a rehabilitation context addressing patient engagement in healthcare, this thesis emerged as the initial study of approaches to perform FER. The target of this ultimate application would be the interaction between the medical staff and the patients that had suffered from breast cancer and would be then going through the rehabilitation process.

Breast cancer has shown to be the most common malignant tumor in women. In Western Europe, its incidence is approximately 90 new cases per 100,000 inhabitants [15]. Despite these figures, mortality in most countries is considerably low. This means that the number of survivors who need to learn how to live with the undesirable side effects of breast cancer treatment is increasing year after year. There are 4 physical restraints that can be a consequence of the treatments performed to save or extend the lives of those affected. These include impaired mobility, strength, and stiffness of the upper limb, the onset of pain, among other effects that can be identified. Regarding physical recovery, as previously mentioned it is recommended that the patient should attend some rehabilitation sessions. However, during these sessions restrictions on mobility are often not visible or easily quantifiable. This is because before the person starts showing a decrease in mobility, such as failing to raise the arm to the head and at a certain point only being able to raise it up to shoulder height, that person will probably begin to express some difficulty in performing this movement. In this context, it will be considered the problem of facial expression recognition

that in a future application will be able to quantify the patient's expression according to a specific model using computer vision.

1.2 Motivation and Objectives

As it was shown in the example above, in a clinical environment, recognition of facial expressions performs a significant role since it defines if the patient is comfortable with the movements that he or she is executing [16]. Accordingly, the great difficulty in this recognition is the fact that it would be considered an uncontrolled environment. This means the patient being evaluated would not be necessarily cooperating, also the acquisition system to use would be low-cost, so it would not be the most appropriate for that purpose. Other problems, now concerning the methods used should be equally taken into consideration. These methods are not guaranteed to be robust to certain characteristics of the chosen data, such as possible variations in head position, variations in illumination or facial occlusions caused by glasses or facial hair.

Data from the rehabilitation sessions was not possible to access and use due to the time constraint to obtain authorizations as well as to the raise of ethical concerns. Therefore, what is intended with this dissertation, is to be able to automatically recognize facial expressions in a chosen set of visual data. The validation will happen in a future application enabling to draw conclusions about the patient's state regarding the complications resulting from the treatment of breast cancer that the patient tries to revert in the rehabilitation sessions. Thereby, initially an existent methodology or group of methodologies for the recognition of facial expressions should be chosen, then they should be studied and, in the future, validated.

1.3 Contributions

The major contributions of this thesis to the scientific community are the following :

- The implementation of a framework for facial expression recognition using conventional techniques achieving accuracy rates close to some state-of-the-art algorithms.
- A comparative study of algorithms used to perform the recognition task is presented in this dissertation. The relevance of this study encompasses the fact that it describes the process of becoming acquainted with different approaches for the task at hand. This might be useful as a starting point if one has little knowledge on the subject and intends to study and explore it more deeply.

1.4 Document Structure

Apart from the introduction, this document contains four more chapters. In chapter 2, it is described the background information and state of the art on recognition of facial expression classification and the existing methods. Chapter 3 addresses the methodology including the approaches

and methods that have been found to be the most feasible and adequate to perform facial expression recognition. In chapter 4, the results are presented and discussed. Chapter 5 refers to the conclusions and the potential future work for the dissertation.

Chapter 2

Literature Review

This chapter will explain the theoretical basis needed to fully comprehend this thesis and study the current state of Facial Expression Recognition as well as to understand how an automatic facial expression recognition system works.

2.1 Facial Expressions

By the time Charles Darwin wrote "The Expression of Emotion in Man and Animals", in the 19th century, the willingness to study and perceive Facial Expressions was notably encouraged [4]. This increasing interest also mirrors the notoriety that has been given to nonverbal communication [17] since the subsequent models highlight their employment as a communicative tool.

Facial Expressions are voluntarily or involuntarily employed as a powerful nonverbal clue by people when interacting with each other [18]. They can provide meaningful information when it comes to communication, by giving feedback about our level of interest, the level of understanding of the transmitted message or simply a way of showing our desire to be the next ones to have the opportunity to talk. Thus, it enables people to communicate more efficiently. Since others can be acknowledged of an individual's emotional state, motivations or intention to deliberately engage in a behaviour. Therefore, the question that arises now is through which mechanisms are the human vision system endowed with the ability to perceive facial expressions. To do that, the focus should be the understanding of the three types of facial perception [19]:

- Holistic;
- Componential;
- Configural.

Regarding the holistic perception models, the human face is perceived as a gestalt (a whole), features are not seen as isolated components of the face. Componential perception, on the other hand, considers that in the human vision system there are determined features separately processed. Finally, in configural processing the spatial relations of two parts of a face (e.g. distance between

mouth and nose) can be variant or invariant depending on the kind of performed movement or the person's facial viewpoint [20].

2.2 Facial Expressions: Methods for Assessing

In the present section, two methods for measuring facial expressions are addressed. Additionally, the advantages and disadvantages of each method.

2.2.1 Electromyography

The first method to be considered is the electromyography (EMG). This technique is for assessing the electrical activity created by the muscles was applied to identify the activation of some facial muscles. Over a long period of time owing to some technical issues just two different facial muscles *M. zygomaticus major* (smiling), *M. corrugator supercilii* (frowning) could be studied. Only recently, the performance of this technique has reached satisfactory results due to the augmented sensitivity [21]. The development of this procedure allowed the identification and record of the activity of slightly visible face muscles. Along with the muscles mentioned before, *M. levator labii superioris* (disgust) is also one of the muscles that provides useful information when trying to assess facial expression.

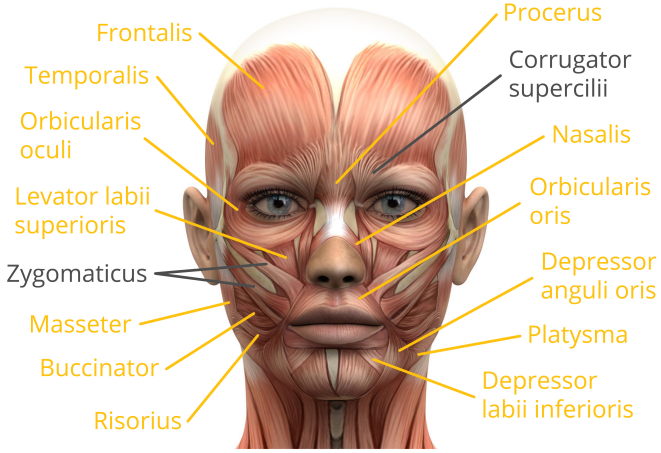

Figure 2.1: Facial Muscles. From [1]

The advantage of the facial electromyography is the fact that it is a precise method, able to perceive the subtle visible facial muscle activity that could not be detectable to the naked eye [22]. It is even capable of registering the response when the participants were taught to suppress their facial expressions. Concerning the disadvantages, this is an intrusive method [23] which means that is highly complex to perform and implies a lot of constraints to the experimental context. This makes it really difficult to use the EMG method really difficult to use the EMG method on participants in a real environment [21].

2.2.2 Facial Action Coding System

The second method, *Facial Action Coding System* (FACS) was first mentioned by Carl-Herman Hjortsjö, a Swedish anatomist, in the book "Man's face and mimic language" [24]. Afterwards, Paul Ekman and Wallace Friesen in 1978 adapted the anatomist previous work and published [25]. Finally, in 2002, a minor revision was carried out with the contribution of Joseph Hager leading to the following publication [26].

FACS is a system that implies the analysis of changes in the expressions of a person's face, the identification of certain facial movements, and the posterior categorization into emotional expressions [22]. Thus, is used to describe facial behaviour [23]. To be performed, the human face is divided into individual components defined by the muscle movements [23]. These individual components are the basic units of measurement in FACS called *Action Units* (AU). The contraction of certain facial muscles is what defines an AU, it can be individual (see Figure 2.2) or combined (see Figure 2.3) [27] and produces a unique defined image feature. One example is the contraction of the *M. frontalis (pars medialis)*. When it occurs, the rising of the inner part of the eyebrows can be observed, this consists in the AU 1 [28].

Table 2.1: Number of the AU and correspondent description. Adapted from [11].

AU	Description	AU	Description	AU	Description
1	*Inner Brow Raiser*	13	*Cheek Puller*	25	*Lips Part*
2	*Outer Brow Raiser*	14	*Dimpler*	26	*Jaw Drop*
4	*Brow Lowerer*	15	*Lip Corner Depressor*	27	*Mouth Stretch*
5	*Upper Lip Raiser*	16	*Lower Lip Depressor*	28	*Lip Suck*
6	*Cheek Raiser*	17	*Chin Raiser*	29	*Jaw Thrust*
7	*Lid Tightener*	18	*Lip Puckerer*	31	*Jaw Clencher*
9	*Nose Wrinkler*	20	*Lip Stretcher*	34	*Cheek Puff*
10	*Upper Lip Raiser*	21	*Neck Tightener*	38	*Nostril Dilator*
11	*Nasolabial Deepener*	23	*Lip Tightener*	39	*Nostril Compressor*
12	*Lip Corner Puller*	24	*Lip Pressor*	43	*Eyes Closed*

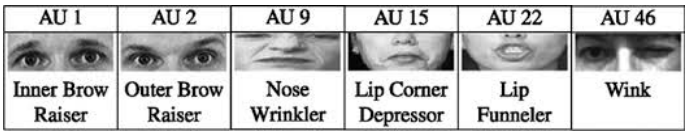

Figure 2.2: Upper and Lower AU examples. From [2].

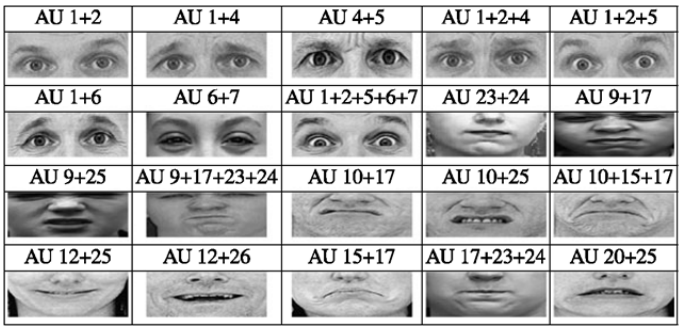

Figure 2.3: Examples of combined AU. Adapted from [3].

Table 2.2: Criteria to define emotions in facial action units. Adapted from [11].

Emotion	**Facial Action Units**
Anger	AU combination should include AU23 and AU24
Contempt	AU14
Disgust	AU9 or AU10
Fear	AU combination of 1+2+4
Happiness	AU12
Sadness	AU combination of 1+4+15 or AU11
Surprise	AU combination of 1+2 or AU5

The advantage of FACS when compared to the EMG method is that the first one is non-intrusive which means it can be easily undertaken in any environment. The performance of FACS can also vary depending on whether it is executed manually or automatically. Automatic FACS allow the attainment of more precise results since the subjects can be studied without biases by the researcher [21]. So, it provides an objective and reliable analysis of expressions [29]. Also, it does not only measure the emotion-relevant movements but all facial movements [22]. On the other hand, the disadvantage when executed manually is its subjectivity as well as the time required to perform this method as it is severely labour-intensive [23].

Of the two methods described above, the observational coding scheme Facial Action Systems is the most notable and used for facial measurement [30].

2.3 Automatic Facial Expression Recognition

Automatic Facial Expression Recognition has been an intensely developed field of research due to the interest that has been given to its large number of applications. As it allows to create adaptive human-computer interfaces, which detect and interpret the human expressions and adapt the interface accordingly [31]. Corneanu et al. [4] provided a summary of some of those applications. Where reference is made to *"Robovie"*, a robot designed to communicate with humans [32], as well as to a pain detection system that monitors the patient's progress [33, 34]. Further examples include the improvement of e-learning scenarios by identifying frustration in students, the improvement of gaming experience, for instance, by adjusting the level of difficulty and, at last, the detection of drowsy driving [35].

Samal et al., Pantic et al. and Fasel et al. [36, 37, 38] are extensive surveys of the past achievements that refer to the end of the 20th century, the beginning of the 21st century. In these, the early works in the field describing the issues that researchers were dealing with at the time can be found. Overcoming variations in the face appearance, for instance, in pose or size [39]. Since these early works addressed barely a single part of the question. After all, they were the result of the first attempts to automatically analyze facial expressions [36, 40]. Afterwards, it is described the performance of facial expression recognition systems in samples generated exclusively from controlled scenarios. In such scenarios, the face is in frontal view due to the camera positioning. Moreover, it is known beforehand that a face is in the image [37].

Zeng et al. [41] and Corneanu et al. [4], on the other hand, gather the literature more recently produced. Their focus was the methods and specifications required to perform the recognition [42]. In [4], Corneanu et al. proposed a way of categorizing these techniques (see Figure 2.4), splitting into two major components, namely, parametrization and recognition of facial expression. The first branch, parametrization is the method that assigns facial expressions to a coding scheme; FACS, for example. Concerning the automatic facial expression recognition, the general approach is detailed in four key steps [4]. These will be described in more detail in the next sub-section.

- **Face Detection** — The purpose of the first step is to find out if the image contains a face and where.
- **Feature Extraction** — Then, the extraction of the features on the obtained samples will be performed, which results in a feature vector.
- **Feature Selection** — This step consists of selecting the most relevant features from a dataset, generating a new subset of features.
- **Expression Classification** — At last, extracted features of the second step are used as an input into the classifier and finally the classifier generates an output with the recognized expression.

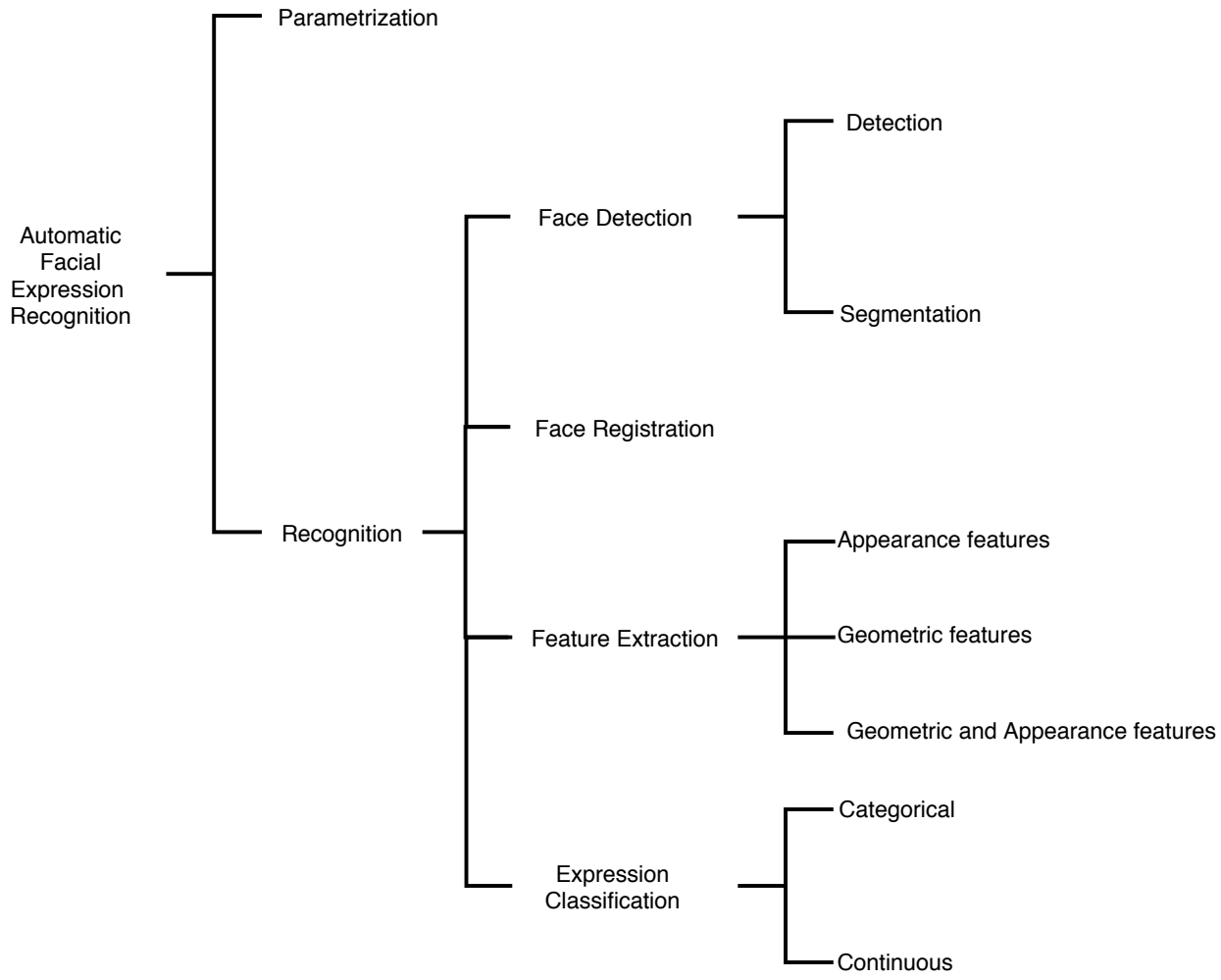

Figure 2.4: Categorization of Automatic Facial Expression Recognition Systems. Adapted from [4].

2.3.1 Face Detection

In this sub-section, the localization of the face in the images will be discussed. There are some applications that do not depend and do not need to perform this step. This happens because the face images used are contained in a normalized dataset. In that situation, the face images are already in a standardized way (e.g., in a criminal dataset). Also, it can be the case that it is not required to know where the face is, namely, in a deep learning approach. However, when this does not happen, the researcher has to deal with images that contain more than the face in question. In this case, there is no other way than performing face localization [43]. Thus, a procedure has to be undertaken to localize and extract the face region from the background. Face localization techniques can be branched in two distinct groups of methods [4]: detection and segmentation. The detection approach is the most frequently used. It can be dealt with as a classification problem where different defined regions within an image are classified as a face or

non-face. While segmentation, on the other hand, is the technique in which the aim is to link a label to each pixel of the image. Thereby, the image is divided into a few segments each one assigned to a label, in which some share the label, that means these segments have identical characteristics. This results in a simpler representation of the image which provides clearer analysis.

Besides that, it should also be taken into consideration the fact that for a distinct types of images, there should be different ways of proceeding. For instance, in the case of RGB[1] images, the Viola-Jones algorithm [8] is the most used and accepted. It is available in the OpenCV[2] library. Furthermore, this algorithm main principle is based on a cascade of weak classifiers. It is considered to be fast since it rapidly eliminates the parts that visibly do not contain face images [8]. However, it has some limitations caused by the different pose variations and when dealing with large occlusions. In order to overcome these limitations methods with multiple pose detectors or probabilistic approaches should be considered. Also, more specific methods such as CNN or SVM should be taken into consideration. For 3D images, the way of proceeding provides the possibility of obtaining better results and a more detailed feature base. So, the aim is to recognize any face regardless of the pose orientation of the input image. To do that, curvature features are used to find high curvature components of the face (e.g., the nose tip).

2.3.2 Dimensionality Reduction

Dimensionality reduction of high dimensional data is an essential step when it is intended to use this data as the input of a machine learning algorithm. In the present case, the handled data are images and to avoid a problem referred to as the curse of dimensionality [44] it has to be performed a transformation into a low dimensional representation of the data. Moreover, a great number of features can affect negatively the learning algorithms as it increases the risk of overfitting, it is more computationally costly, decreases its performance, and requires more memory availability.

From [45], dimensionality reduction is branched out into feature extraction and feature selection. Feature extraction is a transformative method in which the data is projected into a low dimensional feature space. On the other hand, feature selection consists of selecting the most relevant features from the initial dataset, as if it was a filter, creating a new subset of features. These two branches will be studied below.

2.3.3 Feature Extraction

The next step in this system is feature extraction, it can be described as the procedure that allows the extraction of relevant data from a face.

Relevant data such as face regions, measures, and angles are intended to be obtained [43]. To do that, there are two different types of approaches that should be considered: geometric-feature based methods and appearance-feature based methods. Geometric features give information about shape and distances of facial components. These features are well-succeeded when the goal is

[1] System of colors that represents the three primary colors red, green and blue, which combined allow to produce a wide chromatic spectrum.

[2] Open Source Computer Vision.

to describe facial expressions, however, they are not able to detect some attributes that are not so prominent as the wrinkles, for instance. In this approach, the first thing to do is localize and collect a considerable number of facial components so a feature vector can be created representing the face geometry [46]. Geometric-based methods can be more expensive in terms of computing. Nevertheless, they are more robust to changes in, among others, size and head pose. Appearance features, on the other side, are steadier and are not influenced by noise, which allows the detection of a more complex and complete group of facial expressions. Regarding the appearance-based methods, image filters can be tested in both the whole face or certain regions of a face in order to obtain a feature vector.

2.3.4 Feature Selection

In the previous sub-section, a representation of the face was obtained in the form of a vector of features. However, not all those features contribute in the same way to the recognition task. Some of them have little or no significant contribution. In addition, the reduction of the data results in a better performance if the right subset is chosen, less computing time, and a clearer comprehension of the features [47].

Multiple methods for feature selection are accessible in the literature. It should be noted that methods as the Principal Component Analysis, explained in the sub-section 2.4.4, must not be confused with feature selection methods. This is because, although it performs dimensional reduction it does not only select and remove the features from the original set but changes them generating new features. Feature selection methods are usually grouped into Embedded, Filter and Wrapper methods [47]. These 3 groups will be described below.

- **Wrapper Methods-** In this method, the performance of the classifier is taken into account as the method's principle. From the original dataset, a subset of features will be selected and tested. A score will be associated with each subset [48]. In the end, the subset that achieved the highest score will be chosen. Wrapper methods can be seen as a "brute force" technique which requires a substantial computational effort [49].

  Two of the most commonly explored methods are Forward Selection and Backward Elimination.

- **Filter Methods-** Considered as a preprocessing task, this method, through procedures to rank the features orders them and selects the features positioned at the top of the rank, discarding the ones in the lower positions [47]. Its implementation is independent and performed before classification. In addition, it is considered to be faster than the previous method [49].

  Examples of ranking procedures from [50, 47] are the following: Chi-Squared, the Correlation and Mutual Information Criteria.

In the literature, Filter Methods have been presented such as, ReliefF [51], Fisher Score [52] and the Information Gain based on the Mutual Information Criterion [53].

- **Embedded Methods-** At last, contrary to the wrapper methods, the embedded focus on the reduction of the time to compute the classification of each subset. The selection of features, in this case, is carried out in the process of training. These methods are specifically used for certain algorithms [49].

  The Embedded Methods based on regularization achieve successful results and because of that a significant attention has been drawn to them [54]. This branch of the Embedded Methods includes methods as the Lasso [55], and Elastic net regularization [56],

2.3.5 Expression Classification

At last, the final step in which the expression is classified. In this phase, two models that describe how people perceive and identify which facial expression are they observing will be considered:

- Categorical
- Continuous

The first one consists of a determined set of emotions, grouped in emotion categories. Among a certain number of possible strategies, usually, for each of these emotion categories, a classifier is trained. Usually, the six basic emotions, namely anger, disgust, fear, happiness, surprise, and sadness are the categories chosen. However, there are some cases in which other categories are included, for instance, expressions of pain, empathy, or others that indicate the existence of mental disorders. The term categorical means that while a person is changing from a surprise to a sad emotion it can only be identified one of these two emotions [57]. There is no emotion in between. In contrast, the continuous shows that emotion is not a binary variable but can have different intensities, in other words, emotions can be a combination of basic emotions (e.g., happily surprised). This is a more exhaustive model, but it has the advantage of being able to define expressions without any supervision applying clustering. Methods for expression recognition can also be divided into two other group models:

- Static
- Dynamic

The static models evaluate every single frame independently, the techniques that they use for classification can be NN [58], RF, SVM. In early works, Neural Network was the most used classifier, however, in the latest approaches the chosen techniques were the SVM and the BNC. The SVM [18] provides robustness in the process of classification, this can be observed by the high classification accuracy when compared to the other methods. It performed well even in situations that was expected not to, due to the presence of noise caused by illumination variations or head pose

variation [18]. Dynamic models, on the contrary, use features that are separately extracted from each frame, so the evolution of the expression in the course of time can be modelled. The classifier used is Hidden Markov Models (HMM) [59], it provides a method for modelling variable-length expression series. This method was studied before being applied to facial expression classification, however, because the results achieved by other methods had higher levels of accuracy it was seldom used.

It is easier to train and implement a static classifier, as in the case of a dynamic classifier it is necessary to have more training samples and learning parameters. Furthermore, when there are differences among expressions they are robustly modelled by dynamic transitions that occur in the distinct phases of an expression. This is relevant as, while communicating, people only express subtle and sometimes almost invisible facial expressions. Those facial expressions are hard to identify in a single image, but likely noticeable when shown in a video sequence.

2.3.6 Challenges

Although there is a lot of interest in this area and much progress was made, there is still plenty of difficulties to overcome. The complexity of the process and the changeability of the facial expressions [60] do not help to improve the accuracy when performing facial expression recognition. The main challenges in this recognition can be found in the table 2.3 [14, 60, 61]:

Table 2.3: Main challenges in automatic expression recognition.

Challenge	**Description**
Head-pose variations	Head-pose variations occur when considering uncontrolled conditions since the participants can move, or the angle of the camera can change. The ideal scenario would be the employment of only frontal images which it is not likely to happen.
Illumination variations	In the situations where the environment is not controlled, and so pictures can be taken in different lights. Also, even in environments of constant light, some body movements can cause shadows or differences in the intensity of the illumination.
Registration Errors	Registration techniques commonly lead to registration error, so the researcher should be prepared to deal with that to guarantee the accuracy of the results.
Occlusions	It can occur due to head movements, as in the case of the illumination variations, but it can also be the presence of glasses, beard or scarves.
Identity bias	To deal with it, it is required to be able to tell identity-related shape and texture hints for subject-independent recognition.

2.3.7 Algorithms Analysis of Facial Expression Approaches

- Happy et al. [62], 2015 — In this thesis, a framework is described consisting, at first, on the localization of the face using the Viola-Jones algorithm. Secondly, facial landmark

detection was performed followed by extraction of the features using the LBP technique. The posterior application of the PCA allowed the feature vector's dimensionality reduction. At last, the SVM was used as the multi-class classifier to translate the feature vectors in expressions. It presented an accuracy of 94.09% for 329 samples of the CK+ dataset and 92.22% for 183 images in the JAFFE dataset.

- Matsugu et al. [39], 2003 — This work claimed to be the first FER model. In addition, it claimed to be independent of the participant as well as robustly invariant to its appearance and positioning. A CNN model was implemented using the disparities of the local features between a neutral and a face enacting an expression. It followed an approach of one unique CNN structure achieving an accuracy of 97.6% for 5600 images of ten participants.

- Carcagnì et al. [63], 2015- The paper contributes with a study of the HOG implementation to perform facial expression recognition since the goal is to give emphasis to its use in this context. The pipeline includes a first stage which focus is the face detection and registration. The face detection uses the Viola-Jones algorithm. Then, it develops a HOG representation of the images comparing it to other frequently used approaches. In a second stage, tests were carried out in some of the publicly available datasets. The SVM approach was used to classify the images from datasets, such as CK+ and the RFD. The accuracy values were 98.8%, 98.5%, 98.5%, 98.2% for the CK+ 6 expressions, CK+ 7 expressions, RFD 7 expressions and RFD 8 expressions, respectively.

- Shan et al. [64], 2009 — This work provides an empirical analysis of the use of the LBP features in the problem of FER. The classification was performed by means of the application of algorithms on datasets, such as the Cohn-kanade, the JAFFE, and the MMI databases. The algorithms used to classify the expressions were the Template matching, SVM, LDA, and Linear programming. Furthermore, the performance is inspected on different image resolutions and in situations close to the real-world setting. Regarding the CK database, the achieved accuracy was 88.9%, 79.1% and 73.4% for the SVM, Template matching and LDA, respectively, when considering 7 expressions.

- Jia et al. [65], 2016 — The present work proposes a methodology that uses the PCA as a feature extractor applied on a RF classifier. The tested dataset was the Japanese Female Database in which, at first it was performed the preprocessing of the images (i.e. face detection, crop and resize and noise removal), followed by the classification. This last step used SVM and RF whose recognition rate was 73.3% and 77.5%, respectively.

2.3.8 Competitions

- Valstar et al. [66], 2011 — This paper presents the first challenge in automatic FER, the FERA2011. This challenge had 2 variants, one detected Action Units whereas the other focused on discrete expressions. The challenge selected the GEMEP database [67], however,

only a part of this dataset was used. A baseline is described using the LBP, PCA, and SVM for the 2 variants of the challenge.

- Valstar et al. [68], 2015 — The second FER challenge addressed the detection of the AU occurrence and the estimation of its intensity for previously segmented data as well as a fully automated version. The BP4DSpontaneous [69] and the SEMAINE dataset [70] composed the data used in this challenge. To perform the extraction of the appearance features a local LGBP descriptor[71], and the Cascaded Regression facial point detector[72] for the geometric features were used. At last, a linear SVM performed the detection of the AU occurrence, and a linear SVR was used for the intensity.

- Valstar et al. [73], 2017 — Lastly, the third challenge adds to the previous one the difficulty of dealing with data generated when varying the positioning and the camera angle. The sub-challenges are, as previously stated, the AU detection and the estimation of its intensity. In this case, the geometric features were obtained by the Cascaded Continuous Regression facial point detector[74]. In contrast to the previous challenges, for the FERA2015 the temporal dynamics was modeled by using the learning method Conditional Random Field[75] (AU occurrence) and Conditional Ordinal Random Field[76] (AU intensity).

2.4 Feature Methods

2.4.1 Histogram of Oriented Gradients (HOG)

The dissemination of this technique goes back to 2005 when Dalal et al. [77] proposed a work in which they drew attention to human detection in static images at the CVPR[3]. HOG is a feature descriptor comparable to scale-invariant feature transform descriptors. Though, the difference lies in the implementation since the HOG algorithm consists of dividing the image into equally sized cells and computing a local 1-D histogram of gradient directions for each cell. Combining all these local histograms results in a histogram that represents the whole image. Yet, before obtaining this combined histogram and, in order to achieve an invariant system in illumination and shadows, it is advantageous to contrast-normalize local histograms. Toward this end, an accumulated value is obtained through the local histograms over larger regions denominated as blocks, applying this outcome to normalize all the cells in the block [77]. This feature descriptor is a useful tool as it enables a detailed description of the image, in which the presence of elements or features of it are identified by sudden changes in the image. Finally, as a shape descriptor it allows representing an object as a pattern (see Figure 2.5).

2.4.2 Local Binary Patterns (LBP)

LBP is a texture descriptor used for classification and Ojala et al. [78] was one of the first notorious references to it. The response produced by this algorithm comes in the form of a feature vector. In

[3]Conference on Computer Vision and Pattern Recognition

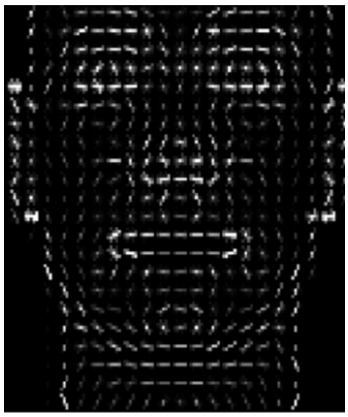

Figure 2.5: HOG of the face. From [5].

practice, to obtain this LBP feature vector a window of determined dimensions is taken, supposed that a 3x3 pixel block is chosen . Moving this window through the image, the value of the pixel at the center of the block is used to threshold its surrounding pixels [6]. This means that the pixel values of each of the 8 neighbours will be compared to the center pixel and so, in the case of the neighbour pixel having an intensity value greater than the center, it will be replaced by "0" if not, becomes a "1". The next step involves reading the modified values in the 3x3 window in the clockwise direction leading to an 8 digits binary pattern that is converted to decimal afterwards. After carrying out this process in the whole image a histogram can be generated giving information about the frequency of the pattern occurrence. At last, the final step implies concatenating the results to obtain the feature vector [78].

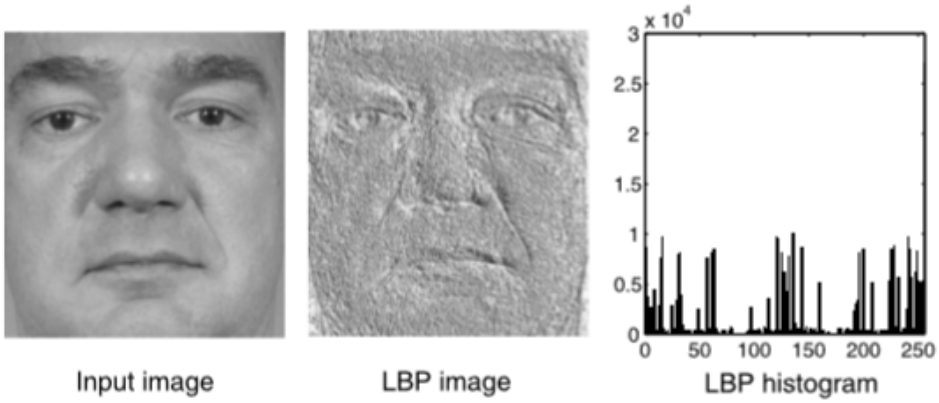

Figure 2.6: Image sequence of the process described above: an input image, LBP image, and the correspondent histogram. From [6].

2.4.3 Scale-Invariant Feature Transform (SIFT)

David Lowe presented this method to generate image features in [79, 80]. The scale-invariant feature transform has been applied to several topics as motion tracking, object and gesture recognition. As the name suggests, this algorithm is used to extract and describe invariant features. That is to say it extracts and describes features that are invariant to image scale, variations in the illumination, translation, and rotation of the element in issue. This approach consists of a great collection of key points descriptors possessing extremely distinctive characteristics. Such characteristics enable this algorithm to find an accurate match in a large set of features [80], which means the same object has a high chance of being detected in another image.

2.4.4 Principal Component Analysis (PCA)

PCA is a statistical method invented by Karl Pearson in 1901 [81]. The method concerned identifies the maximum variance and after that reduces their dimensionality [82]. In fact, it can reduce a large dataset into a smaller dataset preserving most of the information existing in the large dataset. It is used to give emphasis to variation and highlight patterns by converting the initially considered data into principal components [83]. Since these components are ordered by their ability to explain the variability of the data, the first principal component is the one that can account for most of the variability. Thus, the subsequent components can explain the remaining variability, and so on. Eigenfaces [84] consist in the Principal Component Analysis when performed in a dataset of face images. The focus in this method are the significant features which are the areas of maximum change in a face (e.g. the significant variation visible from the eyes to nose). However, those significant features are not necessarily translated in a region of the face as the eyes or the nose [85]. The intention here is to capture the relevant variations among faces so it is possible to differentiate them.

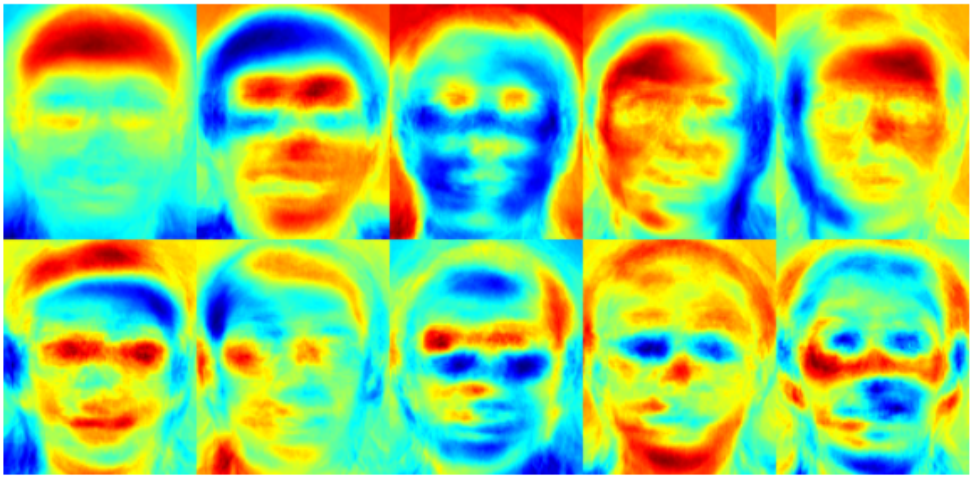

Figure 2.7: Example of the eigenfaces showing that as well as encoding the facial features, it also encodes the illumination in the face images. From [7].

2.5 Feature Selection Techniques

2.5.1 Sequential Forward Selection (SFS)

SFS is an algorithm used to perform feature selection. The process of selection is initialized testing an empty vector of features. Then, one feature is added to the vector at a time and each new generated vector of features is tested. The fact that a feature allows achieving the best performance in the classification is what defines if it is kept or discarded of the vector of features. In the end, the selected set of features is returned.

2.5.2 Sequential Backward Selection (SBS)

Contrary to the previous algorithm, the Sequential Backward Selection starts considering all the features and excludes one at a time. In this case, it is excluded the features that reflect the least reduction of the classifier's performance.

2.5.3 Mutual Information (MI)

The principle of MI consists of calculating the dependency measure between two variables [86]. In machine learning it is used as a feature selection criterion which defines the relevance or redundancy of the features. Therefore, a score is calculated indicating how well descriptive a feature (x) is of the labels (y). In the end, a predefined number of features (k) corresponding to the highest scores is chosen. This score is presented as the mutual information, $MI(x_i, y)$ below:

$$MI(x_i, y) = \sum_{x_i \in \{0,1\}} \sum_{y \in \{0,1\}} p(x_i, y) \log \frac{p(x_i, y)}{p(x_i)p(y)} \tag{2.1}$$

MI will be equal to 0 in the case of x and y be independents and superior if there is a dependency [47].

2.5.4 Lasso Regularization

Lasso, proposed by Robert Tibshirani in 1996 [55] is an effective technique that performs both regularization and feature selection [87]. It formulates that the model specifications are restricted, the sum of its absolute values is upper limited by defined value. To this end, one of the steps performs a shrinking (regularization). The coefficients of the features are penalized being shrunk to 0. The selected features are the ones whose coefficient is other than zero. This process aims to reduce the error in the prediction [87].

2.6 Machine Learning Algorithms

2.6.1 Viola-Jones

Viola-Jones is an extensively used real-time object detection approach published in 2001 in [8, 88]. It is known for its ability to perform rapid image processing with high detection rates. The target of this framework, as well as one of its motivations, was the definition of the face detection problem. The fact that a fast face detector was created made it suitable for a wide range of applications, such as user interfaces and image datasets [8]. There are three main aspects of this system that are worth highlighting. Its robustness, which means there is a high True-Positive rate and a low False-Positive consistently, its capability to process images in real time and, finally, its exclusive use to detect faces in images and not recognition as it can be mistaken. Furthermore, according to this work, to build such a face detection system 3 steps need to be accomplished [89]. These steps are the folowing: obtaining the Integral Image, the implementation of AdaBoost and, at last classification using an Attentional Aascade.

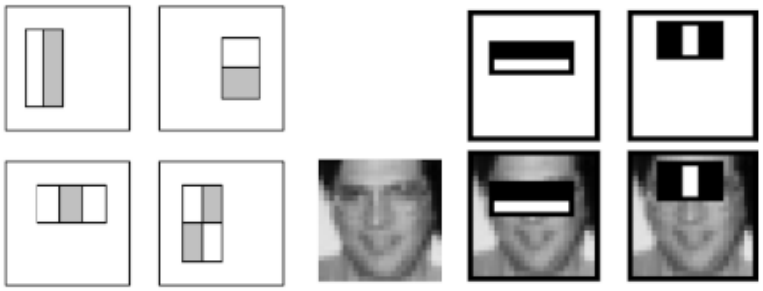

Figure 2.8: On the left, feature examples are shown. On the right it is presented the AdaBoost two first selected features. Adapted from [8].

2.6.1.1 Integral Image

An Integral Image is an image representation that was first presented by the name *Summed-Area Table*, which is used as a fast way of computing Haar-like features at various scales [8]. In practice, it efficiently calculates the sum of intensities over manifold overlapping rectangle regions of an image [9]. See Figure 2.9.

2.6.1.2 AdaBoost

AdaBoost is a learning algorithm which acts in both the selection of a limited number of significant features as well as in the training of classifiers [90]. In this regard, it occurs a boost in the performance due to the combination of weighted “weak” classifiers that yields to this “strong” boosted classifier [88].

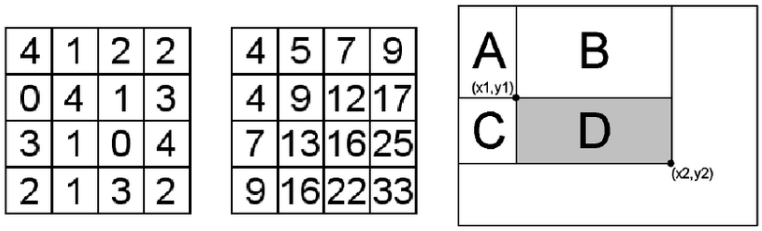

Figure 2.9: On the left and center it is demonstrated how to calculate the integral image. On the right, it is shown D which can be calculated through the integral image. From [9].

2.6.1.3 The Attentional Cascade

This architecture generates a cascade of classifiers with improved performance in the detection of the face [8] and drastically reduced computation time [89]. The focus is that simple boosted classifiers maintain most of the positive sub-windows while discarding the negative ones. It is considered to be a highly efficient system since a negative response will mean the sub-window immediate rejection, and thus it is predictable that the rejection of most of the sub-windows will occur in the initial stages which decreases the computational cost.

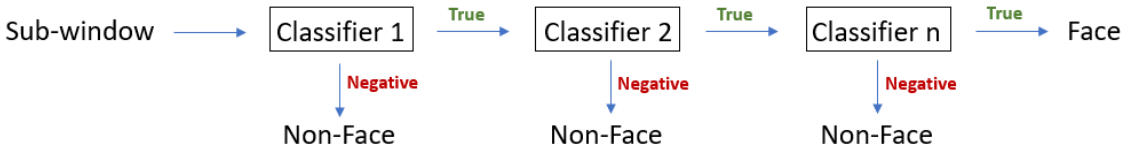

Figure 2.10: The Attentional Cascade.

2.6.2 Support Vector Machines (SVM)

SVM [91] is a machine learning technique widely used in classification problems. An SVM model aims to find the most precise borderline which maximizes the gap between sets of distinct elements (see Figure 2.11). Therefore, it is considered as a maximum margin classifier since it can decrease the error to its minimum and, at the same time, increase the gap between different sets to its maximum [89]. At last, it gained a valuable reputation by achieving better results than other machine learning approaches. A good example is the SVM performance in face detection [92, 93].

2.6.3 Decision Trees (DT)

A DT, as the name suggests is a tree with the ability to make decisions. It is one of the preferred approaches to represent a classifier since it provides a clear way to visualize and interpret the classification problem [94]. What differentiates a DT from our notion of what is a normal tree is the fact that this tree grows downwards. In this way, it starts being built from the roots and

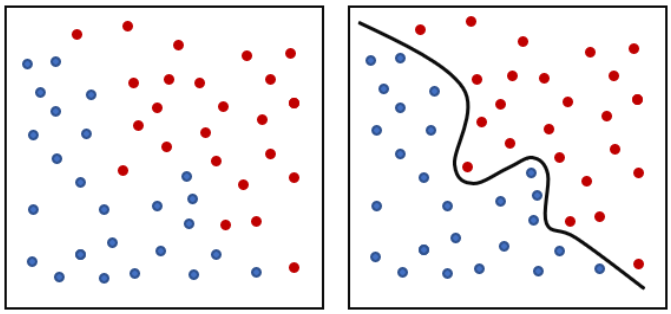

Figure 2.11: On the left it is shown the original feature space whereas on the right, it is the non-linear separation of those features.

goes down to the leaves [95]. It is essentially a binary tree, in which the leaves correspond to the different target class labels. A test node, on the other hand, represents a feature and it is where the decision occurs. The outcome that results from the decision defines which one of the branches to follow, and so on until a leaf is reached, which means the class has been predicted (see Figure 2.12).

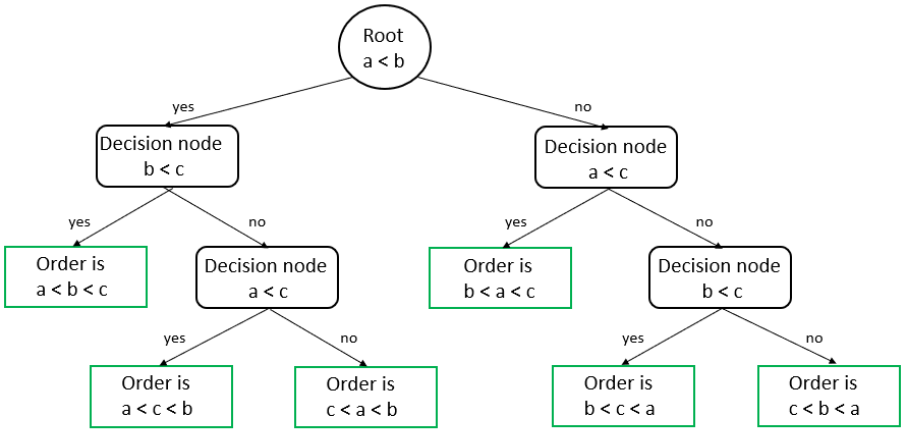

Figure 2.12: Example of Decision Tree, which aim is to sort the variables a, b, and c. Adapted from [10]

2.6.4 Random Forest (RF)

RF [96] is an acknowledged statistical method in a wide variety of subjects [97]. The classifier consists of using multiple Decision Trees [4] combined, whose training process applies the bagging method proposed by Leo Breiman in [98]. As previously mentioned, when a DT is fully-grown a

[4] Quinlan et al. in [95]

prediction is reached. However, in the case of RF, it is the combination of all the interim predictions that yield to a final prediction, achieving notorious improvements in the accuracy values [99]. This way of proceeding corresponds to the aforementioned bagging method. In addition, the fact that it is used sub-set of randomly selected features from the training set as the input for each tree leads to favourable error rates comparable to the AdaBoost algorithm [97] [5].

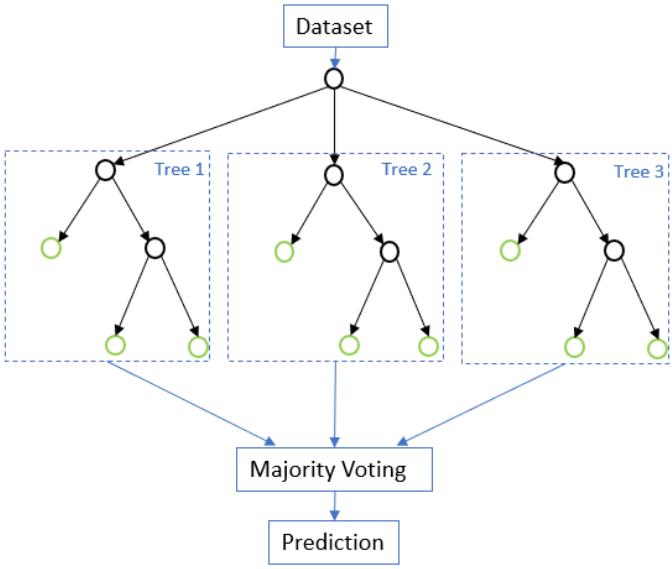

Figure 2.13: Example of a simple RF.

[5] Freund et al. in [90]

2.7 Facial Expression Databases

When benchmarking techniques, it is highly important to use the most appropriate dataset. Therefore, it is extremely important to take into consideration the final goal of the task. In this work, since it is aimed to recognize facial expressions it is likely to use databases, such as the following:

- Japanese Female Facial Expressions (JAFFE) — This database consists in the record of 10 Japanese female models enacting 7 expressions making a total of 213 images (Lyons et al. [100], 1998).
- Cohn-Kanade AU-Coded Expression Database (CK) — The CMU-Pittsburgh AU-Coded Face Expression Image Database contains 2105 image sequences, in which were included 182 participants from diverse ethnic group obtaining a description in facial expression labels (e.g. happiness) and FACS basic units (AU) (Kanade et al. [101], 2000)
- MMI Facial Expression Database (MMI) — This database consists of 1500 samples divided in static and image sequences. The faces are positioned in a frontal angle enacting different expressions measured in AUs from the Facial Action Coding System (FACS) (Pantic et al. [102], 2005)
- Taiwanese Facial Expression Image Database (TFEID) — TFEID contains 7200 images from 40 particIpants, half are women. Eight expressions are represented, with some pose variations (Chen et al. [103], 2007)
- Extended Cohn–Kanade (CK+) — The CK+ represents an increase of 22% in the number of sequences and 27% in the case of the participants when compared to the first release of the CK. Also, in this extended version, it was added spontaneous sequences and their respective description in FACS and expression labels (Lucey et al. [11], 2010).
- Multimedia Understanding Group (MUG) — Mug is organized in two groups, the first one contains data from 86 models performing the six main expressions (anger, disgust, fear, happiness, sadness, surprise) defined in FACS, whereas the second one contains induced expressions performed in lab environment by the same group of participants (Aifanti et al. [104], 2010).
- Facial Expressions In The Wild Project (AFEW/SFEW) — Acted Facial Expressions in the Wild (AFEW) is a dynamic temporal database in which the samples were collected from movies. The selection of 700 frames from the AFEW database originated a static subset labelled for 6 expressions called Static Facial Expressions in the Wild (SFEW) (Dhall et al. [105], 2012).
- Facial Expression Recognition 2013 (FER2013) — FER2013 was first made public for the Kaggle competition. The dataset contains 35887 grayscale face images labelled for 7 expressions (Goodfellow et al. [106], 2013)

- AffectNet — This database contains roughly 1,000,000 face images in the wild setting obtained from the Internet, half of these were manually annotated for 7 emotions and the intensity of valence and arousal. The remaining were automatically annotated training the ResNext Neural Network on the manually annotated set. (Mollahosseini et al. [13], 2017)

The properties of a database can be organized in three main categories, this organization is based on the content, in the capture modality and in the participants [4]. Content includes information as the type of labels, which expressions are present, whether the samples were taken with an intention or not (posed or spontaneous), and, at last, if it contains images (static) or video sequences (dynamic). On the other hand, the capture modality describes if the data was captured in laboratory conditions or not, changes in perspective, illumination and finally occlusions. Lastly, it is the compilation of the data in statistical terms, such as age, gender and ethnic group [4].

Table 2.4: RGB Dataset.

Dataset	**Description**	**Intention**	**Gray/Color**
CK	The first dataset to be made public. This first version is considerably small.	Posed primary facial expressions	Mostly gray
CK+	Extended version of CK with an increased number of samples both posed and spontaneous.	Spontaneous images added plus the previous posed ones	Mostly gray
MMI	Marked an improvement by adding profile views of primary expressions and almost all existing AUs of the FACS.	Spontaneous and Posed	Color
JAFFE	A dataset of static images captured in a lab environment. It contains 213 samples with 7 expressions acted by 10 Japanese women	Posed	Gray
AFEW	It is a dynamic dataset, carefully describing the age, gender, and pose of the images, one of the 6 primary expressions	Posed	Color

Table 2.5: 3D Dataset.

Dataset	**Description**	**Intention**	**Gray/Color**
BU-3DFE [107]	6 expressions out of 100 distinct subjects, taken under 4 different intensity levels.	Posed	Color
Bosphorus [108]	Low ethnic diversity, however, it contains many expressions, head poses, and occlusions.	Posed	Color texture images
BU-4DFE (video) [109]	High-resolution 3D dynamic facial expression dataset.	Posed	Color texture video

Table 2.6: Thermal Dataset.

Dataset	Description	Intention	Gray/Color
IRIS [110]	Images from 30 subjects. It includes a set of images labelled with 3 posed primary emotions capture on different illuminations.	Posed	Gray
NIST [111]	Consists of 1573 images, of which 78 are from women and the rest from men.	Posed	Gray
NVIE [112]	The 215 subjects enact six expressions. In the posed setting it is included also some occlusions and illumination from different angles.	Spontaneous and Posed	Gray
KTFE [113]	As the NVIE, this database contains the 6 expressions. Includes samples from 26 subjects from Vietnam, Japan, and Thailand	Spontaneous and Posed	-

2.8 Final Considerations

In this chapter, the topic of study Facial Expressions was introduced, as well as the structure of an Automatic Facial Expression Recognition System, depicting each one of the steps and how they were performed in other similar works. Moreover, the most appropriate datasets to deal with the problem of expression recognition are presented.

Gathering all this information was a fundamental milestone to be able to decide which of those methods and algorithms would be implemented hereafter. Also, it was taken into consideration the computational cost of some techniques and the public availability of the datasets. With this in mind, the chosen techniques were the following:

- Viola-Jones approach to perform face detection as it is still widely used in current works due to its effectiveness in the localization of the faces;
- HOG, LBP and PCA to obtain the facial features, the first because of its ability to detect abrupt changes, the second for being a robust texture descriptor that can deal with illumination variations, and the last one which is able to create a representation that explains the variance of the images and discard the redundant features making it faster to run;
- MI to select the features due to its ability to deal with inconsistent relations between the features and the target variables, also it is not computationally intensive;
- SVM and RF to perform classification, as the first is one of the most used algorithms able to achieve high accuracy values, and the second one, a classifier known for its great performance due to the combination of predictions that allows achieving a more reliable final prediction.

Chapter 3

Methodology

In the present chapter, the methodology of this work is described. More specifically, the approaches and methods used to perform feature extraction and classification so, in the end, it is possible to classify face images according to the expression shown in the categorical domain. The decisions made at each step are also duly explained. This approach was organized as shown in the following Figure 3.1:

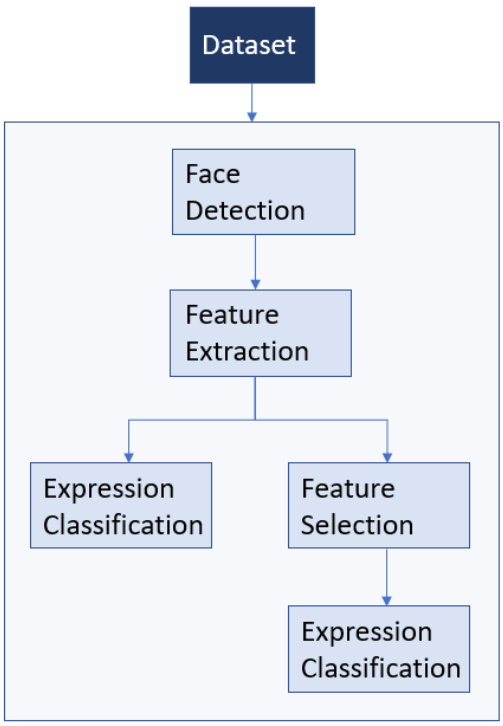

Figure 3.1: Automatic Facial Expression Recognition System.

3.1 Face Localization and Crop

The aim of this stage is to detect and crop the faces present in the images. Nevertheless, there was a slight difference in the pre-processing of these two datasets. The CK+ had no annotations for the location of the face in the image, which meant that a face detection technique would have to be applied. Toward this end, the OpenCV library seemed to be a reasonable option, since it is acknowledged by their Object Detection approach with a few of pre-trained classifiers for the face and, moreover, some more specific regions of the face as the eyes or the mouth (smile). This detector uses a Haar Feature-based Cascade Classifier originally proposed by Paul Viola and Michael Jones [8] (see Section 2.6.1) which continues to be one of the most frequently used [114] methods. On the contrary, the AffectNet Database provided already the location of the faces in the images (see Figure 4.3). In this case, a bounding box for each face has been previously found by using the OpenCV face detector. The provided coordinates represent that bounding box expanded in fifteen percent.

Hereupon, regardless the way the location of the faces in the images was obtained, we ended up with 4 values (x,y,w,h) which are the required information to crop the images, and so our final image would only have the desired region of interest, the face. Finally, and because the preprocessing step is to produce an image that can be used with a certain efficiency and straight by the feature extractor, the images from both datasets were converted to grayscale and resized to a fixed size, in this case, 256x256 pixels [13].

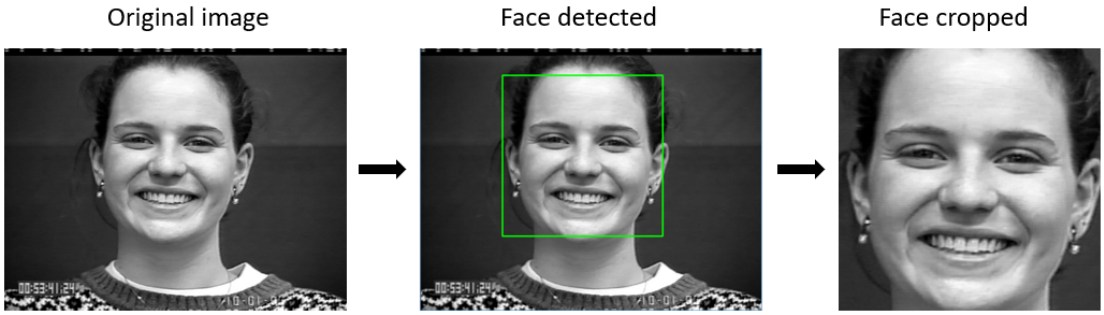

Figure 3.2: Representation of the performed steps to obtain a face image on the CK+ dataset.

3.2 Facial Features

Objects are effortlessly recognized by the human eye due to the ability of our brain to associate them with some specific characteristics. The mastery of this skill is the result of its development since the day we were born by observing the world around us. The aim of Computer Vision is, precisely, to imitate the human eye. For this purpose, information from an image is acquired using feature extraction techniques. In chapter 2, a few of these techniques were reviewed and some of them implemented so it would be possible to draw conclusions on how well they would be able to describe the image faces. In this experiment, the chosen feature extraction techniques consider the image as a whole [115]: HOG, LBP, and PCA.

3.2.1 HOG

Different facial expressions trigger different changes in the face, as can be observed in Figure 4.1. The distinct characteristics among different facial expressions are easily identified, for instance, surprise is represented by arching the eyebrows, and keeping the eyes and mouth wide open. On the contrary, to lower the eyebrows and press the lips together defines another facial expression, anger. These are the features that are intended to be extracted. The Hog algorithm, previously presented, was used due to its capability to detect abrupt changes in the face images. In practice, it can detect the transition from the skin to other elements as the lips, eyebrows or nose. It is considered a shape descriptor as it distributes the intensity gradients in the direction of the element's edges.

The procedure starts by converting the cropped face image to grayscale, this is a necessary step because it prevents the occurrence of errors provoked by the channels. Finally, the feature vector is generated in the form of a histogram that represents the image. See Figure 3.3.

3.2.2 LBP

In some instances, the image after being converted to grayscale shows almost no noticeable distinction in the different levels of gray, this can be caused by illumination variations. The LBP is a robust texture descriptor able to deal with situations like this. Another important particularity is its computational simplicity due to the low complexity steps that need to be performed, explained in the literature review (See 3.4).

The first step involves converting the image to grayscale, followed by the repetition of some basic steps in the whole image obtaining a decimal number to each position of the window and, subsequently, generating a histogram with the frequency of the number. In the end, the results are concatenated and the feature vector obtained.

3.2.3 PCA

PCA's importance is reflected in its ability to discard the redundant components and preserve only a few components that can describe most of the variation of the original dataset (See Figure 2.7).

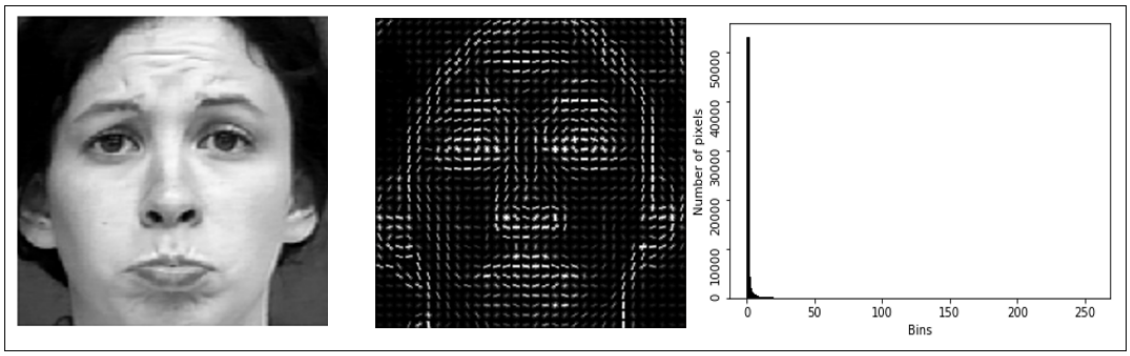

a) CK+

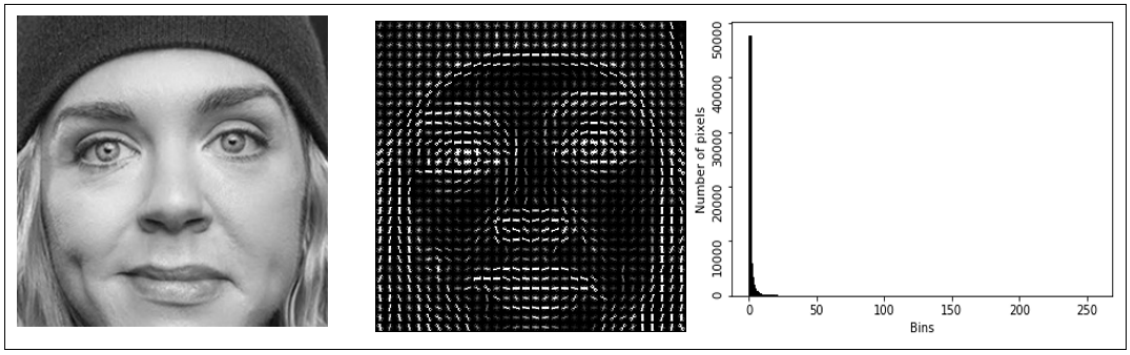

b) AffectNet

Figure 3.3: Example of the HOG implementation on the CK+ and AffectNet dataset, on the upper and lower images respectively. Starting from the left it shows the original image, followed by the HOG image and the respective histogram.

In practice, this performs dimensionality reduction which enables the speed up of the facial expression recognition system.

In this algorithm, the sufficient number of components to explain 95% of the variance of the training set are preserved. So, it starts with the extraction of the first eigenfaces from the training set and, at last, it projects both the training and test set on the eigenfaces orthonormal basis.

Figure 3.5 shows the 'mean' face computed by the PCA explaining 95% of the variance applied to the training set from the CK+ and on the training set from the AffectNet. As it can be observed there is a discernible difference of sharpness in the images. In the image on the right, it is less evident that it corresponds to a facial structure. This can be justified by the fact that the AffectNet images are highly variant in characteristics such as the occlusions, the subject's age, the lighting conditions, and the head pose.

Figure 3.7 and 3.6 illustrate the 30 first principal components, organized by their significance from the upper left corner to the lower right corner. Hence, the first ones, on the top left corner appears to handle the lighting conditions, whereas the rest focuses on certain specific features of the human face, such as the mouth, eyes, eyebrows and, nose.

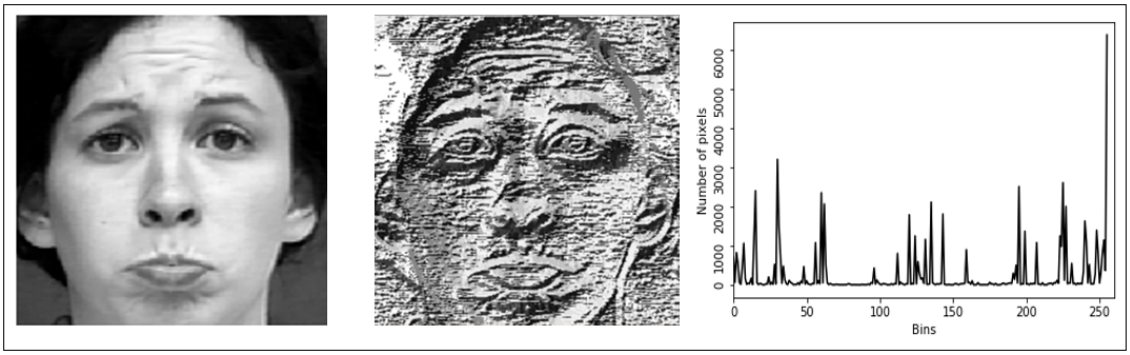

a) CK+

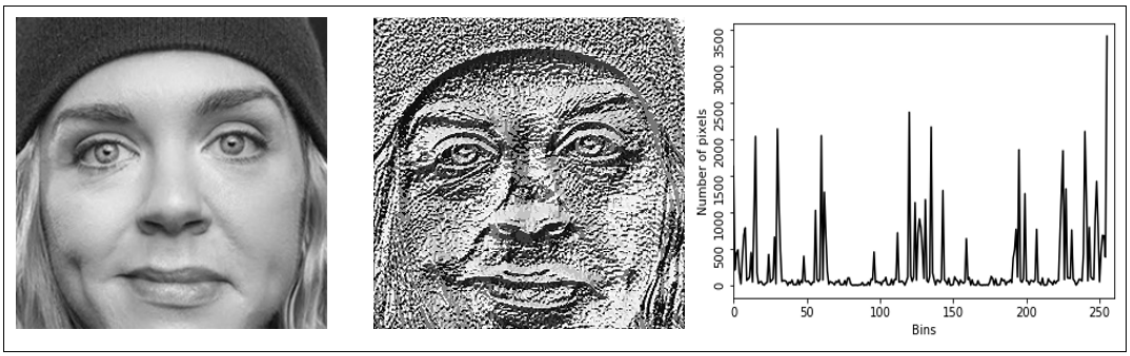

b) AffectNet

Figure 3.4: Example of the LBP implementation on the CK+ and AffectNet dataset, on the upper and lower images respectively. Starting from the left it shows the original image, followed by the LBP image and the respective histogram.

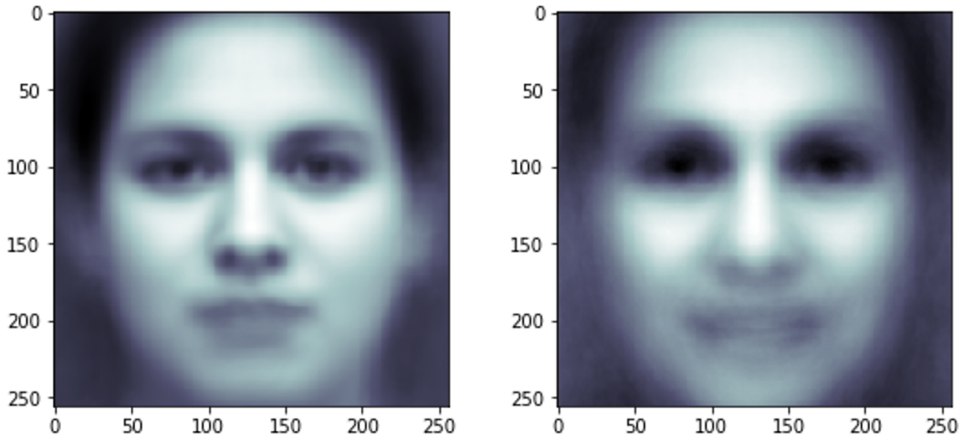

a) CK+ b) AffectNet

Figure 3.5: 'Mean' face computed by the PCA.

Figure 3.6: Representation of the first principal components on the CK+ dataset.

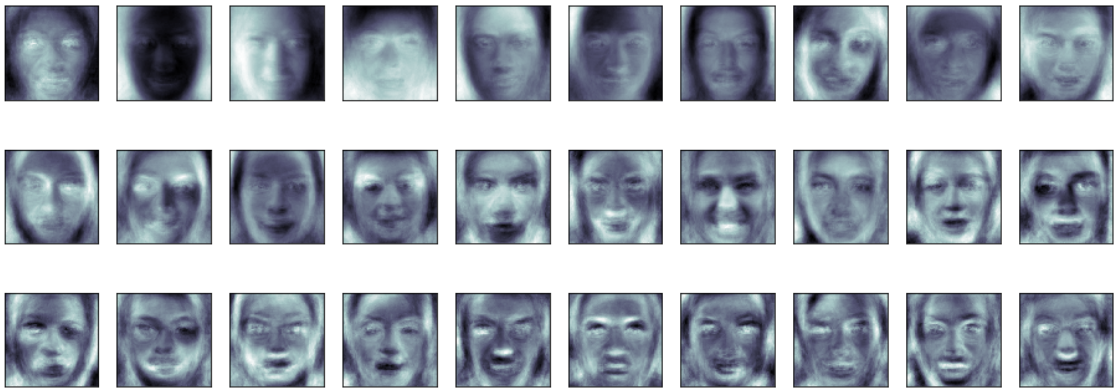

Figure 3.7: Representation of the first principal components on the AffectNet dataset.

3.3 Feature Selection

In the previous section, a vector of features was obtained. However, it is possible that not all the features are needed to create a meaningful representation of face. That is what a feature selection algorithm tries to find out, whether a smaller set of features would be able to achieve the same or even superior accuracy comparing to the complete set of features. Such reduction would have multiple advantages, as it would allow a better understanding of the features keeping only the features that are relevant, minimizing the vector of features making the algorithms to run faster and, at last, to avoid overfitting [87]. In Chapter 2, some feature selection algorithms were studied.

3.3.1 MI Based Approach

As studied in 2.5.3 the MI criterion [116] consists of obtaining a score which is determined by what is shared or not between features. The MI's principle was used as a straight measure to choose a subset of features that enable the system to perform the most accurate separation of the aimed labels. Other conventional feature selection techniques, for instance techniques based in correlation

when compared to the MI are not able to calculate the score for associations between random features [117]. This approach might be advantageous when dealing with situations to which a linear relations technique fails to deal with. In addition, it is not a computationally complex technique.

3.4 Classification

From the two datasets a set of seven emotions (anger, contempt, disgust, fear, happy, sad, surprise) and, additionally, the neutral one were considered.

In this section, the methods used to classify the datasets for the above facial expressions will be discussed. For this purpose, the goal was to find an accurate, robust, and feasible classifier. Of the two types of machine learning techniques, supervised learning is the one used to train a model on a known training set (considering both, the input and the output response data). Thereby, and after having built the classification model it can be finally used to predict a new test set. This experiment tested two distinct supervised learning algorithms, so the behaviour of the different features could be analyzed: SVM and RF.

3.4.1 SVM

The SVM, previously studied in section 2.6.2, is one of the most used algorithms as it has the ability to perform classification with high accuracy, outperforming other classification algorithms.

The feature vectors obtained through the HOG, LBP or PCA algorithm performed on the training set, along with the respective labels, were used to feed the classifier. Then, a model is built and the features were distributed depending on their associated label. By doing this, the features that belong to different classes are separated from one another and positioned in the correspondent group.

Some tests were carried out varying some parameters so it would be possible to analyze the behaviour of the classifier, which parameters would have more influence and how it would affect the system accuracy.

3.4.2 RF

The second method tested was the Random Forest, explained in section 2.6.4. The great performance of the RF is due to the combination of a considerable number of interim predictions that lead to a more reliable prediction in the end. Also, its randomness when selecting the features from the training set that are feeding each tree allows the method to estimate the importance of each feature in relation to the others.

As the SVM, the input for this classifier is also the output of the previously mentioned feature extraction methods. An RF model with certain parameters is built and the model and those feature vectors together with the labels are given to fit the model. At last, it makes the predictions to the test set and provides a final prediction value.

A vast set of parameters were tested in order to find the best parameter choice that would achieve the highest accuracy, as well as to study the influence of each one the parameters.

3.5 Final Considerations

In this chapter, the proposed methodology for this project was described. By starting with the choice of the datasets to the last step, the algorithms chosen for the classification. In order to obtain a more reliable analysis more than one technique was tested at each step. The following chapter presents the results of the implementation of these methods as well as its interpretation in order to understand how feasible they are to perform the proposed task.

Chapter 4

Results and Discussion

This chapter covers the discussion and analysis of the results for all the methods implemented in each step of the Methodology (Chapter 3). As it was mentioned before, each phase involved the test of different approaches. The final goal was to understand how reliable an Automatic Facial Expression Recognition system can be in different situations. For this purpose, whenever the results were not satisfactory some modifications were made and even other techniques considered. This entire process will be discussed as well as the respectively obtained outcomes.

4.1 Dataset

The initial step to perform any recognition task is to choose the adequate data. As in this case, the focus was the benchmarking of different techniques to recognize facial expressions, a reliable and well-known dataset was required. In this way, the CK+ was chosen. The fact that this dataset was generated in a controlled environment and it is been used countless times since its release makes it a valuable addition. A second dataset was also considered the AffectNet Database. The choice for this dataset was due to the fact that this is a recent dataset, in-the-wild and with a large number of samples. These characteristics reflect the current needs in the field.

4.1.1 The Extended Cohn – Kanade (CK+)

The CK+ is a publicly available dataset, and as it was stated before is an extension of the CK database which the main purpose was to promote the development of automatic systems to detect the individual's facial expressions. This new version has augmented in 22 percent the posed samples and added the spontaneous ones (see Figure 4.1). The subjects that were taking part in the experiment were 210 adults which facial movements were recorded using the following equipment: two hardware synchronized Panasonic AG-7500 cameras [11]. The age of the individuals ranged from 18 to 50 years of age, given that sixty-nine percent were female, eighty-one percent were Euro-American, thirteen percent Afro-American, and six percent from other groups. During the experiment, the subjects were instructed to execute 23 facial displays which comprehended

both single and combined action units. In the observation room where the experiment was taking place, image sequences were obtained by the two cameras there positioned, one of them was directly in front and the other was 30 degrees to the right of the subject [101]. In the end, the result was both an 8-bit grayscale and a 24-bit color values pixel arrays with dimension 640x490 or 640x480. The number of frames in the image sequences can vary between 10 and 30 and it always starts and finishes with a neutral expression. However, the arranged sequence in the dataset only includes the frames from the neutral to the peak of the expression (See Figure 4.2). This last one characterizes the emotion label that is assigned to the alluding sequence. The group of the possible labelled emotions can be seen in Figure 4.1 below: anger (e), contempt (f), disgust (a), fear (d), happiness (b), neutral (h), sadness (g) and surprise (c).

Figure 4.1: Examples of the CK+ dataset. In the upper part, there are some images originally from the CK dataset and those below are the data included in the new version. Adapted from [11].

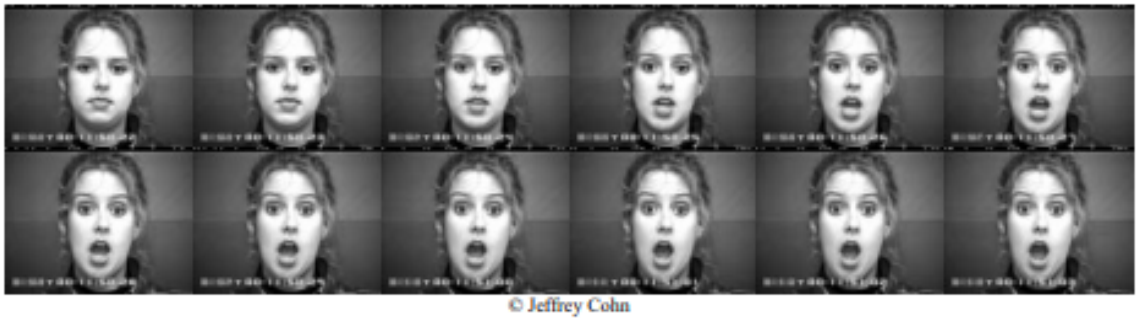

Figure 4.2: Images sequence obtained from a subject when the labelled emotion is “Surprise”. From [12].

4.1.2 AffectNet

AffectNet, which name arose from the merge of the words Affect and InterNet, is the largest existing dataset only released in the second semester of 2017. This dataset contains approximately

Table 4.1: Frequency of each expression represented in the peak frames on the CK+ database.

Expression	**Number**
Angry (An)	45
Contempt (Co)	18
Disgust (Di)	59
Fear (Fe)	25
Happy (Ha)	69
Sadness (Sa)	28
Surprise (Su)	83

one million face images. Images that were gathered from the Internet through 3 search engines (Bing, Google, and Yahoo) when queried with 1250 keywords associated with emotion vocabulary in 6 distinct languages (English, Spanish, Portuguese, German, Arabic, and Farsi). Afterwards, a bounding box for each face was found by using the OpenCV face recognition approach mentioned above. Then, this bounding box was expanded in fifteen percent. Besides that, via regression local binary features (a face alignment technique) [118] sixty-six facial landmarks points were detected. The resolution of the face images is, on average, 425x425. In order to take some facial characteristics, the *Microsoft cognitive face API* [119] was used and according to the outcome: Forty-nine percent of the samples were identified as men and the average age is 33.01 years old, with a standard deviation of 16.96 years. The Microsoft cognitive face API also allowed the detection of the occurrence of some occlusions. For instance, eye (0.49 percent), forehead (4.5 percent) and mouth (1.08 percent) occlusions were found in the face images. Additionally, several faces have eye (51.7 percent) and lip (41.4 percent) make-up, and others were wearing glasses (9.63 percent). The dataset is branched in two different sets, such as:

- Manually Annotated;
- Automatically Annotated.

The present need of having an extensive dataset in the wild which would contain a huge number of the individual's variation provided the justification for its creation. Apart from that, there is also the fact that this dataset embraces more than one model of affect [120]. In this case two different emotion models [121]: the categorical, which represents the discrete facial expressions, for instance, here are considered seven distinct facial expressions; and the dimensional which is the intensity of valence and arousal (see [122]). The manually annotated set, as the name implies is an annotated set by expertise human labelers. It has around 420000 images which are labelled by the annotators for the two models of affect aforementioned. The remaining images belong to the automatically annotated set (more than 550000), which was obtained through the training of the ResNext Neural Network on the manually annotated training set, achieving an average accuracy of sixty-five percent.

4.1.2.1 Annotation Procedure

To perform the annotation of the face images some options were considered as the *Amazon Mechanical Truck* (MTurk), a crowd-sourcing service. Although it is a cheap and straightforward approach to label large datasets, it is not fully reliable in terms of the quality of labelling. Since it ranges significantly depending on the annotators. Also, the fact that it is required to annotate this dataset in the dimensional model makes this task impossible for any annotator with no knowledge in this model of affect. Thus, after taking in consideration these limitations the crowd-sourcing service was discarded, and the solution found was hiring twelve annotators at the University of Denver. These expertise annotators were given 450000 samples to perform the labelling of the face in the images, each image annotated by one annotator. To annotate the two models of affect (categorical and dimensional) a software application was designed (See Figure 4.3).

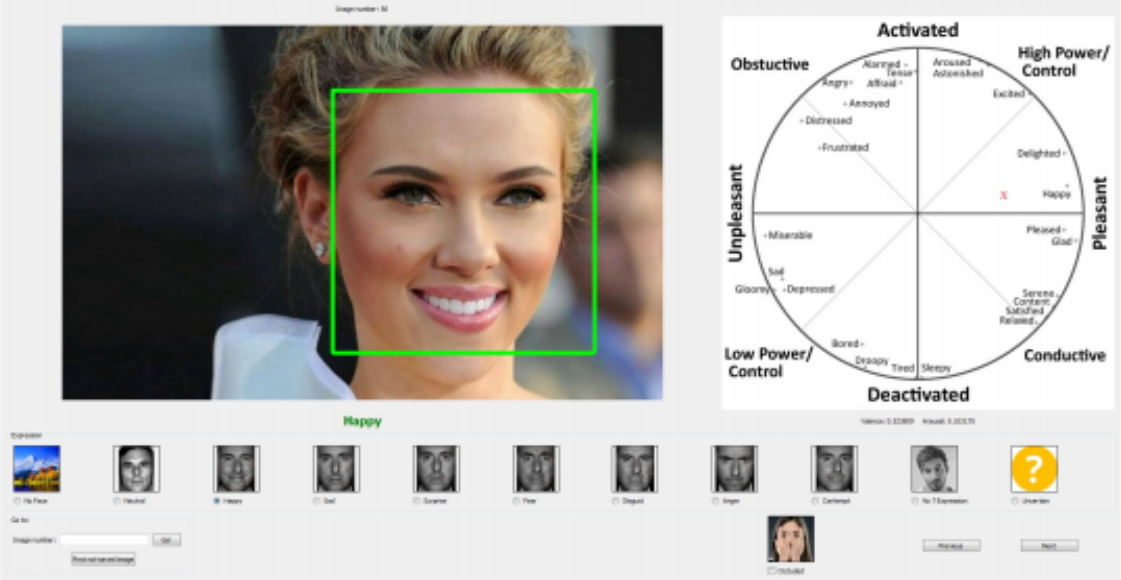

Figure 4.3: Software application used by the annotators to label into the categorical and dimensional models of affect. An image has only one face annotated (for instance, the one in the green box). From [13].

4.1.2.2 Annotation in the Categorical Model

Each sample was identified as one out of 11 emotion and non-emotion categorical labels. These eleven labels are Neutral, Happiness, Sadness, Surprise, Fear, Disgust, Anger, Contempt, None, Uncertain and Non-Face. Next, some of the categories will be explained as they are not so common. Specifically, the **None** label, which means "None of the eight emotions" [**?**] represents all the images that the annotator could not assign to any of the 8 expressions. If it existed they could, in some cases, belong to categories as shy, impressed or focused. On the other hand, the **Non-Face** refers to images in which: the face detection algorithm does not draw the bounding box where the face is located; the face is not a human face (e.g. can be a painting or an animation); in the face

there is a watermark; and, at last, the shape of the face is distorted. The choice of the label would fall in the **Uncertain** category for the situations in which the annotators were not sure about the facial expressions. For the faces categorized as a Non-face or Uncertain, it would not be feasible to continue with the annotation procedure so for these situations no value for the valence and the arousal would be attached to the respective sample.

Table 4.2: Frequency of each annotated image in each category.

Expression	**Number**
Neutral	80276
Happy	146198
Sad	29487
Surprise	16288
Fear	8191
Disgust	5264
Anger	28130
Contempt	5135
None	35322
Uncertain	13163
Non-Face	88895

4.1.2.3 Annotation in the Dimensional Model

Although this model for affect was not used in this work a brief explanation will be given. The circumplex model first introduced in [122] claims that emotional information can be characterized in a two-dimensional circular space: Arousal and Valence. As we can see in Figure 4.4 the vertical axis indicates the arousal and the horizontal one the valence. The arousal can be translated as how exciting or calming, whereas the valence represents how positive or negative is the expressed emotion. To execute this task the annotators were instructed to be able to decide where in the circumplex they would locate the images. For that, the annotators were provided with a tutorial which allowed them to have a reference and to be trained. That tutorial included an example of a circumplex from [123], in which were placed about thirty-four emotion labels for instance, worried, courageous or polite. While the process was occurring, the annotators were subjected to close monitoring which allowed them to be clarified in any situation of doubt. A specific region for each discrete expression (from the categorical model) was defined in advance in the software application (see Figure 4.3). Values of arousal or valence outside the circumplex were not admissible, so whenever the annotators tried to choose one of those values a warning message was issued, and the annotation of the respective image had to be revised. The purpose was to be as accurate as possible, thus practices as the one mentioned above prevented the occurrence of mistakes in this model.

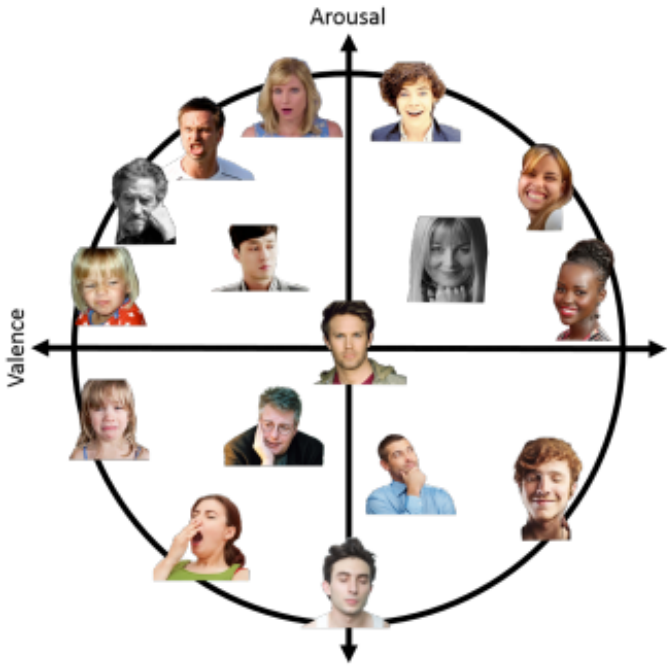

Figure 4.4: Images distributed in the Valence and Arousal dimensions of the circumplex model. From [13].

4.1.2.4 Inter-annotator agreement

The measure of the inter-annotator agreement defines how frequently the same annotation for a specific category is made by multiple annotators. This means the labelers are systematic in their annotation decision [124]. But, what is known already beforehand is that we should be aware that there is a variation in the performance of the labelers and that is what has the interest in being explored. The study of the annotation agreement among several annotators is a frequent practice because, by doing this, annotations can be authenticated and boosted, as well as the ambiguities identified. Hence, the main purpose can be achieved, and it can be made a meaningful use out of the annotations. For this dataset, 36000 samples were provided to only two annotators, those samples were labelled and the annotation agreement between them measured afterwards. To produce a reliable measurement during the whole process the annotators did not have any information about the other's choice for the annotation or even the query by which the image was found. As a result, there was an agreement in 60.7 percent of the samples (see Figure 4.5 for more details).

4.1.3 AffectNet Adapted

As it was mentioned before, the AffectNet has around 420000 samples for the manually annotated set, of which almost 300000 belonging to the expressions considered in this work. This proved to be a limitation as it was computationally heavy for the available resources. So, since the multiple attempts did not result in the desired outcome, this dataset, taken as a whole, was considered

Agreement Between Two Annotators in Categorical Model of Affect (%)

	Neutral	Happy	Sad	Surprise	Fear	Disgust	Anger	Contempt	None	Uncertain	Non-Face
Neutral	**50.8**	7.0	9.1	2.8	1.1	1.0	4.8	5.3	11.1	1.9	5.1
Happy	6.3	**79.6**	0.6	1.7	0.3	0.4	0.5	3.0	4.6	1.0	2.2
Sad	11.8	0.9	**69.7**	1.2	3.4	1.3	4.0	0.3	3.5	1.2	2.6
Surprise	2.0	3.8	1.6	**66.5**	14.0	0.8	1.9	0.6	4.2	1.9	2.7
Fear	3.1	1.5	3.8	15.3	**61.1**	2.5	7.2	0.0	1.9	0.4	3.3
Disgust	1.5	0.8	3.6	1.2	3.5	**67.6**	13.1	1.7	2.7	2.3	2.1
Anger	8.1	1.2	7.5	1.7	2.9	4.4	**62.3**	1.3	5.5	1.9	3.3
Contempt	10.2	7.5	2.1	0.5	0.5	4.4	2.1	**66.9**	3.7	1.5	0.6
None	**22.6**	12.0	14.5	8.0	6.0	2.3	16.9	1.3	9.6	4.3	2.6
Uncertain	13.5	12.1	7.8	7.3	4.0	4.5	6.2	2.6	12.3	**20.6**	8.9
Non-Face	3.7	3.8	1.7	1.1	0.9	0.4	1.7	0.4	1.2	1.4	**83.9**

Figure 4.5: Percentages of the agreement between the two annotators for the different expressions. From [13].

impractical. However, there was still a great interest in the fact that this dataset would bring the spontaneity of expressions close to a real-world setting as well as containing more than one face in one image.

For this reason, only a part of this dataset was used, containing a number of samples similar to the CK+ dataset to ensure its feasibility. Nevertheless, the creation of this subset followed the characteristics of the AffectNet. Being, the percentage of men in the images (49%), the percentage of samples for each expression (see Table 4.3), the percentage of forehead, mouth, and eye occlusions(see Table 4.4) and the percentage of other elements(see Table 4.5). These numbers were originally obtained for the AffectNet dataset by the Microsoft cognitive face API. In the end, a subset of 719 samples was created.

Table 4.3: Number of images and the correspondent percentage of each Expression on the Manually Annotated set.

Expression	**Manually Annotated Images**	**Percentage (%)**
Neutral	75374	25.83
Happy	134915	46.25
Sad	25959	8.90
Surprise	14590	5.00
Fear	6878	2.36
Disgust	4303	1.48
Anger	25382	8.70
Contempt	4250	1.48
Total	291651	100

Table 4.4: Percentage of the occlusions present in the AffectNet dataset.

Occlusion	**(%)**
Forehead	4.50
Mouth	1.08
Eye	0.49

Table 4.5: Percentage of other elements present in the images of AffectNet dataset.

Others	**(%)**
Glasses	9.63
Eye make-up	51.07
Lips make-up	41.4

4.1.4 Splitting Method: Train and Test Set

For the experiments, the datasets had to be split into two, the training and test set. In order to test how different splits would affect the final result, 5 splits were considered. The referred splits took the following proportions: 50:50, 60:40, 70:30, 80:20, 90:10. This procedure took into account the number of samples of each expression for the split. For instance, if there would be 40 samples for the happy expression and the aim was to perform a $50:50$ split, the training set would get 20 samples for that same expression and the test set the remaining 20. The procedure was the same for both the CK+ and AffectNet datasets.

4.2 Face Detector Validation

As proposed in the section 3.1, for the CK+ dataset, face detection was performed using Haar Cascades. However, a validation test was needed to justify the use of this detector. Since the AffecNet dataset provided the location of the faces in the images, a proper way of doing the validation would be comparing the annotated coordinates with the coordinates that would result from the implementation of the OpenCV[1]. approach on that same dataset.

To measure the accuracy of the face detector the evaluation metric considered was the IoU[2]. The application of this metric only depends on having a ground truth and a predicted bounding box. The ground truth corresponded to the location of faces provided with the AffectNet dataset, whereas the predicted bounding boxes were the output of the classifier. The following expression illustrates how IoU is calculated (see Figure 4.6):

$$IoU = \frac{Intersection_{area}}{Union_{area}}$$

In order to consider that a face was detected in the image, an overlap of at least 0.50 concerning IoU was necessary as this is the standard value commonly used [126]. Otherwise, it would be considered a failed detection. Additionally, if the output of the classifier corresponding to an

[1] In [13], it is only mentioned that "The OpenCV face recognition was used to detect faces in the images"

[2] IoU was used in Computer Vision for the first time in the work [125], in which it was interpreted what could be learned by the IoU loss limited to bounding boxes.

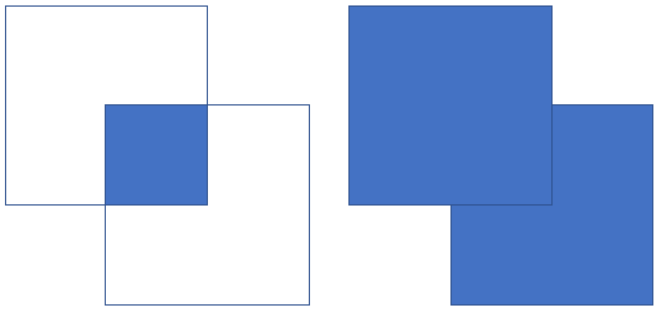

Figure 4.6: On the right, an example of the overlapping area between two objects. On the left, an example of the area of union of those objects.

empty vector of the predicting bounding box coordinates that would also be treated as a failed detection.

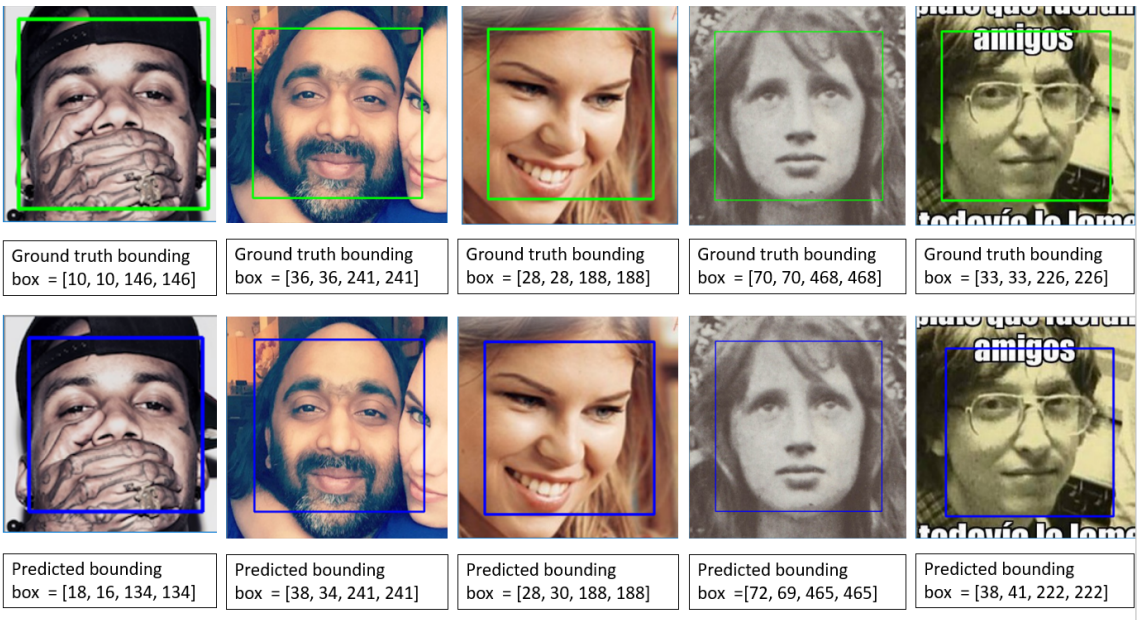

Figure 4.7: Some samples with both the representation of the ground truth and the predicted bounding boxes.

As can be seen in Figure 4.7 above when a face was detected the predicted bounding box coordinates were very close to those of the ground truth bounding box. The method was even able to detect faces in situations where there was more than one person in the same image or where there were multiple occlusions.

In contrast, Figure 4.8 addresses the cases in which the detection failed. By observing these images a few characteristics that might be the reason for the failure in the detection can be easily

Figure 4.8: Some samples in which a face could not be detected in the image.

noticed. From left to right, what stands out most:

- 1^{st} column, images containing the subject's side view of the face;
- 2^{nd} column, there's also a variation in the head pose, plus an eye occlusion;
- 3^{rd} and 4^{th} columns, the images correspond to an enlarged and cropped face, not containing a whole face;
- 5^{th} column, the rotation of the face in the upper image as well as the poor lighting in the lower one.

4.2.1 Face Detector Validation Approach Results

Primarily, the aim was to obtain vector coordinates that would define the predicted bounding box to further comparison. However, a few times this did not happen and an empty vector was returned. This has restricted the images that could potentially contain a face in 87.92%.

After this, the IoU metric could finally be calculated in 87.92% of the initially considered images. The Table 4.6 shows the mean value of the IoU, which was calculated to each image that had both the predicted bounding box and the ground truth coordinates. From those, 97.77% of the predictions corresponded to a value of the IoU superior to 0.50. This value drops to 86.89% when all the images are considered, including the ones discarded when no vector was returned.

These values mentioned above can be translated in the percentage of detected faces as the condition of having an IoU value greater than 0.50 is guaranteed. This means that from the set of images in which OpenCV performed a detection, 97.7% of the cases corresponded to face detection, whereas, when considering the whole initial set of images, 86.89% was the percentage of face detection.

Therefore, the results obtained when implementing the Haar Feature-based Cascade Classifier from the OpenCV library suggested that this approach would not be the most appropriate to be implemented on the AffectNet dataset. However, it does not discard the use on the CK+ dataset since this dataset does not contain images with settings as the shown in Figure 4.8. On the contrary, the CK+ (see Figure 4.1 and 4.2) contains face images mostly in a frontal view taken in a controlled environment where there was almost no variation in the lighting conditions. Furthermore, it was known a priori that each image contained only one face to be detected.

Table 4.6: Results of the IoU evaluation metric.

IoU	**%**
Mean value	85.53
> 0.50 (when considering the set of images in which the OpenCV approach performed a detection)	97.77
> 0.50 (when considering the whole initial set of images)	86.77

4.3 Classifier Results

Having extracted the features from the two datasets and used them as an input to the classifiers, the result of the prediction in the test set was obtained. The current section presents those results.

4.3.1 SVM Classifier Results

At this point, the SVM for classification from the machine learning package scikit-learn [127] was used. Its implementation was built upon the libsvm from [128]. This is not an easily scalable approach due to the fact that its fit time complexity is more than the square number of images. Thus, it becomes difficult to use it in a large dataset with over ten thousand images. In order to understand the influence of each parameter as well as to be able to achieve better results, the parameters of the classifier were varied in a range of values. Additionally, to manage multi-class classification an one-vs-one approach is implemented.

Parameters:

- **C -** is the control parameter that allows to effectively balance the misclassifications and the margin's width. If C corresponds to a large value, it will be avoided misclassifying the samples which will lead to a smaller margin. On the contrary, if assumes a small value the samples will be effortlessly misclassified and the margin will be enlarged. The tested C values ranged from 1 (the default value) to 100000 with increments of the exponent with base e: $1.00e+00$, $1.00e+01$, $1.00e+02$, $5.00e+02$, $1.00e+03$, $5.00e+03$, $1.00e+04$, $5.00e+04$, $1.00e+05$.

- **kernel -** it defines which type of kernel is applied. The tested kernels were linear, polynomial (poly) and radial basis function (rbf). The default kernel is the rbf.

- **gamma -** the parameter used by all the kernels except for the linear one. As this value increases it also increases the effort to precisely fit the training set. The default value for gamma is the inverse of the number of features. The gamma value ranged from the default value defined by 'auto' to 1: 'auto',$1.00e-04$, $5.00e-04$, $1.00e-03$, $5.00e-03$, $1.00e-02$, $1.00e-01$, 1.00.

- **degree -** this parameter is only considered when the kernel is the polynomial, its value corresponds to the degree of the polynomial used. The default degree is equal to 3. For this parameter were considered the following values: 1,2,3.

Table 4.7: Results for the 50:50 split using the SVM classifier.

Split (train:test)		**50:50**				
		Accuracy (%)	**Parameters**			
			C	**kernel**	**gamma**	**degree**
HOG	**CK+**	87.30	500	rbf	'auto'	-
	AffectNet	67.13	500	poly	0.0005	2
LBP	**CK+**	79.68	100	rbf	0.1	-
	AffectNet	63.51	100	linear	-	-
PCA	**CK+**	77.14	100	rbf	0.0001	-
	AffectNet	54.60	10	rbf	0.001	-

Table 4.8: Results for the 60:40 split using the SVM classifier.

Split (train:test)		**60:40**				
		Accuracy (%)	**Parameters**			
			C	**kernel**	**gamma**	**degree**
HOG	**CK+**	90.48	500	rbf	'auto'	-
	AffectNet	69.26	100	rbf	0.0005	-
LBP	**CK+**	83.33	1000	rbf	0.01	-
	AffectNet	65.37	100	rbf	0.1	-
PCA	**CK+**	79.37	1	poly	'auto'	1
	AffectNet	55.48	10	rbf	0.005	-

Table 4.9: Results for the 70:30 split using the SVM classifier.

Split (train:test)		**70:30**				
		Accuracy (%)	**Parameters**			
			C	**kernel**	**gamma**	**degree**
HOG	**CK+**	91.40	500	rbf	'auto'	-
	AffectNet	71.83	100	rbf	0.001	-
LBP	**CK+**	83.33	500	rbf	0.005	-
	AffectNet	67.61	500	rbf	0.005	-
PCA	**CK+**	79.57	1	poly	0.01	1
	AffectNet	58.22	10	rbf	0.005	-

Table 4.10: Results for the 80:20 split using the SVM classifier.

Split (train:test)		**80:20**				
		Accuracy (%)	**Parameters**			
			C	**kernel**	**gamma**	**degree**
HOG	**CK+**	94.31	500	rbf	'auto'	-
	AffectNet	72.86	1	poly	0.1	2
LBP	**CK+**	91.06	500	rbf	0.005	-
	AffectNet	67.14	100	rbf	0.01	-
PCA	**CK+**	86.18	10	poly	0.001	1
	AffectNet	60.00	100	rbf	0.001	-

Table 4.11: Results for the 90:10 split using the SVM classifier.

Split (train:test)		**90:10**				
		Accuracy (%)	**Parameters**			
			C	**kernel**	**gamma**	**degree**
HOG	**CK+**	96.55	500	poly	0.001	3
	AffectNet	70.00	1	linear	-	-
LBP	**CK+**	96.55	500	rbf	0.005	-
	AffectNet	67.14	100	rbf	0.01	-
PCA	**CK+**	93.10	10	rbf	0.0005	-
	AffectNet	57.14	10	rbf	0.005	-

Tables 4.7 to 4.11 present the obtained results for each of the considered splits. Each table depicts the outcome for the different facial features (HOG, LBP, PCA) tested on the CK+ and the AffectNet dataset. In addition, it details the parameters to which these results were obtained. Note that the accuracy values presented correspond only to the highest accuracy achieved from the implementation of the methods. However, is it important to have in mind that to obtain these values the parameters were varied; only choosing, in the end, the best result. The system's behaviour for the different values of the parameters will be analyzed below (see Appendix A for more detailed results).

Regarding the CK+ dataset, the 90:10 split generated the highest accuracy values for all the 3 algorithms (HOG, LBP, PCA). However, depending on one of those specific algorithms the parameters in use were different. On the contrary, for the AffectNet dataset the 70:30 split obtained the best result for the LBP features and the 80:20 split for the HOG and PCA.

- For both datasets, the linear kernel produced a constant result regardless the C value for the HOG and the PCA algorithm, 89.66% and 79.31% for the CK+; 71.43% and 57.86% for the AffectNet dataset. The LBP, on the other hand, despite following the constant tendency was disrupted for C equal to 10 corresponding to the peak of accuracy of 93.10%.

- For the rbf, the behaviour was similar for both datasets. For different values of C, the variation of the accuracy occurred in a similar way which suggested that this parameter had little impact on the system. In contrast, the variation of the value of gamma defined the improvement or worsening of the results. C equal to 1 was proven not to be enough to predict the images, as it presented a low accuracy specially when combined with small values of gamma. This kernel generated the highest values of accuracy when using the LBP and PCA features as the input of the SVM classifier on both datasets, for relatively small values of C and gamma.

- The third kernel tested was the polynomial which implies the variation of 3 parameters. The two already mentioned (C and gamma) and a third one exclusive for this kernel, the degree.

The results, for the CK+ and AffectNet dataset indicate that the greater the value of the degree, the greater the dependence on the other parameters to reach good accuracy values. This means that for a value of the degree equal to 1, varying the remaining parameters does not affect the outcome as much as for superior values of the degree. Except for the PCA which produces the greatest decline in the accuracy for degree values superior to 1 to which the classifier is not able to correctly predict the images.

4.3.2 RF Classifier Resuls

The RF classifier was implemented using the previously mentioned machine learning package scikit-learn. This classifier fits multiple decision trees into multiple subsets of the input set and increases the number of correctly predicted images as well as is able to better regulate overfitting by using averaging [129].

Parameters:

- **n_estimators -** The number of estimators represents the number of trees considered in the forest. The default value is 10. For the tests, this parameter ranged from 1 to 10000: 1, 100, 1000, 10000.

- **max_features -** This parameter defines the size of the subsets of features randomly generated that are to be taken into account when it is aimed to split a node. The default value for classification is the square root of the number of features defined by 'auto'. This parameter takes the value 1, 'auto' and 'None' which is the maximum number of features considered (21632 for the hog, 12544 for the LBP, 129 and 196 for the PCA on the CK+ and AffectNet respectively).

- **max_depth -** Corresponds to the maximum depth of each tree in the forest. The default value is 'None' which means that while not all the leaves are pure or possess a number of samples inferior to the value of the parameter min_samples_split, the tree continues growing.

- **min_samples_split -** In order to know when to split a node, this parameter is used. Thus, when the minimum number of samples is reached the internal node split occurs. The default value is 2.

- **min_samples_leaf -** The min_samples_leaf follows the same concept as the previous parameter. In this case, it is defined the minimum samples needed at a leaf node. The default value is 1.

In a first stage, all the parameters introduced above were considered for a range of values. The outcome from these tests suggested that varying parameters, such as min_samples_split and min_samples_leaf for values away from the default value, which is 2 and 1 respectively, would result in a poor performance. Accordingly, keeping those parameters equal to the default values together with max_depth defined as 'None' (i.e., so the trees were fully grown) proved to be a good approach. Since the default values for these parameters were the ones able to produce higher values of accuracy. To obtain the following results the previous considerations were taken into account; therefore, only the remaining parameters, n_estimators, and max_features were adjusted.

Table 4.12: Results for the 50:50 split using the RF classifier.

Split (train:test)		**50:50**		
		Accuracy (%)	**Parameters**	
			n_estimators	**max_features**
HOG	**CK+**	80.63	100	'auto'
	AffectNet	59.05	1000	'None'
LBP	**CK+**	74.60	1000	'None'
	AffectNet	57.38	1000	'None'
PCA	**CK+**	66.03	1000	'None'
	AffectNet	50.42	10000	'None'

Table 4.13: Results for the 60:40 split using the RF classifier.

Split (train:test)		**60:40**		
		Accuracy (%)	**Parameters**	
			n_estimators	**max_features**
HOG	**CK+**	80.95	1000	'auto'
	AffectNet	62.54	100	'auto'
LBP	**CK+**	75.79	10000	'None'
	AffectNet	60.78	1000	'None'
PCA	**CK+**	65.87	10000	'None'
	AffectNet	50.53	1000	'None'

Table 4.14: Results for the 70:30 split using the RF classifier.

Split (train:test)		**70:30**		
		Accuracy (%)	**Parameters**	
			n_estimators	**max_features**
HOG	**CK+**	82.26	100	'auto'
	AffectNet	64.79	1000	'None'
LBP	**CK+**	75.27	1000	'None'
	AffectNet	62.44	1000	'None'
PCA	**CK+**	67.74	1000	'None'
	AffectNet	50.23	1000	'None'

Table 4.15: Results for the 80:20 split using the RF classifier.

Split (train:test)		**80:20**		
		Accuracy (%)	**Parameters**	
			n_estimators	**max_features**
HOG	**CK+**	84.55	10000	'auto'
	AffectNet	61.43	100	'None'
LBP	**CK+**	78.86	10000	'None'
	AffectNet	<u>62.86</u>	10000	'None'
PCA	**CK+**	66.67	100	'None'
	AffectNet	52.14	100	'None'

Table 4.16: Results for the 90:10 split using the RF classifier.

Split (train:test)		**90:10**		
		Accuracy (%)	**Parameters**	
			n_estimators	**max_features**
HOG	**CK+**	<u>87.93</u>	100	'auto'
	AffectNet	61.43	100	'auto'
LBP	**CK+**	<u>79.31</u>	100	'None'
	AffectNet	57.14	1000	'auto'
PCA	**CK+**	<u>75.86</u>	100	'None'
	AffectNet	<u>57.14</u>	1000	'None'

Tables 4.12 to 4.16 show the result for each of the considered splits. The outcome is presented by each table for the considered facial features (HOG, LBP, PCA) tested on the CK+ and the AffectNet dataset. Furthermore, it specifies the parameters to which these results were obtained. Once more, the underlined values are the best results achieved for the considered methods on a specific dataset. The analysis of the variation of the RF classifier parameters made it possible to find these values of accuracy which will be presented below.

On the CK+ dataset the peak of accuracy was reached for the 90:10 split of the training and test set regardless of the input features. Conversely, for the AffectNet dataset the HOG features obtained its highest accuracy value for the 70:30 split, the LBP for the 80:20 split and the PCA for the 90:10.

The outcome of the tests using the RF classifier indicated that the accuracy values increase as the number of features considered also increases for both the CK+ and the AffectNet dataset. For the HOG, the peak of accuracy for the CK+ occurred for the default value of the max_features ($\sqrt{max\_features}$) and a relatively small number of estimators, whereas, for the AffectNet dataset the best result was for the maximum number of features and a larger value for the n_estimators. The LBP features as an input presented a good performance for values of the max_features greater than or equal to the default value ($\sqrt{max\_features} = \sqrt{12544} \approx 112$) and greater values of the n_estimators on the CK+ dataset. In contrast, the AffectNet requires the complete set of features to

achieve its best result. As well as to the HOG, when considering the PCA features the parameters variation produced approximately the same behaviour regardless of the number of estimators. Additionally, the peak of accuracy occurred for the the maximum number of features for both datasets.

4.3.3 Feature Selection Based on MI Results

To implement this approach the previously mentioned machine learning package scikit-learn was used. The purpose is the estimation of the mutual information for a discrete variable. The obtained MI's score represents a positive value, it only takes the value zero when the considered variables are independent. This algorithm is based on [130, 131].

In the previous sections some results were obtained considering the complete set of features. What was not very clear was whether all the features were needed or not to achieve those values of accuracy. Trying to provide an answer this feature selection approach was implemented for the underlined values in Tables 4.7 to 4.11 and Tables 4.12 to 4.16, using the SVM and RF classifier, respectively.

The outcome was, for the highest accuracy achieved on this study (the HOG features generated from the CK+ dataset tested on the SVM) the same accuracy value, 96.55% with only 11000 features, a reduction of almost 50% in the number of the features (21632 to 11000). For the LBP on the same dataset and classifier, it were necessary only 4000 features from the 12544 complete set to achieve 96.55% of accuracy. The AffectNet had the same behaviour in this test being able to reduce the number of features needed to keep the same value of accuracy.

The RF classifier provided an even higher performance since it was able to maintain the accuracy values as well as to reduce the number of required features. In this case, the optimal number of features for the HOG considering the CK+ was 5000 achieving the same accuracy of 87.93%. For the LBP on the same dataset the updated number of features was 1500 with an accuracy of 79.31%. For the AffectNet, the same number of features generated a slightly inferior value of accuracy.

4.3.4 Discussion

4.3.4.1 CK+

A comparison was made between the results obtained by the implemented tests and the approaches mentioned in the literature. This comparison has proved not to be as straightforward as expected since there is a shortage of information on the data involved and the evaluation process for the different literature proposals. Therefore, the obtained results were compared with other works that used approximately the same approach for the CK+ dataset. From the implemented tests the SVM classifier outperforms, by a wide margin, the RF classifier for the accuracy of the prediction of the images. The highest achieved values of accuracy were 96.55% and 87.93% for the SVM and RF classifier, respectively, when tested on the CK+ dataset. The previously mentioned results were obtained when considering the largest training set, whereas the smallest training set resulted in an accuracy of 87.30% for the SVM and 80.63% for the RF classifier. The gap between the values of accuracy for the two classifiers can be explained due to the greater influence that a small and imbalanced training set has on the RF classifier which reveals itself less able to handle this scenario in comparison to the SVM. Nugrahaeni et al. in [132] conducted a research in which the performance of these two classifiers was compared. It was observed the behaviour of the classifiers to different sizes of the training set and consistent with the present work the accuracy was increasing to larger training sets. In the paper, the increase in the accuracy for the largest training set was of 10% and 23.7% for the SVM and RF, respectively. Conversely, in their research, the RF (98.55%) surpassed the SVM (90%) for the largest training sets which were not observed in this study. However, a reason for that might be the fact that, for the SVM it was considered, in this work, beyond the linear kernel the rbf and the polynomial kernel functions which lead to better outcomes. Also, the data used in this study was significantly imbalanced which was a disadvantage for the RF classifier. As an input for the classifiers were used the HOG, LBP and PCA algorithms. The results for each implemented test can be observed in Table 4.17. Happy et al. in [62] reported a similar methodology using LBP features and the SVM for the classification, achieving an accuracy of 94.09% on the CK+ dataset. Another approach, in this case for dynamic texture recognition presented by Zhao et al. in [133] obtained an accuracy of 96.2% on that same dataset. In this paper, an LBP version was implemented combining both the appearance and motion. Regarding the HOG features, Carcagnì et al. in [63] conducted a study on the implementation of this feature extractor achieving an accuracy of 98.5% when considering the CK+ dataset. More recently, Chen et al. in [134] proposed a hierarchical random forest model to perform facial expression recognition that resulted in an accuracy of 94.3%. El Meguid in [135] proposed a framework to perform classification of facial expressions in a non-controlled scenario under the observation of cameras using RF, it achieved an accuracy of 90.26%.

Regarding the last performed test, through the implementation of a feature selection approach it was found that a significantly smaller number of features can be used and the same value of accuracy maintained. Li et al. in [136] aims to explore a MI technique which obtained an accuracy of 96.7% with only $2/3$ of features, even superior to their obtained value for the complete set of

features. Lajevardi et al. in [117] presented a study comparing different approaches to perform feature selection for an optimal number of features of 4096 and increasing its overall accuracy in approximately 5%.

Table 4.17: Summary of the best achieved results on the CK+ dataset.

	RF	**SVM**
HOG	87.93	96.55
LBP	79.31	96.55
PCA	75.86	93.10

The obtained results in this study represent a good performance of the implemented algorithms. In some cases, these results were outperformed by the literature. However, bearing in mind that this is an extensively studied topic much has been done to improve the accuracy rate. For instance, the development of improved versions of the considered algorithms is been used to obtain considerably better results. Furthermore, in this study, it was considered imbalanced data. All the facial expressions available on the CK+ dataset: anger (45), disgust (59), fear (25), happiness (69), sadness (28), surprise (83), and contempt (18), plus the neutral (309). For the studied literature in most of the cases the data was more balanced, and at least, one less facial expression was considered, this means one less class, which is likely to be translated in an increase of the accuracy rate.

4.3.4.2 AffectNet

The need to reach out to other scenarios where people were not performing the facial expressions justified the choice of the AffectNet. The goal was to add an approximation of what would have been the scenario to test these algorithms in the clinical environment application. Testing on this dataset has shown some weaknesses at first because it was not feasible to test the complete dataset, and second, as the methods implemented proved not to be robust enough to achieve accuracy values close to the ones achieved on the CK+ dataset. The best results for this dataset can be found below. They follow the same tendency as the CK+ dataset. The SVM surpasses the RF for all the considered features. Also, the HOG features as an input obtain the highest accuracy followed by the LBP and at last, the PCA whose performance is the poorest.

Conversely, in [137], a recent paper from Zeng et al., it is addressed the issue of the in-the-wild datasets, and the example of the AffectNet is given as the annotations bias on this dataset trigger inconsistent predictions. This means that for different labelled expressions it can be found similar face images and that is likely to cause the classifier to wrongly predict the expression. In [137], both the AffectNet and the CK+ were used to perform FER. Having in mind that this result can not be used to prove the consistency of the obtained results in this study for the adapted AffectNet it is still interesting to compare the obtained accuracy for both datasets when testing the same method (an end-to-end trainable network LTNet). Thus, for both the AffectNet (the complete dataset) and the CK+ dataset the achieved accuracy was 57.31% and 86.64%, respectively. This highlights

how challenging it is to perform facial expression classification on the AffectNet, an in-the-wild dataset, which is confirmed by the fact that even for the annotators this was not a straightforward task as the agreement rate between them was not more than 60.7%.

Table 4.18: Summary of the best achieved results on the AffectNet dataset.

	RF	**SVM**
HOG	64.79	72.86
LBP	62.86	67.61
PCA	57.14	60.00

Chapter 5

Conclusions and Future Work

5.1 Conclusions

Facial Expression Recognition can be seen as a trivial task, however, even humans or experience annotators have difficulties to assertively identify the expression. The present work focused on the automatic identification of expressions, by its face images.

The initial step consisted of studying the literature in order to be able to choose the most adequate methods to perform FER. Once the methods were chosen it was the moment to search for appropriate and relevant datasets which included both the images of the subjects performing different expressions and the correspondent annotated labels for the expressions in the categorical domain. This was the starting point to explore some Computer Vision techniques. One of the datasets did not provide annotations for the face localization in the image, in this case, a face detection algorithm had to be applied. Then, it were implemented methods to extract the features that were able to represent the images in the most accurate way. From those methods, the first two produced a representation for each image whereas the third one considered the whole training set to build a model of representation.

Having a good representation for the images as well as the labels, the necessary requirements to apply the classifiers were fulfilled. Those image faces could be classified in 7 different expressions, such as happiness, sadness, surprise, fear, disgust, anger, contempt and additionally, the neutral. Multiple experiments were carried out, testing the previously extracted features so it would be inspected to which features the best accuracy was achieved.

The best performance was generated by the SVM classifier when applied to the HOG features with 96.55% of accuracy for the CK+. The exact same approach achieved an accuracy of only 72.86% on the AffectNet dataset. At last, it was also found that for approximately less than 50% of the total of features these accuracy values could be kept.

The number of expressions considered together with the imbalanced sets did not allow the system to perform better. So, it would be expectable to achieve a higher value for the accuracy if fewer expressions, as well as a more balanced set, would be taken into account for the classification.

In short, the study allowed to draw some conclusions about the behaviour of a recognition system. Although these approaches achieve good performance on the CK+ dataset, they proved not to be the most adequate to deal with a dataset as the AffectNet. For that purpose, less conventional approaches would have to be considered, for instance, deep Convolutional Neural Networks, regarded as a valuable technique that allows learning straight from the images as well as take advantage of a large number of samples contained on the original AffectNet.

5.2 Future Work

Regarding the framework of this dissertation, the following steps are easy to identify. The creation of a new dataset would be the first. This new dataset would contain pictures of patients already in a clinical setting which would allow having as a starting point the subjects in the aimed environment. Having the most appropriate dataset would help to ensure that the approach was reliably enough and performed well in such a setting. This was not feasible to accomplish since this is a time-bounded project and the fact that it would be needed to record sessions with real patients raises major and complex ethical issues. The process to obtain the required authorizations would be extensive and it was not guaranteed that would result in a positive response. Also, apart from obtaining the samples, it would be also required to annotate them. For that, experienced annotators willing to perform this task would have to be found.

Secondly, as it was mentioned before, primarily deep CNNs would have to be implemented. In addition, the latest approaches and methods would have to start being explored. Again, the time constraint, as well as the computational availability, have not made it possible to study and introduce less conventional approaches.

At last, the final goal would be the application in the field and, in the case of wanting to provide the professionals with immediate feedback from the patient expressions a real-time approach would be desired. The previous steps would presumably promote this step as this would be a natural step forward.

Appendix A

Detailed Results

In this chapter, it is shown the graphs that led to the presented and discussed results in the the chapter 4.

A.1 Results in the form of graphs obtained from the use of the SVM and RF Classifiers.

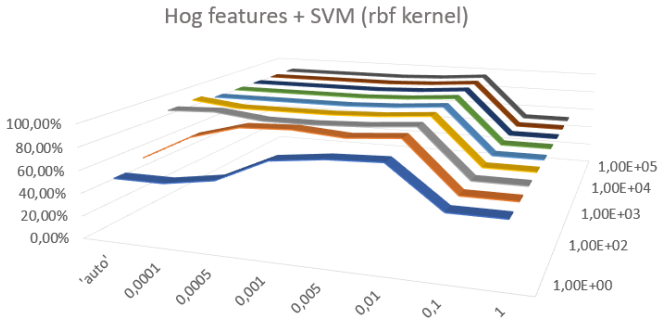

gamma

C	'auto'	0,0001	0,0005	0,001	0,005	0,01	0,1	1
1,00E+00	51,72%	51,72%	58,62%	79,31%	84,48%	86,21%	51,72%	51,72%
1,00E+01	58,62%	81,03%	93,10%	94,83%	91,38%	94,83%	51,72%	51,72%
1,00E+02	93,10%	94,83%	89,66%	89,66%	91,38%	94,83%	51,72%	51,72%
5,00E+02	94,83%	89,66%	89,66%	89,66%	91,38%	94,83%	51,72%	51,72%
1,00E+03	89,66%	89,66%	89,66%	89,66%	91,38%	94,83%	51,72%	51,72%
5,00E+03	89,66%	89,66%	89,66%	89,66%	91,38%	94,83%	51,72%	51,72%
1,00E+04	89,66%	89,66%	89,66%	89,66%	91,38%	94,83%	51,72%	51,72%
5,00E+04	89,66%	89,66%	89,66%	89,66%	91,38%	94,83%	51,72%	51,72%
1,00E+05	89,66%	89,66%	89,66%	89,66%	91,38%	94,83%	51,72%	51,72%

Figure A.1: Graph representing the HOG features from the CK+ dataset classified using the SVM classifier with a rbf kernel.

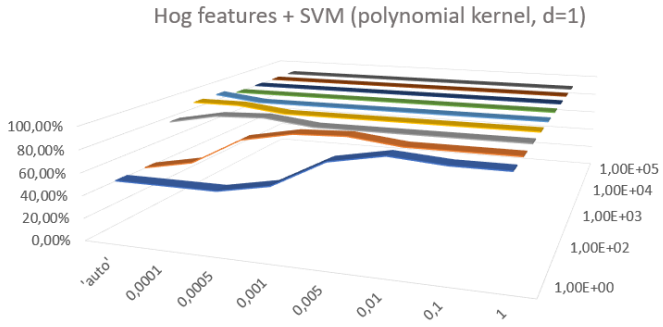

gamma

C	'auto'	0,0001	0,0005	0,001	0,005	0,01	0,1	1
1,00E+00	51,72%	51,72%	51,72%	60,34%	84,48%	93,10%	89,66%	89,66%
1,00E+012	51,72%	60,34%	84,48%	93,10%	94,83%	89,66%	89,66%	89,66%
1,00E+02	84,48%	93,10%	94,83%	89,66%	89,66%	89,66%	89,66%	89,66%
5,00E+02	94,83%	94,83%	89,66%	89,66%	89,66%	89,66%	89,66%	89,66%
1,00E+03	94,83%	89,66%	89,66%	89,66%	89,66%	89,66%	89,66%	89,66%
5,00E+03	89,66%	89,66%	89,66%	89,66%	89,66%	89,66%	89,66%	89,66%
1,00E+04	89,66%	89,66%	89,66%	89,66%	89,66%	89,66%	89,66%	89,66%
5,00E+04	89,66%	89,66%	89,66%	89,66%	89,66%	89,66%	89,66%	89,66%
1,00E+05	89,66%	89,66%	89,66%	89,66%	89,66%	89,66%	89,66%	89,66%

Figure A.2: Graph representing the HOG features from the CK+ dataset classified using the SVM classifier with a polynomial kernel (degree equal to 1).

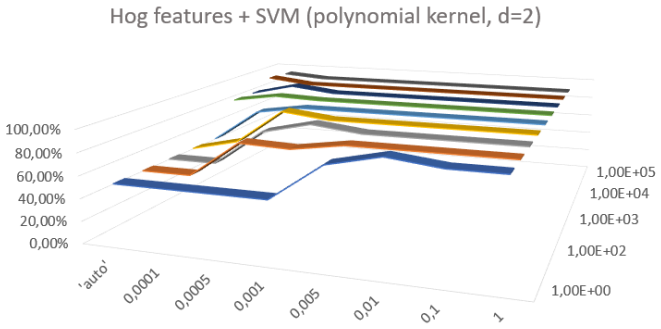

gamma

C	'auto'	0,0001	0,0005	0,001	0,005	0,01	0,1	1
1,00E+00	51,72%	51,72%	51,72%	51,72%	84,48%	94,83%	89,66%	89,66%
1,00E+012	51,72%	51,72%	84,48%	82,76%	89,66%	89,66%	89,66%	89,66%
1,00E+02	51,72%	51,72%	84,48%	94,83%	89,66%	89,66%	89,66%	89,66%
5,00E+02	51,72%	62,07%	94,83%	89,66%	89,66%	89,66%	89,66%	89,66%
1,00E+03	51,72%	82,76%	89,66%	89,66%	89,66%	89,66%	89,66%	89,66%
5,00E+03	84,48%	91,38%	89,66%	89,66%	89,66%	89,66%	89,66%	89,66%
1,00E+04	84,48%	94,83%	89,66%	89,66%	89,66%	89,66%	89,66%	89,66%
5,00E+04	94,83%	89,66%	89,66%	89,66%	89,66%	89,66%	89,66%	89,66%
1,00E+05	93,10%	89,66%	89,66%	89,66%	89,66%	89,66%	89,66%	89,66%

Figure A.3: Graph representing the HOG features from the CK+ dataset classified using the SVM classifier with a polynomial kernel (degree equal to 2).

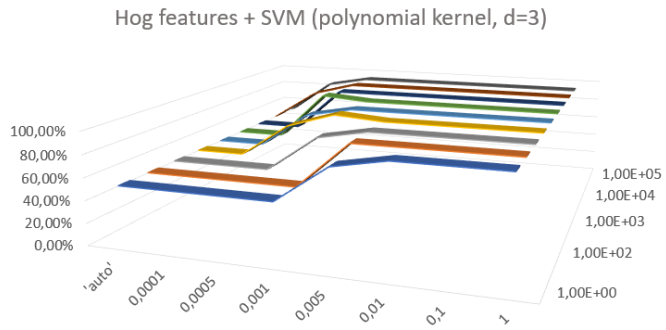

gamma

C	'auto'	0,0001	0,0005	0,001	0,005	0,01	0,1	1
1,00E+00	51,72%	51,72%	51,72%	51,72%	84,48%	93,10%	93,10%	93,10%
1,00E+012	51,72%	51,72%	51,72%	51,72%	93,10%	93,10%	93,10%	93,10%
1,00E+02	51,72%	51,72%	51,72%	84,48%	93,10%	93,10%	93,10%	93,10%
5,00E+02	51,72%	51,72%	82,76%	96,55%	93,10%	93,10%	93,10%	93,10%
1,00E+03	51,72%	51,72%	84,48%	93,10%	93,10%	93,10%	93,10%	93,10%
5,00E+03	51,72%	51,72%	96,55%	93,10%	93,10%	93,10%	93,10%	93,10%
1,00E+04	51,72%	51,72%	93,10%	93,10%	93,10%	93,10%	93,10%	93,10%
5,00E+04	51,72%	81,03%	93,10%	93,10%	93,10%	93,10%	93,10%	93,10%
1,00E+05	51,72%	84,48%	93,10%	93,10%	93,10%	93,10%	93,10%	93,10%

Figure A.4: Graph representing the HOG features from the CK+ dataset classified using the SVM classifier with a polynomial kernel (degree equal to 3).

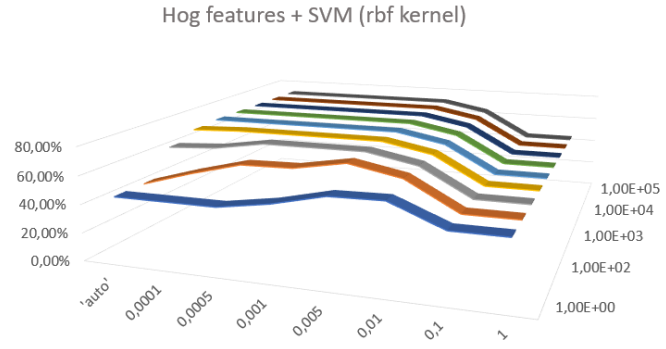

gamma

C	'auto'	0,0001	0,0005	0,001	0,005	0,01	0,1	1
1,00E+00	44,29%	44,29%	44,29%	50,00%	58,57%	59,29%	44,29%	44,29%
1,00E+01	44,29%	55,00%	64,29%	65,00%	71,43%	64,29%	44,29%	44,29%
1,00E+02	63,57%	65,71%	71,43%	71,43%	71,43%	64,29%	44,29%	44,29%
5,00E+02	70,00%	71,43%	71,43%	71,43%	71,43%	64,29%	44,29%	44,29%
1,00E+03	71,43%	71,43%	71,43%	71,43%	71,43%	64,29%	44,29%	44,29%
5,00E+03	71,43%	71,43%	71,43%	71,43%	71,43%	64,29%	44,29%	44,29%
1,00E+04	71,43%	71,43%	71,43%	71,43%	71,43%	64,29%	44,29%	44,29%
5,00E+04	71,43%	71,43%	71,43%	71,43%	71,43%	64,29%	44,29%	44,29%
1,00E+05	71,43%	71,43%	71,43%	71,43%	71,43%	64,29%	44,29%	44,29%

Figure A.5: Graph representing the HOG features from the AffectNet dataset classified using the SVM classifier with a rbf kernel.

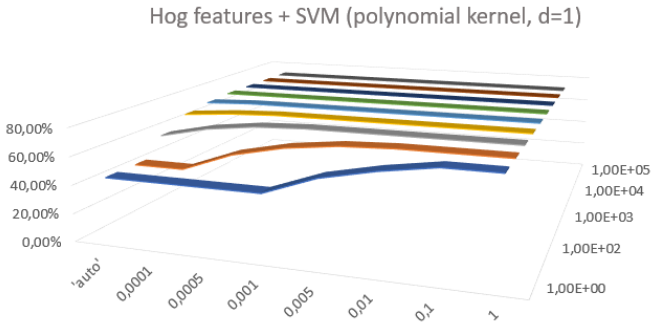

gamma

C	'auto'	0,0001	0,0005	0,001	0,005	0,01	0,1	1
1,00E+00	44,29%	44,29%	44,29%	44,29%	57,86%	65,71%	71,43%	71,43%
1,00E+01	44,29%	44,29%	57,86%	65,71%	70,00%	71,43%	71,43%	71,43%
1,00E+02	57,86%	65,71%	70,00%	71,43%	71,43%	71,43%	71,43%	71,43%
5,00E+02	67,14%	70,00%	71,43%	71,43%	71,43%	71,43%	71,43%	71,43%
1,00E+03	70,00%	71,43%	71,43%	71,43%	71,43%	71,43%	71,43%	71,43%
5,00E+03	71,43%	71,43%	71,43%	71,43%	71,43%	71,43%	71,43%	71,43%
1,00E+04	71,43%	71,43%	71,43%	71,43%	71,43%	71,43%	71,43%	71,43%
5,00E+04	71,43%	71,43%	71,43%	71,43%	71,43%	71,43%	71,43%	71,43%
1,00E+05	71,43%	71,43%	71,43%	71,43%	71,43%	71,43%	71,43%	71,43%

Figure A.6: Graph representing the HOG features from the AffectNet dataset classified using the SVM classifier with a polynomial kernel (degree equal to 1).

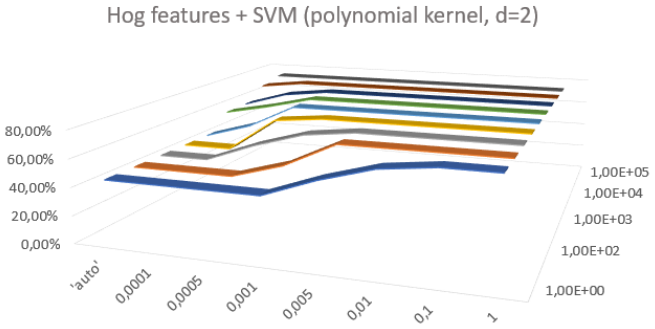

gamma

C	'auto'	0,0001	0,0005	0,001	0,005	0,01	0,1	1
1,00E+00	44,29%	44,29%	44,29%	44,29%	57,86%	68,57%	72,86%	72,86%
1,00E+01	44,29%	44,29%	44,29%	55,00%	72,86%	72,86%	72,86%	72,86%
1,00E+02	44,29%	44,29%	57,86%	68,57%	72,86%	72,86%	72,86%	72,86%
5,00E+02	44,29%	44,29%	69,29%	72,86%	72,86%	72,86%	72,86%	72,86%
1,00E+03	44,29%	55,00%	72,86%	72,86%	72,86%	72,86%	72,86%	72,86%
5,00E+03	57,14%	64,29%	72,86%	72,86%	72,86%	72,86%	72,86%	72,86%
1,00E+04	57,86%	68,57%	72,86%	72,86%	72,86%	72,86%	72,86%	72,86%
5,00E+04	68,57%	72,86%	72,86%	72,86%	72,86%	72,86%	72,86%	72,86%
1,00E+05	72,86%	72,86%	72,86%	72,86%	72,86%	72,86%	72,86%	72,86%

Figure A.7: Graph representing the HOG features from the AffectNet dataset classified using the SVM classifier with a polynomial kernel (degree equal to 2).

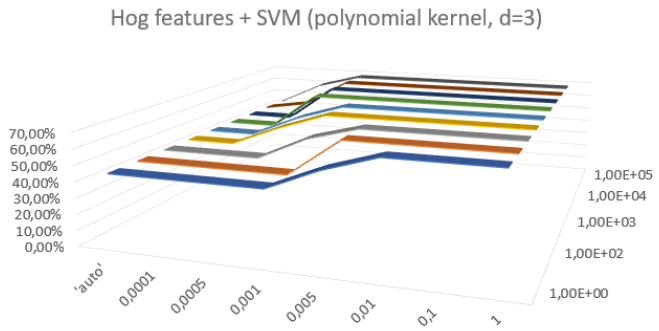

gamma

C	'auto'	0,0001	0,0005	0,001	0,005	0,01	0,1	1
1,00E+00	44,29%	44,29%	44,29%	44,29%	57,86%	67,86%	67,86%	67,86%
1,00E+012	44,29%	44,29%	44,29%	44,29%	67,86%	67,86%	67,86%	67,86%
1,00E+02	44,29%	44,29%	44,29%	59,29%	67,86%	67,86%	67,86%	67,86%
5,00E+02	44,29%	44,29%	57,14%	67,86%	67,86%	67,86%	67,86%	67,86%
1,00E+03	44,29%	44,29%	57,86%	67,86%	67,86%	67,86%	67,86%	67,86%
5,00E+03	44,29%	44,29%	67,86%	67,86%	67,86%	67,86%	67,86%	67,86%
1,00E+04	44,29%	44,29%	67,86%	67,86%	67,86%	67,86%	67,86%	67,86%
5,00E+04	44,29%	49,29%	67,86%	67,86%	67,86%	67,86%	67,86%	67,86%
1,00E+05	44,29%	59,29%	67,86%	67,86%	67,86%	67,86%	67,86%	67,86%

Figure A.8: Graph representing the HOG features from the AffectNet dataset classified using the SVM classifier with a polynomial kernel (degree equal to 3).

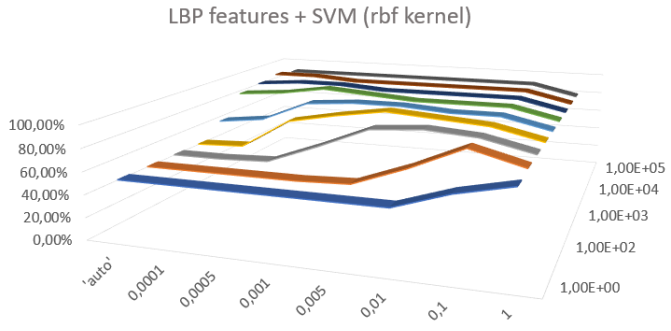

gamma

C	'auto'	0,0001	0,0005	0,001	0,005	0,01	0,1	1
1,00E+00	51,72%	51,72%	51,72%	51,72%	51,72%	51,72%	67,24%	77,59%
1,00E+01	51,72%	51,72%	51,72%	51,72%	53,45%	70,69%	91,38%	79,31%
1,00E+02	51,72%	51,72%	53,45%	70,69%	89,66%	93,10%	89,66%	79,31%
5,00E+02	51,72%	53,45%	81,03%	89,66%	96,55%	93,10%	89,66%	79,31%
1,00E+03	65,52%	70,69%	89,66%	93,10%	93,10%	89,66%	89,66%	79,31%
5,00E+03	86,21%	89,66%	96,55%	93,10%	89,66%	89,66%	89,66%	79,31%
1,00E+04	89,66%	93,10%	93,10%	89,66%	89,66%	89,66%	89,66%	79,31%
5,00E+04	93,10%	93,10%	89,66%	89,66%	89,66%	89,66%	89,66%	79,31%
1,00E+05	89,66%	89,66%	89,66%	89,66%	89,66%	89,66%	89,66%	79,31%

Figure A.9: Graph representing the LBP features from the CK+ dataset classified using the SVM classifier with a rbf kernel.

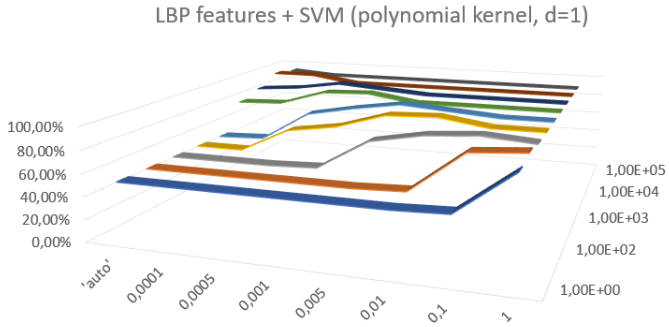

gamma

C	'auto'	0,0001	0,0005	0,001	0,005	0,01	0,1	1
1,00E+00	51,72%	51,72%	51,72%	51,72%	51,72%	51,72%	53,44%	89,66%
1,00E+01	51,72%	51,72%	51,72%	51,72%	51,72%	53,44%	89,66%	93,10%
1,00E+02	51,72%	51,72%	51,72%	53,45%	81,03%	89,66%	93,10%	89,66%
5,00E+02	51,72%	51,72%	74,14%	81,03%	94,83%	96,55%	89,66%	89,66%
1,00E+03	51,72%	53,45%	81,03%	89,66%	96,55%	93,10%	89,66%	89,66%
5,00E+03	79,31%	81,03%	94,83%	96,55%	89,66%	89,66%	89,66%	89,66%
1,00E+04	86,21%	89,66%	96,55%	93,10%	89,66%	89,66%	89,66%	89,66%
5,00E+04	96,55%	96,55%	89,66%	89,66%	89,66%	89,66%	89,66%	89,66%
1,00E+05	93,10%	89,66%	89,66%	89,66%	89,66%	89,66%	89,66%	89,66%

Figure A.10: Graph representing the LBP features from the CK+ dataset classified using the SVM classifier with a polynomial kernel (degree equal to 1).

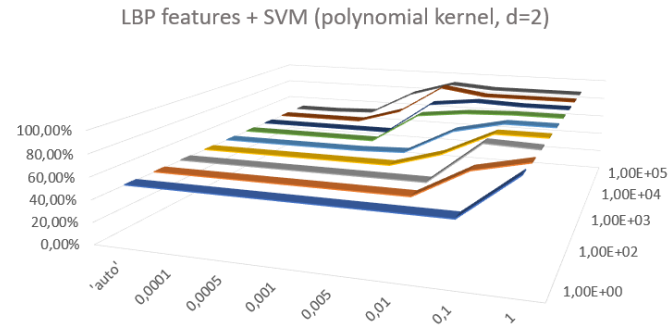

gamma

C	'auto'	0,0001	0,0005	0,001	0,005	0,01	0,1	1
1,00E+00	51,72%	51,72%	51,72%	51,72%	51,72%	51,72%	51,72%	89,66%
1,00E+01	51,72%	51,72%	51,72%	51,72%	51,72%	51,72%	77,59%	87,93%
1,00E+02	51,72%	51,72%	51,72%	51,72%	51,72%	51,72%	89,66%	87,93%
5,00E+02	51,72%	51,72%	51,72%	51,72%	51,72%	65,52%	87,93%	87,93%
1,00E+03	51,72%	51,72%	51,72%	51,72%	53,45%	77,59%	87,93%	87,93%
5,00E+03	51,72%	51,72%	51,72%	51,72%	81,03%	86,21%	87,93%	87,93%
1,00E+04	51,72%	51,72%	51,72%	51,72%	84,49%	89,66%	87,93%	87,93%
5,00E+04	51,72%	51,72%	51,72%	65,52%	94,83%	87,93%	87,93%	87,93%
1,00E+05	51,72%	51,72%	53,45%	77,59%	91,38%	87,93%	87,93%	87,93%

Figure A.11: Graph representing the LBP features from the CK+ dataset classified using the SVM classifier with a polynomial kernel (degree equal to 2).

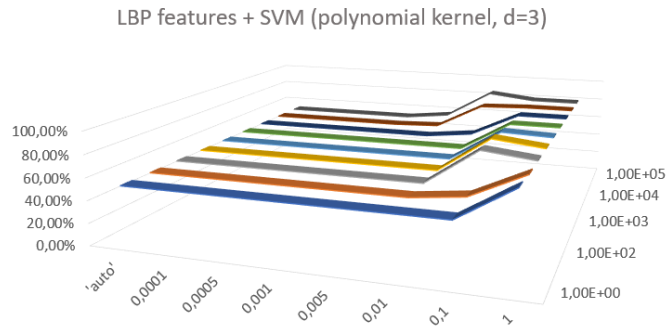

C	'auto'	0,0001	0,0005	0,001	0,005	0,01	0,1	1
1,00E+00	51,72%	51,72%	51,72%	51,72%	51,72%	51,72%	51,72%	81,03%
1,00E+012	51,72%	51,72%	51,72%	51,72%	51,72%	51,72%	56,90%	79,31%
1,00E+02	51,72%	51,72%	51,72%	51,72%	51,72%	51,72%	84,48%	79,31%
5,00E+02	51,72%	51,72%	51,72%	51,72%	51,72%	51,72%	84,48%	79,31%
1,00E+03	51,72%	51,72%	51,72%	51,72%	51,72%	51,72%	81,03%	79,31%
5,00E+03	51,72%	51,72%	51,72%	51,72%	51,72%	51,72%	79,31%	79,31%
1,00E+04	51,72%	51,72%	51,72%	51,72%	51,72%	56,90%	79,31%	79,31%
5,00E+04	51,72%	51,72%	51,72%	51,72%	53,45%	77,59%	79,31%	79,31%
1,00E+05	51,72%	51,72%	51,72%	51,72%	56,90%	84,48%	79,31%	79,31%

Figure A.12: Graph representing the LBP features from the CK+ dataset classified using the SVM classifier with a polynomial kernel (degree equal to 3).

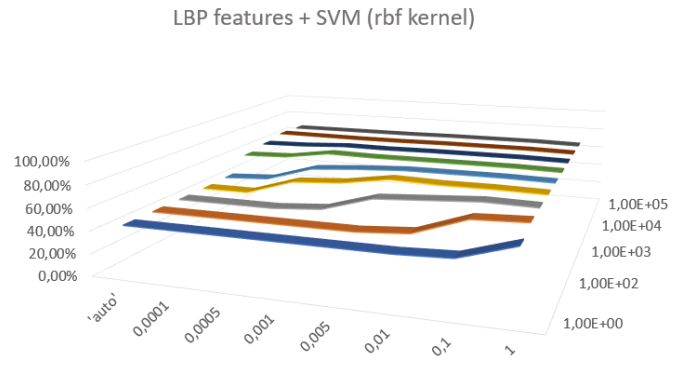

C	'auto'	0,0001	0,0005	0,001	0,005	0,01	0,1	1
1,00E+00	43,66%	43,66%	43,66%	43,66%	43,66%	43,66%	45,54%	60,09%
1,00E+01	43,66%	43,66%	43,66%	43,66%	43,66%	46,95%	63,38%	65,26%
1,00E+02	43,66%	43,66%	43,66%	46,95%	60,56%	63,38%	66,20%	65,26%
5,00E+02	43,66%	43,66%	57,75%	60,56%	67,61%	66,20%	66,20%	65,26%
1,00E+03	44,60%	46,95%	60,56%	63,85%	66,20%	66,20%	66,20%	65,26%
5,00E+03	59,15%	60,56%	67,14%	66,20%	66,20%	66,20%	66,20%	65,26%
1,00E+04	62,91%	63,85%	66,20%	65,73%	66,20%	66,20%	66,20%	65,26%
5,00E+04	66,67%	66,20%	65,73%	65,73%	66,20%	66,20%	66,20%	65,26%
1,00E+05	65,73%	65,73%	65,73%	65,73%	66,20%	66,20%	66,20%	65,26%

Figure A.13: Graph representing the LBP features from the AffectNet dataset classified using the SVM classifier with a rbf kernel.

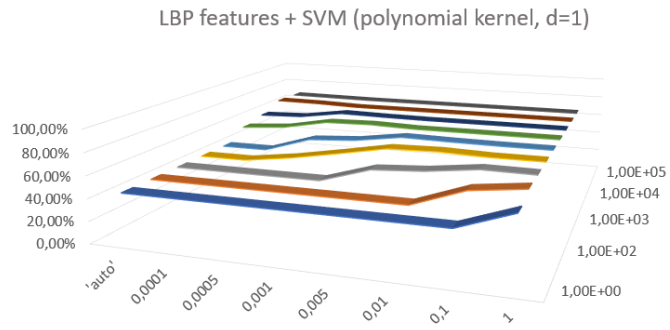

gamma

C	'auto'	0,0001	0,0005	0,001	0,005	0,01	0,1	1
1,00E+00	43,66%	43,66%	43,66%	43,66%	43,66%	43,66%	43,66%	60,56%
1,00E+012	43,66%	43,66%	43,66%	43,66%	43,66%	43,66%	60,56%	66,20%
1,00E+02	43,66%	43,66%	43,66%	43,66%	57,75%	60,56%	66,20%	65,73%
5,00E+02	43,66%	43,66%	49,77%	57,75%	66,20%	67,14%	65,73%	65,73%
1,00E+03	43,66%	43,66%	57,75%	60,56%	67,14%	66,20%	65,73%	65,73%
5,00E+03	54,46%	57,75%	66,20%	67,14%	65,73%	65,73%	65,73%	65,73%
1,00E+04	59,15%	60,56%	67,14%	66,20%	65,73%	65,73%	65,73%	65,73%
5,00E+04	67,61%	67,14%	65,73%	65,73%	65,73%	65,73%	65,73%	65,73%
1,00E+05	66,67%	66,20%	65,73%	65,73%	65,73%	65,73%	65,73%	65,73%

Figure A.14: Graph representing the LBP features from the AffectNet dataset classified using the SVM classifier with a polynomial kernel (degree equal to 1).

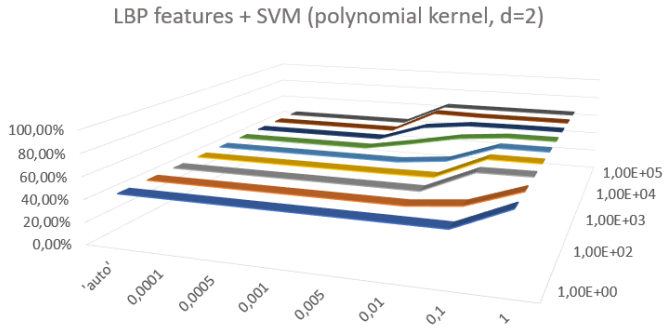

gamma

C	'auto'	0,0001	0,0005	0,001	0,005	0,01	0,1	1
1,00E+00	43,66%	43,66%	43,66%	43,66%	43,66%	43,66%	43,66%	64,32%
1,00E+01	43,66%	43,66%	43,66%	43,66%	43,66%	43,66%	48,36%	64,79%
1,00E+02	43,66%	43,66%	43,66%	43,66%	43,66%	43,66%	64,32%	64,79%
5,00E+02	43,66%	43,66%	43,66%	43,66%	43,66%	44,13%	64,79%	64,79%
1,00E+03	43,66%	43,66%	43,66%	43,66%	43,66%	48,36%	64,79%	64,79%
5,00E+03	43,66%	43,66%	43,66%	43,66%	51,64%	60,56%	64,79%	64,79%
1,00E+04	43,66%	43,66%	43,66%	43,66%	59,15%	64,32%	64,79%	64,79%
5,00E+04	43,66%	43,66%	43,66%	43,66%	65,73%	64,79%	64,79%	64,79%
1,00E+05	43,66%	43,66%	43,66%	43,66%	64,79%	64,79%	64,79%	64,79%

Figure A.15: Graph representing the LBP features from the AffectNet dataset classified using the SVM classifier with a polynomial kernel (degree equal to 2).

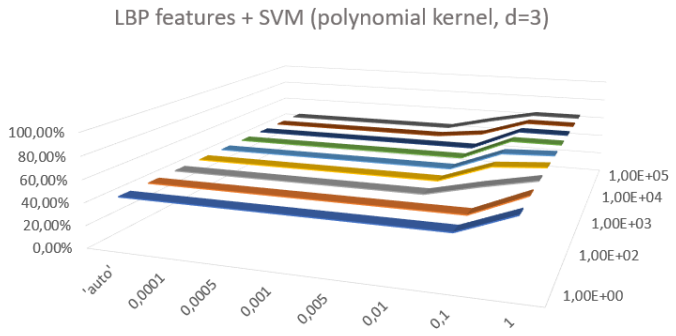

gamma

C	'auto'	0,0001	0,0005	0,001	0,005	0,01	0,1	1
1,00E+00	43,66%	43,66%	43,66%	43,66%	43,66%	43,66%	43,66%	61,97%
1,00E+01	43,66%	43,66%	43,66%	43,66%	43,66%	43,66%	43,66%	63,85%
1,00E+02	43,66%	43,66%	43,66%	43,66%	43,66%	43,66%	54,46%	63,85%
5,00E+02	43,66%	43,66%	43,66%	43,66%	43,66%	43,66%	60,56%	63,85%
1,00E+03	43,66%	43,66%	43,66%	43,66%	43,66%	43,66%	61,97%	63,85%
5,00E+03	43,66%	43,66%	43,66%	43,66%	43,66%	43,66%	63,85%	63,85%
1,00E+04	43,66%	43,66%	43,66%	43,66%	43,66%	43,66%	63,85%	63,85%
5,00E+04	43,66%	43,66%	43,66%	43,66%	43,66%	48,83%	63,85%	63,85%
1,00E+05	43,66%	43,66%	43,66%	43,66%	43,66%	54,46%	63,85%	63,85%

Figure A.16: Graph representing the LBP features from the AffectNet dataset classified using the SVM classifier with a polynomial kernel (degree equal to 3).

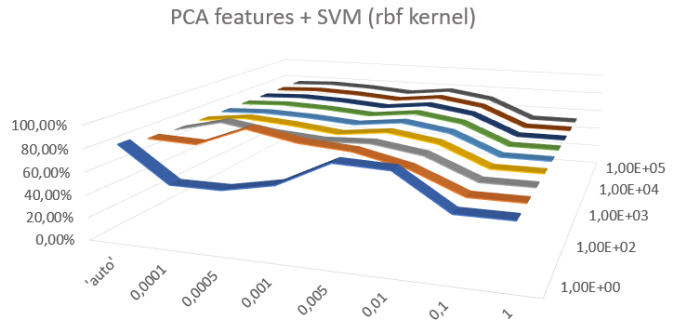

gamma

C	'auto'	0,0001	0,0005	0,001	0,005	0,01	0,1	1
1,00E+00	82,76%	51,72%	51,72%	60,34%	82,76%	81,03%	51,72%	51,72%
1,00E+01	77,59%	75,86%	93,10%	84,48%	81,03%	70,69%	51,72%	51,72%
1,00E+02	75,86%	86,21%	79,31%	75,86%	77,59%	70,69%	51,72%	51,72%
5,00E+02	75,86%	81,03%	77,59%	72,41%	77,59%	70,69%	51,72%	51,72%
1,00E+03	75,86%	77,59%	75,86%	72,41%	77,59%	70,69%	51,72%	51,72%
5,00E+03	75,86%	77,59%	75,86%	72,41%	77,59%	70,69%	51,72%	51,72%
1,00E+04	75,86%	77,59%	75,86%	72,41%	77,59%	70,69%	51,72%	51,72%
5,00E+04	75,86%	77,59%	75,86%	72,41%	77,59%	70,69%	51,72%	51,72%
1,00E+05	75,86%	77,59%	75,86%	72,41%	77,59%	70,69%	51,72%	51,72%

Figure A.17: Graph representing the PCA obtained from the CK+ dataset classified using the SVM classifier with a rbf kernel.

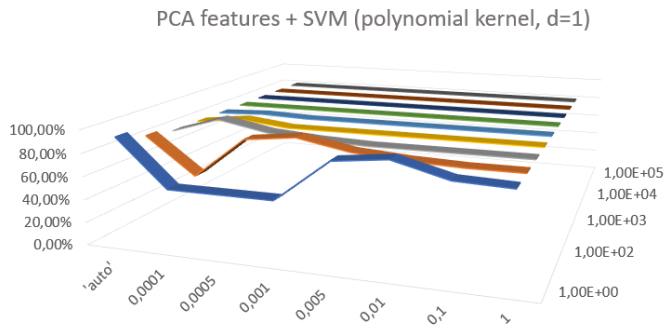

gamma

C	'auto'	0,0001	0,0005	0,001	0,005	0,01	0,1	1
1,00E+00	93,10%	51,71%	51,71%	51,71%	87,93%	93,10%	81,03%	79,31%
1,00E+01	84,48%	51,71%	87,93%	93,10%	84,48%	81,03%	79,31%	79,31%
1,00E+02	79,31%	93,10%	84,48%	81,03%	79,31%	79,31%	79,31%	79,31%
5,00E+02	79,31%	84,48%	79,31%	79,31%	79,31%	79,31%	79,31%	79,31%
1,00E+03	79,31%	81,03%	79,31%	79,31%	79,31%	79,31%	79,31%	79,31%
5,00E+03	79,31%	79,31%	79,31%	79,31%	79,31%	79,31%	79,31%	79,31%
1,00E+04	79,31%	79,31%	79,31%	79,31%	79,31%	79,31%	79,31%	79,31%
5,00E+04	79,31%	79,31%	79,31%	79,31%	79,31%	79,31%	79,31%	79,31%
1,00E+05	79,31%	79,31%	79,31%	79,31%	79,31%	79,31%	79,31%	79,31%

Figure A.18: Graph representing the PCA obtained from the CK+ dataset classified using the SVM classifier with a polynomial kernel (degree equal to 1).

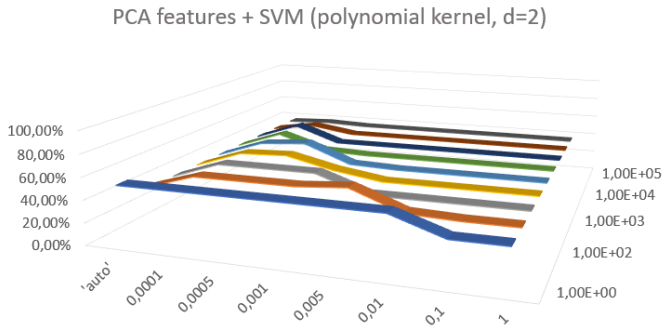

gamma

C	'auto'	0,0001	0,0005	0,001	0,005	0,01	0,1	1
1,00E+00	51,72%	51,72%	51,72%	51,72%	51,72%	51,72%	36,21%	36,21%
1,00E+01	37,93%	51,72%	51,72%	51,72%	55,17%	37,93%	36,21%	36,21%
1,00E+02	36,21%	51,72%	51,72%	51,72%	36,21%	36,21%	36,21%	36,21%
5,00E+02	36,21%	51,72%	53,45%	43,10%	36,21%	36,21%	36,21%	36,21%
1,00E+03	36,21%	51,72%	55,17%	37,93%	36,21%	36,21%	36,21%	36,21%
5,00E+03	36,21%	51,72%	37,93%	36,21%	36,21%	36,21%	36,21%	36,21%
1,00E+04	36,21%	51,72%	36,21%	36,21%	36,21%	36,21%	36,21%	36,21%
5,00E+04	36,21%	43,10%	36,21%	36,21%	36,21%	36,21%	36,21%	36,21%
1,00E+05	36,21%	37,93%	36,21%	36,21%	36,21%	36,21%	36,21%	36,21%

Figure A.19: Graph representing the PCA obtained from the CK+ dataset classified using the SVM classifier with a polynomial kernel (degree equal to 2).

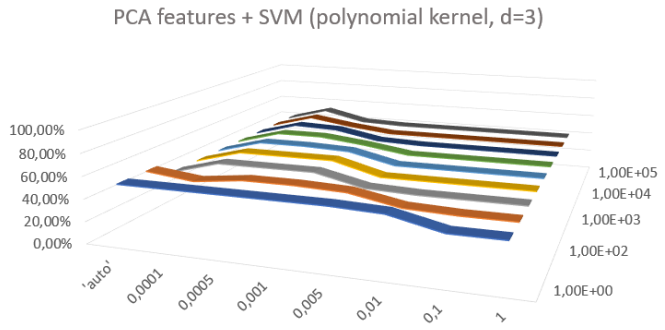

gamma

C	'auto'	0,0001	0,0005	0,001	0,005	0,01	0,1	1
1,00E+00	51,72%	51,72%	51,72%	51,72%	51,72%	50,00%	39,66%	39,66%
1,00E+01	51,72%	46,55%	51,72%	51,72%	50,00%	41,38%	39,66%	39,66%
1,00E+02	39,66%	51,72%	51,72%	51,72%	41,38%	39,66%	39,66%	39,66%
5,00E+02	39,66%	51,72%	51,72%	51,72%	39,66%	39,66%	39,66%	39,66%
1,00E+03	39,66%	51,72%	51,72%	50,00%	39,66%	39,66%	39,66%	39,66%
5,00E+03	39,66%	51,72%	51,72%	46,55%	39,66%	39,66%	39,66%	39,66%
1,00E+04	39,66%	51,72%	50,00%	41,38%	39,66%	39,66%	39,66%	39,66%
5,00E+04	39,66%	51,72%	44,83%	39,66%	39,66%	39,66%	39,66%	39,66%
1,00E+05	39,66%	51,72%	41,38%	39,66%	39,66%	39,66%	39,66%	39,66%

Figure A.20: Graph representing the PCA obtained from the CK+ dataset classified using the SVM classifier with a polynomial kernel (degree equal to 3).

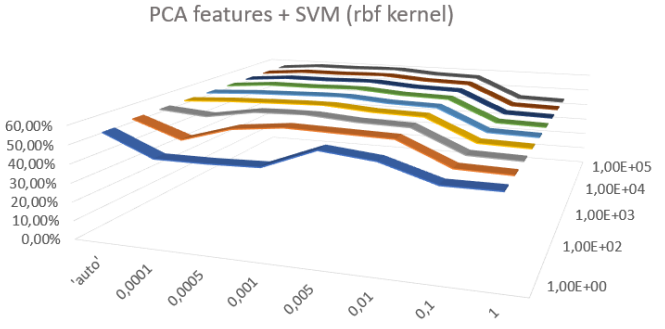

gamma

C	'auto'	0,0001	0,0005	0,001	0,005	0,01	0,1	1
1,00E+00	55,71%	44,29%	44,29%	45,00%	55,71%	52,86%	44,29%	44,29%
1,00E+01	57,14%	47,86%	55,71%	58,57%	57,86%	57,14%	45,00%	44,29%
1,00E+02	57,14%	55,00%	59,29%	60,00%	57,86%	57,14%	45,00%	44,29%
5,00E+02	57,14%	58,57%	59,29%	60,00%	57,86%	57,14%	45,00%	44,29%
1,00E+03	57,14%	58,57%	59,29%	60,00%	57,86%	57,14%	45,00%	44,29%
5,00E+03	57,14%	59,29%	59,29%	60,00%	57,86%	57,14%	45,00%	44,29%
1,00E+04	57,14%	59,29%	59,29%	60,00%	57,86%	57,14%	45,00%	44,29%
5,00E+04	57,14%	59,29%	59,29%	60,00%	57,86%	57,14%	45,00%	44,29%
1,00E+05	57,14%	59,29%	59,29%	60,00%	57,86%	57,14%	45,00%	44,29%

Figure A.21: Graph representing the PCA obtained from the AffectNet dataset classified using the SVM classifier with a rbf kernel.

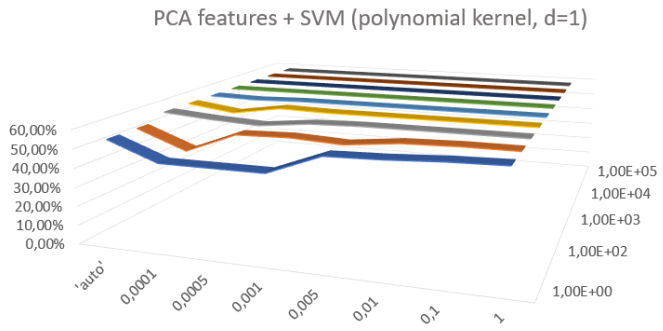

gamma

C	'auto'	0,0001	0,0005	0,001	0,005	0,01	0,1	1
1,00E+00	54,29%	44,29%	44,29%	44,29%	55,00%	55,71%	57,14%	57,86%
1,00E+01	54,29%	44,29%	55,00%	55,71%	54,29%	57,14%	57,86%	57,86%
1,00E+02	57,86%	55,71%	54,29%	57,14%	57,86%	57,86%	57,86%	57,86%
5,00E+02	57,86%	54,29%	58,57%	57,86%	57,86%	57,86%	57,86%	57,86%
1,00E+03	57,86%	57,14%	57,86%	57,86%	57,86%	57,86%	57,86%	57,86%
5,00E+03	57,86%	57,86%	57,86%	57,86%	57,86%	57,86%	57,86%	57,86%
1,00E+04	57,86%	57,86%	57,86%	57,86%	57,86%	57,86%	57,86%	57,86%
5,00E+04	57,86%	57,86%	57,86%	57,86%	57,86%	57,86%	57,86%	57,86%
1,00E+05	57,86%	57,86%	57,86%	57,86%	57,86%	57,86%	57,86%	57,86%

Figure A.22: Graph representing the PCA obtained from the AffectNet dataset classified using the SVM classifier with a polynomial kernel (degree equal to 1).

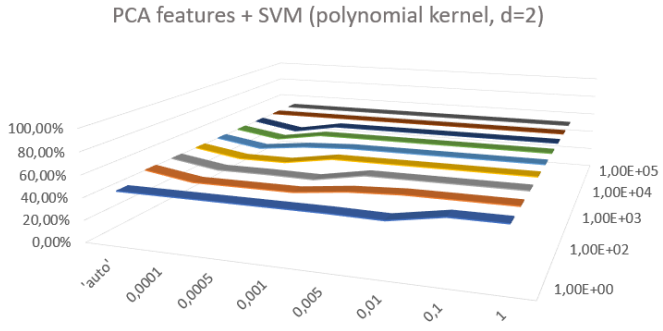

gamma

C	'auto'	0,0001	0,0005	0,001	0,005	0,01	0,1	1
1,00E+00	44,29%	44,29%	44,29%	44,29%	44,29%	43,57%	51,43%	51,43%
1,00E+01	51,43%	44,29%	44,29%	44,29%	49,29%	51,43%	51,43%	51,43%
1,00E+02	51,43%	44,29%	44,29%	43,57%	51,43%	51,43%	51,43%	51,43%
5,00E+02	51,43%	44,29%	44,29%	51,43%	51,43%	51,43%	51,43%	51,43%
1,00E+03	51,43%	44,29%	49,29%	51,43%	51,43%	51,43%	51,43%	51,43%
5,00E+03	51,43%	44,29%	51,43%	51,43%	51,43%	51,43%	51,43%	51,43%
1,00E+04	51,43%	43,57%	51,43%	51,43%	51,43%	51,43%	51,43%	51,43%
5,00E+04	51,43%	51,43%	51,43%	51,43%	51,43%	51,43%	51,43%	51,43%
1,00E+05	51,43%	51,43%	51,43%	51,43%	51,43%	51,43%	51,43%	51,43%

Figure A.23: Graph representing the PCA obtained from the AffectNet dataset classified using the SVM classifier with a polynomial kernel (degree equal to 2).

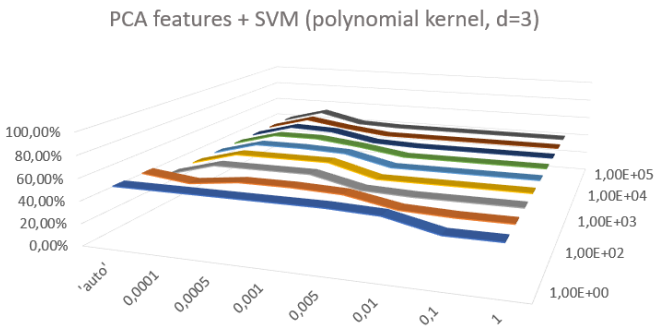

gamma

C	'auto'	0,0001	0,0005	0,001	0,005	0,01	0,1	1
1,00E+00	51,72%	51,72%	51,72%	51,72%	51,72%	50,00%	39,66%	39,66%
1,00E+01	51,72%	46,55%	51,72%	51,72%	50,00%	41,38%	39,66%	39,66%
1,00E+02	39,66%	51,72%	51,72%	51,72%	41,38%	39,66%	39,66%	39,66%
5,00E+02	39,66%	51,72%	51,72%	51,72%	39,66%	39,66%	39,66%	39,66%
1,00E+03	39,66%	51,72%	51,72%	50,00%	39,66%	39,66%	39,66%	39,66%
5,00E+03	39,66%	51,72%	51,72%	46,55%	39,66%	39,66%	39,66%	39,66%
1,00E+04	39,66%	51,72%	50,00%	41,38%	39,66%	39,66%	39,66%	39,66%
5,00E+04	39,66%	51,72%	44,83%	39,66%	39,66%	39,66%	39,66%	39,66%
1,00E+05	39,66%	51,72%	41,38%	39,66%	39,66%	39,66%	39,66%	39,66%

Figure A.24: Graph representing the PCA obtained from the AffectNet classified using the SVM classifier with a polynomial kernel (degree equal to 3).

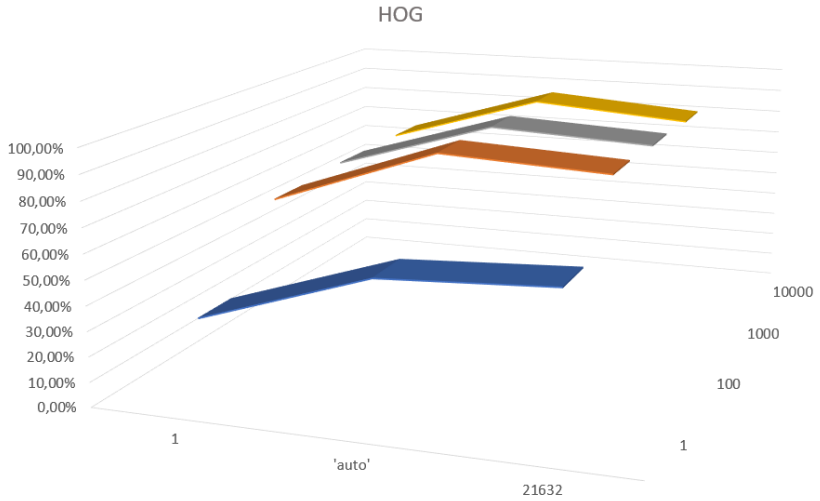

max_features

n_estimators	1	'auto'	21632
1	32,76%	55,17%	58,62%
100	63,79%	87,93%	84,48%
1000	65,52%	86,21%	82,76%
10000	65,52%	86,21%	81,03%

Figure A.25: Graph representing the HOG features from the CK+ dataset classified using the RF classifier.

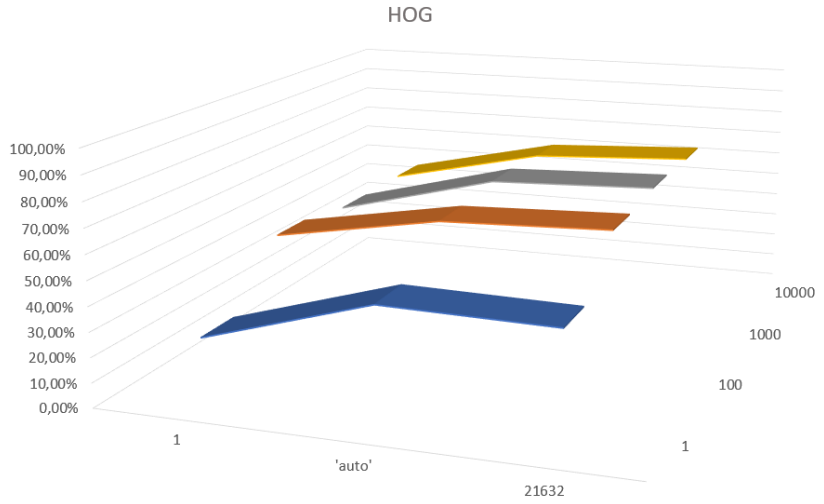

max_features

n_estimators	1	'auto'	21632
1	25,35%	45,54%	44,13%
100	48,83%	60,56%	62,91%
1000	45,07%	62,44%	64,79%
10000	45,54%	60,56%	63,85%

Figure A.26: Graph representing the HOG features from the AffectNet dataset classified using the RF classifier.

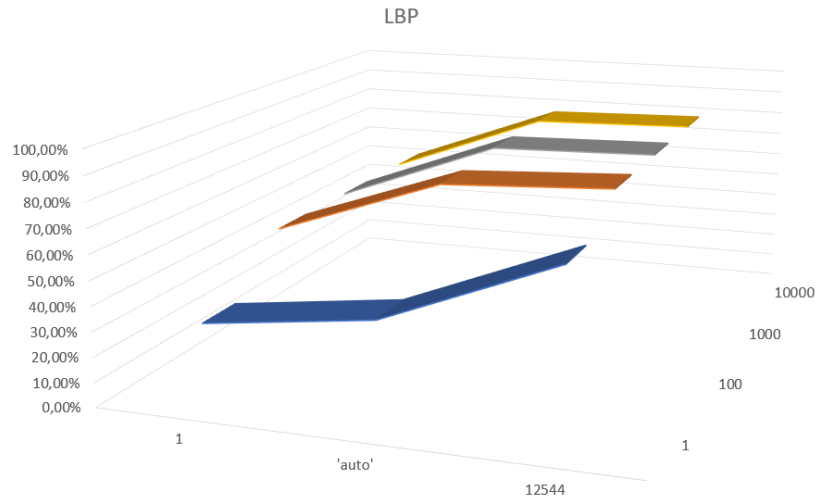

max_features

n_estimators	1	'auto'	12544
1	31,03%	39,66%	67,24%
100	51,72%	75,86%	79,31%
1000	51,72%	77,59%	79,31%
10000	51,72%	77,59%	79,31%

Figure A.27: Graph representing the LBP features from the CK+ dataset classified using the RF classifier.

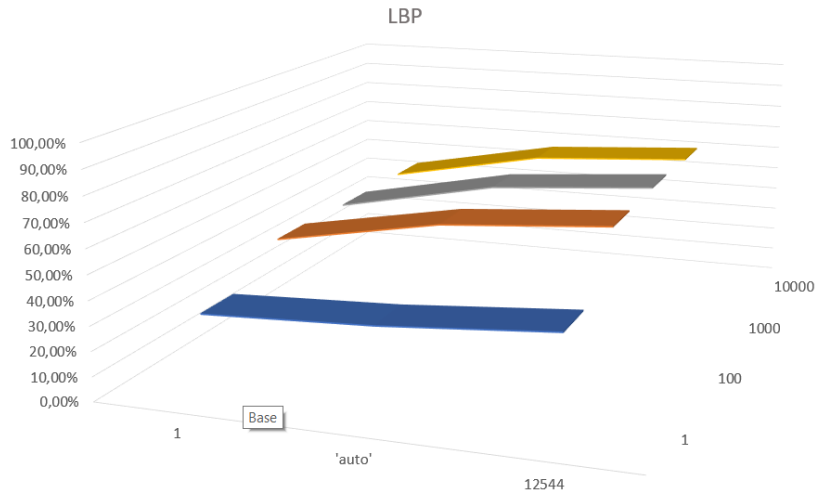

max_features

n_estimators	1	'auto'	12544
1	32,39%	35,21%	40,38%
100	44,60%	56,81%	61,97%
1000	43,66%	57,28%	62,44%
10000	43,66%	56,81%	61,03%

Figure A.28: Graph representing the LBP features from the AffectNet dataset classified using the RF classifier.

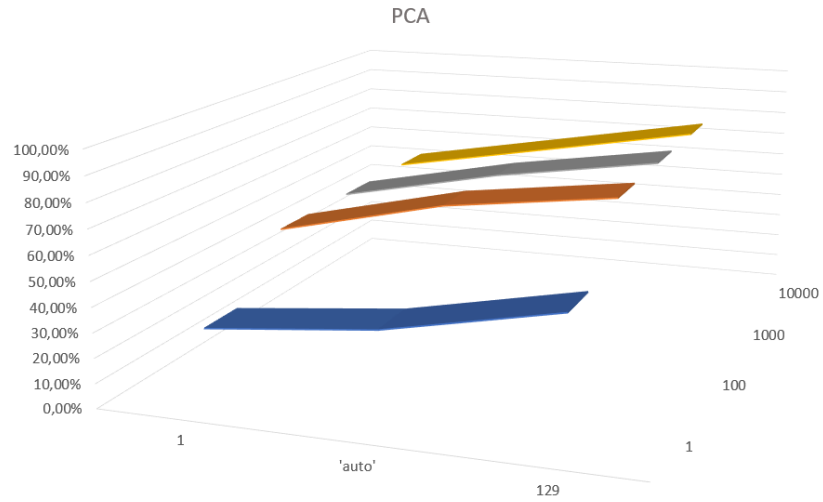

max_features

n_estimators	1	'auto'	129
1	29,31%	36,21%	50,00%
100	51,72%	67,24%	75,86%
1000	51,72%	65,52%	75,86%
10000	51,72%	63,79%	75,86%

Figure A.29: Graph representing the PCA obtained from the CK+ dataset classified using the RF classifier.

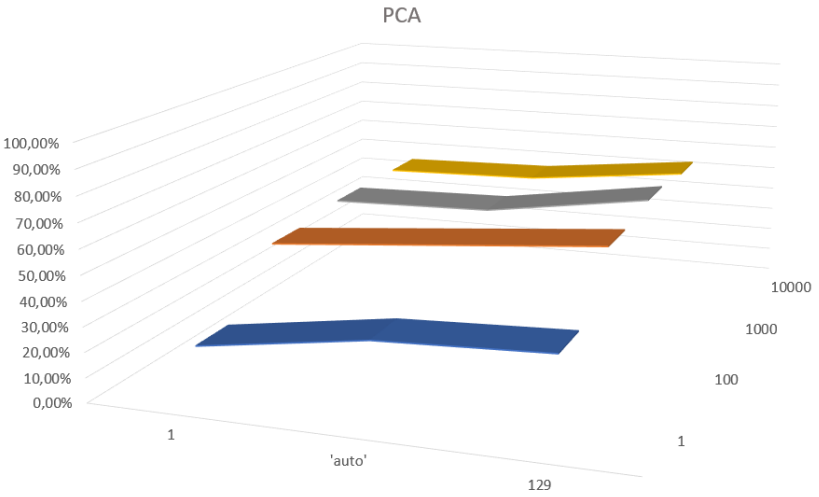

max_features

n_estimators	1	'auto'	129
1	20,00%	30,00%	32,86%
100	42,86%	48,57%	54,28%
1000	45,71%	47,14%	57,14%
10000	45,71%	47,14%	54,29%

Figure A.30: Graph representing the PCA obtained from the AffectNet dataset classified using the RF classifier.

References

[1] DCMA. Diagram body of anatomy. URL: https://anatomybodydiagram.com [last accessed 19.01.2019].

[2] Ciprian Adrian Corneanu, Marc Oliu Simón, Jeffrey F Cohn, and Sergio Escalera Guerrero. Survey on rgb, 3d, thermal, and multimodal approaches for facial expression recognition: History, trends, and affect-related applications. *IEEE transactions on pattern analysis and machine intelligence*, 38(8):1548–1568, 2016.

[3] Y-I Tian, Takeo Kanade, and Jeffrey F Cohn. Recognizing action units for facial expression analysis. *IEEE Transactions on pattern analysis and machine intelligence*, 23(2):97–115, 2001.

[4] C. A. Corneanu, M. O. Simon, J. F. Cohn, and S. E. Guerrero. Survey on rgb, 3d, thermal, and multimodal approaches for facial expression recognition: History, trends, and affect-related applications. *IEEE Transactions on Pattern Analysis Machine Intelligence*, 38(8):1548–1568, Aug. 2016. URL: doi.ieeecomputersociety.org/10.1109/TPAMI.2016.2515606, doi:10.1109/TPAMI.2016.2515606.

[5] Mario Rojas, David Masip, Alexander Todorov, and Jordi Vitria. Automatic prediction of facial trait judgments: Appearance vs. structural models. *PloS one*, 6(8):e23323, 2011.

[6] Matti Pietikäinen, Abdenour Hadid, Guoying Zhao, and Timo Ahonen. Local binary patterns for still images. In *Computer vision using local binary patterns*, pages 13–47. Springer, 2011.

[7] OpenCV. Face recognition with opencv. URL: https://docs.opencv.org/2.4/modules/contrib/doc/facerec/facerec_tutorial.html [last accessed 07.01.2019].

[8] Paul Viola and Michael Jones. Rapid object detection using a boosted cascade of simple features. In *Computer Vision and Pattern Recognition, 2001. CVPR 2001. Proceedings of the 2001 IEEE Computer Society Conference on*, volume 1, pages I–I. IEEE, 2001.

[9] Derek Bradley and Gerhard Roth. Adaptive thresholding using the integral image. *Journal of graphics tools*, 12(2):13–21, 2007.

[10] Alfred V Aho and John E Hopcroft. *The design and analysis of computer algorithms*. Pearson Education India, 1974.

[11] Patrick Lucey, Jeffrey F Cohn, Takeo Kanade, Jason Saragih, Zara Ambadar, and Iain Matthews. The extended cohn-kanade dataset (ck+): A complete dataset for action unit and emotion-specified expression. In *Computer Vision and Pattern Recognition Workshops (CVPRW), 2010 IEEE Computer Society Conference on*, pages 94–101. IEEE, 2010.

[12] C Anitha, MK Venkatesha, and B Suryanarayana Adiga. A survey on facial expression databases. *International Journal of Engineering Science and Technology*, 2(10):5158–5174, 2010.

[13] Ali Mollahosseini, Behzad Hasani, and Mohammad H Mahoor. Affectnet: A database for facial expression, valence, and arousal computing in the wild. *arXiv preprint arXiv:1708.03985*, 2017.

[14] Evangelos Sariyanidi, Hatice Gunes, and Andrea Cavallaro. Automatic analysis of facial affect: A survey of registration, representation, and recognition. *IEEE transactions on pattern analysis and machine intelligence*, 37(6):1113–1133, 2015.

[15] World Cancer Research Fund International. World cancer research fund. URL: https://www.wcrf.org/dietandcancer/cancer-trends/breast-cancer-statistics [last accessed 21.01.2019].

[16] Kenneth M Prkachin. Assessing pain by facial expression: facial expression as nexus. *Pain Research and Management*, 14(1):53–58, 2009.

[17] Paul Ekman and Harriet Oster. Facial expressions of emotion. *Annual review of psychology*, 30(1):527–554, 1979.

[18] Philipp Michel. Support vector machines in automated emotion classification. *Churchill College, June*, 2003.

[19] P Ekman. Basic emotions, handbook of cognition and emotion (pp. 45±60), 1999.

[20] Daniel Piepers and Rachel Robbins. A review and clarification of the terms "holistic,""configural," and "relational" in the face perception literature. *Frontiers in psychology*, 3:559, 2012.

[21] Karsten Wolf. Measuring facial expression of emotion. *Dialogues in clinical neuroscience*, 17(4):457, 2015.

[22] H Davies, I Wolz, J Leppanen, F Fernandez-Aranda, U Schmidt, and K Tchanturia. Facial expression to emotional stimuli in non-psychotic disorders: A systematic review and meta-analysis. *Neuroscience & Biobehavioral Reviews*, 64:252–271, 2016.

[23] Ying Jiang. Measuring facial expression and emotional experience under diverse social context in a negative emotional setting. *Measuring Behavior 2014*, 2014.

[24] Carl-Herman Hjortsjö. *Man's face and mimic language*. Studen litteratur, 1969.

[25] E Friesen and P Ekman. Facial action coding system: a technique for the measurement of facial movement. *Palo Alto*, 1978.

[26] P EKMAN-WV FRIESEN-JC HAGER. Facial action coding system. the manual on cd rom, 2002.

[27] Ying-li Tian, Takeo Kanade, and Jeffrey F Cohn. Recognizing lower face action units for facial expression analysis. In *Automatic face and gesture recognition, 2000. proceedings. fourth ieee international conference on*, pages 484–490. IEEE, 2000.

[28] Shichuan Du and Aleix M Martinez. Compound facial expressions of emotion: from basic research to clinical applications. *Dialogues in clinical neuroscience*, 17(4):443, 2015.

[29] Michael A Sayette, Jeffrey F Cohn, Joan M Wertz, Michael A Perrott, and Dominic J Parrott. A psychometric evaluation of the facial action coding system for assessing spontaneous expression. *Journal of Nonverbal Behavior*, 25(3):167–185, 2001.

[30] Paul Ekman and Erika L Rosenberg. *What the face reveals: Basic and applied studies of spontaneous expression using the Facial Action Coding System (FACS)*. Oxford University Press, USA, 1997.

[31] Zoran Duric, Wayne D Gray, Ric Heishman, Fayin Li, Azriel Rosenfeld, Michael J Schoelles, Christian Schunn, and Harry Wechsler. Integrating perceptual and cognitive modeling for adaptive and intelligent human-computer interaction. *Proceedings of the IEEE*, 90(7):1272–1289, 2002.

[32] Hiroshi Ishiguro, Tetsuo Ono, Michita Imai, Takeshi Maeda, Takayuki Kanda, and Ryohei Nakatsu. Robovie: an interactive humanoid robot. *Industrial robot: An international journal*, 28(6):498–504, 2001.

[33] Patrick Lucey, Jeffrey F Cohn, Iain Matthews, Simon Lucey, Sridha Sridharan, Jessica Howlett, and Kenneth M Prkachin. Automatically detecting pain in video through facial action units. *IEEE Transactions on Systems, Man, and Cybernetics, Part B (Cybernetics)*, 41(3):664–674, 2011.

[34] Sebastian Kaltwang, Ognjen Rudovic, and Maja Pantic. Continuous pain intensity estimation from facial expressions. In *International Symposium on Visual Computing*, pages 368–377. Springer, 2012.

[35] Esra Vural, Müjdat Çetin, Aytül Erçil, Gwen Littlewort, Marian Bartlett, and Javier Movellan. Automated drowsiness detection for improved driving safety. 2008.

[36] Ashok Samal and Prasana A Iyengar. Automatic recognition and analysis of human faces and facial expressions: A survey. *Pattern recognition*, 25(1):65–77, 1992.

[37] Maja Pantic and Leon J. M. Rothkrantz. Automatic analysis of facial expressions: The state of the art. *IEEE Transactions on pattern analysis and machine intelligence*, 22(12):1424–1445, 2000.

[38] Beat Fasel and Juergen Luettin. Automatic facial expression analysis: a survey. *Pattern recognition*, 36(1):259–275, 2003.

[39] Masakazu Matsugu, Katsuhiko Mori, Yusuke Mitari, and Yuji Kaneda. Subject independent facial expression recognition with robust face detection using a convolutional neural network. *Neural Networks*, 16(5-6):555–559, 2003.

[40] Motoi Suwa. A preliminary note on pattern recognition of human emotional expression. In *Proc. of The 4th International Joint Conference on Pattern Recognition*, pages 408–410, 1978.

[41] Zhihong Zeng, Maja Pantic, Glenn I Roisman, and Thomas S Huang. A survey of affect recognition methods: Audio, visual, and spontaneous expressions. *IEEE transactions on pattern analysis and machine intelligence*, 31(1):39–58, 2009.

[42] Dhwani Mehta, Mohammad Faridul Haque Siddiqui, and Ahmad Y Javaid. Facial emotion recognition: A survey and real-world user experiences in mixed reality. *Sensors*, 18(2):416, 2018.

[43] Proyecto Fin De Carrera and Ion Marques. Face recognition algorithms. *Master's thesis in Computer Science, Universidad Euskal Herriko*, 2010.

[44] Richard E Bellman. *Adaptive control processes: a guided tour*, volume 2045. Princeton university press, 2015.

[45] Jundong Li, Kewei Cheng, Suhang Wang, Fred Morstatter, Robert P Trevino, Jiliang Tang, and Huan Liu. Feature selection: A data perspective. *ACM Computing Surveys (CSUR)*, 50(6):94, 2018.

[46] S Dhall and P Sethi. Geometric and appearance feature analysis for facial expression recognition. *International Journal of Advanced Engineering Technology*, 7(111):01–11, 2014.

[47] Girish Chandrashekar and Ferat Sahin. A survey on feature selection methods. *Computers & Electrical Engineering*, 40(1):16–28, 2014.

[48] Ron Kohavi and George H John. Wrappers for feature subset selection. *Artificial intelligence*, 97(1-2):273–324, 1997.

[49] Isabelle Guyon and André Elisseeff. An introduction to variable and feature selection. *Journal of machine learning research*, 3(Mar):1157–1182, 2003.

[50] George Forman. An extensive empirical study of feature selection metrics for text classification. *Journal of machine learning research*, 3(Mar):1289–1305, 2003.

[51] Marko Robnik-Šikonja and Igor Kononenko. Theoretical and empirical analysis of relieff and rrelieff. *Machine learning*, 53(1-2):23–69, 2003.

[52] Quanquan Gu, Zhenhui Li, and Jiawei Han. Generalized fisher score for feature selection. *arXiv preprint arXiv:1202.3725*, 2012.

[53] Hanchuan Peng, Fuhui Long, and Chris Ding. Feature selection based on mutual information criteria of max-dependency, max-relevance, and min-redundancy. *IEEE Transactions on pattern analysis and machine intelligence*, 27(8):1226–1238, 2005.

[54] Jiliang Tang, Salem Alelyani, and Huan Liu. Feature selection for classification: A review. *Data classification: Algorithms and applications*, page 37, 2014.

[55] Robert Tibshirani. Regression shrinkage and selection via the lasso. *Journal of the Royal Statistical Society. Series B (Methodological)*, pages 267–288, 1996.

[56] Hui Zou and Trevor Hastie. Regularization and variable selection via the elastic net. *Journal of the Royal Statistical Society: Series B (Statistical Methodology)*, 67(2):301–320, 2005.

[57] Aleix Martinez and Shichuan Du. A model of the perception of facial expressions of emotion by humans: Research overview and perspectives. *Journal of Machine Learning Research*, 13(May):1589–1608, 2012.

[58] Zhengyou Zhang, Michael Lyons, Michael Schuster, and Shigeru Akamatsu. Comparison between geometry-based and gabor-wavelets-based facial expression recognition using multi-layer perceptron. In *Automatic Face and Gesture Recognition, 1998. Proceedings. Third IEEE International Conference on*, pages 454–459. IEEE, 1998.

[59] Karan Sikka, Abhinav Dhall, and Marian Bartlett. Exemplar hidden markov models for classification of facial expressions in videos. In *Proceedings of the IEEE Conference on Computer Vision and Pattern Recognition Workshops*, pages 18–25, 2015.

[60] S Mahto and Y Yadav. A survey on various facial expression recognition techniques. *Int. J. Adv. Res. Electr., Electron. Instrum. Eng*, 3:13028–13031, 2014.

[61] Alka Gupta and ML Garg. A human emotion recognition system using supervised self-organising maps. In *Computing for Sustainable Global Development (INDIACom), 2014 International Conference on*, pages 654–659. IEEE, 2014.

[62] SL Happy and Aurobinda Routray. Automatic facial expression recognition using features of salient facial patches. *IEEE transactions on Affective Computing*, 6(1):1–12, 2015.

[63] Pierluigi Carcagnì, Marco Del Coco, Marco Leo, and Cosimo Distante. Facial expression recognition and histograms of oriented gradients: a comprehensive study. *SpringerPlus*, 4(1):645, 2015.

[64] Caifeng Shan, Shaogang Gong, and Peter W McOwan. Facial expression recognition based on local binary patterns: A comprehensive study. *Image and vision Computing*, 27(6):803–816, 2009.

[65] Ju Jia, Yan Xu, Sida Zhang, and Xianglong Xue. The facial expression recognition method of random forest based on improved pca extracting feature. In *Signal Processing, Communications and Computing (ICSPCC), 2016 IEEE International Conference on*, pages 1–5. IEEE, 2016.

[66] Michel F Valstar, Bihan Jiang, Marc Mehu, Maja Pantic, and Klaus Scherer. The first facial expression recognition and analysis challenge. In *Automatic Face & Gesture Recognition and Workshops (FG 2011), 2011 IEEE International Conference on*, pages 921–926. IEEE, 2011.

[67] Tanja Bänziger and Klaus R Scherer. Introducing the geneva multimodal emotion portrayal (gemep) corpus. *Blueprint for affective computing: A sourcebook*, pages 271–294, 2010.

[68] Michel F Valstar, Timur Almaev, Jeffrey M Girard, Gary McKeown, Marc Mehu, Lijun Yin, Maja Pantic, and Jeffrey F Cohn. Fera 2015-second facial expression recognition and analysis challenge. In *Automatic Face and Gesture Recognition (FG), 2015 11th IEEE International Conference and Workshops on*, volume 6, pages 1–8. IEEE, 2015.

[69] Xing Zhang, Lijun Yin, Jeffrey F Cohn, Shaun Canavan, Michael Reale, Andy Horowitz, Peng Liu, and Jeffrey M Girard. Bp4d-spontaneous: a high-resolution spontaneous 3d dynamic facial expression database. *Image and Vision Computing*, 32(10):692–706, 2014.

[70] Gary McKeown, Michel Valstar, Roddy Cowie, Maja Pantic, and Marc Schroder. The semaine database: Annotated multimodal records of emotionally colored conversations between a person and a limited agent. *IEEE Transactions on Affective Computing*, 3(1):5–17, 2012.

[71] Wenchao Zhang, Shiguang Shan, Wen Gao, Xilin Chen, and Hongming Zhang. Local gabor binary pattern histogram sequence (lgbphs): a novel non-statistical model for face representation and recognition. In *Computer Vision, 2005. ICCV 2005. Tenth IEEE International Conference on*, volume 1, pages 786–791. IEEE, 2005.

[72] Xuehan Xiong and Fernando De la Torre. Supervised descent method and its applications to face alignment. In *Proceedings of the IEEE conference on computer vision and pattern recognition*, pages 532–539, 2013.

[73] Michel F Valstar, Enrique Sánchez-Lozano, Jeffrey F Cohn, László A Jeni, Jeffrey M Girard, Zheng Zhang, Lijun Yin, and Maja Pantic. Fera 2017-addressing head pose in the third facial expression recognition and analysis challenge. In *Automatic Face & Gesture Recognition (FG 2017), 2017 12th IEEE International Conference on*, pages 839–847. IEEE, 2017.

[74] Enrique Sánchez-Lozano, Brais Martinez, Georgios Tzimiropoulos, and Michel Valstar. Cascaded continuous regression for real-time incremental face tracking. In *European Conference on Computer Vision*, pages 645–661. Springer, 2016.

[75] John Lafferty, Andrew McCallum, and Fernando CN Pereira. Conditional random fields: Probabilistic models for segmenting and labeling sequence data. 2001.

[76] Minyoung Kim and Vladimir Pavlovic. Structured output ordinal regression for dynamic facial emotion intensity prediction. In *European conference on computer vision*, pages 649–662. Springer, 2010.

[77] Navneet Dalal and Bill Triggs. Histograms of oriented gradients for human detection. In *Computer Vision and Pattern Recognition, 2005. CVPR 2005. IEEE Computer Society Conference on*, volume 1, pages 886–893. IEEE, 2005.

[78] Timo Ojala, Matti Pietikäinen, and David Harwood. A comparative study of texture measures with classification based on featured distributions. *Pattern recognition*, 29(1):51–59, 1996.

[79] David G Lowe. Object recognition from local scale-invariant features. In *Computer vision, 1999. The proceedings of the seventh IEEE international conference on*, volume 2, pages 1150–1157. Ieee, 1999.

[80] David G Lowe. Distinctive image features from scale-invariant keypoints. *International journal of computer vision*, 60(2):91–110, 2004.

[81] Karl Pearson. Liii. on lines and planes of closest fit to systems of points in space. *The London, Edinburgh, and Dublin Philosophical Magazine and Journal of Science*, 2(11):559–572, 1901.

[82] Pablo Navarrete and Javier Ruiz-del Solar. Comparative study between different eigenspace-based approaches for face recognition. In *AFSS International Conference on Fuzzy Systems*, pages 178–184. Springer, 2002.

[83] Lindsay I Smith. A tutorial on principal components analysis. Technical report, 2002.

[84] Marian Stewart Bartlett, Javier R Movellan, and Terrence J Sejnowski. Face recognition by independent component analysis. *IEEE transactions on neural networks/a publication of the IEEE Neural Networks Council*, 13(6):1450, 2002.

[85] Dulal Chakraborty, Sanjit Kumar Saha, and Md Al-Amin Bhuiyan. Face recognition using eigenvector and principle component analysis. *International Journal of Computer Applications*, 50(10), 2012.

[86] Zhihong Zhang and Edwin R Hancock. Mutual information criteria for feature selection. In *International Workshop on Similarity-Based Pattern Recognition*, pages 235–249. Springer, 2011.

[87] Valeria Fonti and Eduard Belitser. Feature selection using lasso. *VU Amsterdam Research Paper in Business Analytics*, 2017.

[88] Michael J Jones and Paul Viola. Robust real-time object detection. In *Workshop on statistical and computational theories of vision*, volume 266, page 56, 2001.

[89] Cha Zhang and Zhengyou Zhang. A survey of recent advances in face detection. 2010.

[90] Yoav Freund and Robert E Schapire. A decision-theoretic generalization of on-line learning and an application to boosting. *Journal of computer and system sciences*, 55(1):119–139, 1997.

[91] Corinna Cortes and Vladimir Vapnik. Support-vector networks. *Machine learning*, 20(3):273–297, 1995.

[92] Edgar Osuna, Robert Freund, and Federico Girosit. Training support vector machines: an application to face detection. In *Computer vision and pattern recognition, 1997. Proceedings., 1997 IEEE computer society conference on*, pages 130–136. IEEE, 1997.

[93] Bernd Heisele, Massimilinao Pontil, et al. Face detection in still gray images. Technical report, MASSACHUSETTS INST OF TECH CAMBRIDGE MA CENTER FOR BIOLOGICAL AND . . . , 2000.

[94] Lior Rokach and Oded Maimon. Decision trees. In *Data mining and knowledge discovery handbook*, pages 165–192. Springer, 2005.

[95] J. Ross Quinlan. Induction of decision trees. *Machine learning*, 1(1):81–106, 1986.

[96] Tin Kam Ho. Random decision forests. In *Document analysis and recognition, 1995., proceedings of the third international conference on*, volume 1, pages 278–282. IEEE, 1995.

[97] D Richard Cutler, Thomas C Edwards Jr, Karen H Beard, Adele Cutler, Kyle T Hess, Jacob Gibson, and Joshua J Lawler. Random forests for classification in ecology. *Ecology*, 88(11):2783–2792, 2007.

[98] Leo Breiman. Bagging predictors. *Machine learning*, 24(2):123–140, 1996.

[99] Leo Breiman. Random forests. *Machine learning*, 45(1):5–32, 2001.

[100] Michael J Lyons, Shigeru Akamatsu, Miyuki Kamachi, Jiro Gyoba, and Julien Budynek. The japanese female facial expression (jaffe) database. In *Proceedings of third international conference on automatic face and gesture recognition*, pages 14–16, 1998.

[101] Takeo Kanade, Yingli Tian, and Jeffrey F Cohn. Comprehensive database for facial expression analysis. In *fg*, page 46. IEEE, 2000.

[102] Maja Pantic, Michel Valstar, Ron Rademaker, and Ludo Maat. Web-based database for facial expression analysis. In *2005 IEEE international conference on multimedia and Expo*, page 5. IEEE, 2005.

[103] Li-Fen Chen and Yu-Shiuan Yen. Taiwanese facial expression image database. *Brain Mapping Laboratory, Institute of Brain Science, National Yang-Ming University, Taipei, Taiwan*, 2007.

[104] Niki Aifanti, Christos Papachristou, and Anastasios Delopoulos. The mug facial expression database. In *Image analysis for multimedia interactive services (WIAMIS), 2010 11th international workshop on*, pages 1–4. IEEE, 2010.

[105] Abhinav Dhall, Roland Goecke, Simon Lucey, Tom Gedeon, et al. Collecting large, richly annotated facial-expression databases from movies. *IEEE multimedia*, 19(3):34–41, 2012.

[106] Ian J Goodfellow, Dumitru Erhan, Pierre Luc Carrier, Aaron Courville, Mehdi Mirza, Ben Hamner, Will Cukierski, Yichuan Tang, David Thaler, Dong-Hyun Lee, et al. Challenges in representation learning: A report on three machine learning contests. In *International Conference on Neural Information Processing*, pages 117–124. Springer, 2013.

[107] Lijun Yin, Xiaozhou Wei, Yi Sun, Jun Wang, and Matthew J Rosato. A 3d facial expression database for facial behavior research. In *Automatic face and gesture recognition, 2006. FGR 2006. 7th international conference on*, pages 211–216. IEEE, 2006.

[108] Arman Savran, Neşe Alyüz, Hamdi Dibeklioğlu, Oya Çeliktutan, Berk Gökberk, Bülent Sankur, and Lale Akarun. Bosphorus database for 3d face analysis. In *European Workshop on Biometrics and Identity Management*, pages 47–56. Springer, 2008.

[109] Lijun Yin, Xiaochen Chen, Yi Sun, Tony Worm, and Michael Reale. A high-resolution 3d dynamic facial expression database. In *Automatic Face & Gesture Recognition, 2008. FG'08. 8th IEEE International Conference on*, pages 1–6. IEEE, 2008.

[110] James W Davis and Mark A Keck. A two-stage template approach to person detection in thermal imagery. In *Application of Computer Vision, 2005. WACV/MOTIONS'05 Volume 1. Seventh IEEE Workshops on*, volume 1, pages 364–369. IEEE, 2005.

[111] Alexander Kramida, Yuri Ralchenko, Joseph Reader, et al. Nist atomic spectra database (ver. 5.2), 2015.

[112] Shangfei Wang, Zhilei Liu, Siliang Lv, Yanpeng Lv, Guobing Wu, Peng Peng, Fei Chen, and Xufa Wang. A natural visible and infrared facial expression database for expression recognition and emotion inference. *IEEE Transactions on Multimedia*, 12(7):682–691, 2010.

[113] Hung Nguyen, Kazunori Kotani, Fan Chen, and Bac Le. A thermal facial emotion database and its analysis. In *Pacific-Rim Symposium on Image and Video Technology*, pages 397–408. Springer, 2013.

[114] Albert Ali Salah, Nicu Sebe, and Theo Gevers. Communication and automatic interpretation of affect from facial expressions. In *Affective Computing and Interaction: Psychological, Cognitive and Neuroscientific Perspectives*, pages 157–183. IGI Global, 2011.

[115] Aliaa AA Youssif and Wesam AA Asker. Automatic facial expression recognition system based on geometric and appearance features. *Computer and Information Science*, 4(2):115, 2011.

[116] Roberto Battiti. Using mutual information for selecting features in supervised neural net learning. *IEEE Transactions on neural networks*, 5(4):537–550, 1994.

[117] Seyed Mehdi Lajevardi and Zahir M Hussain. Feature selection for facial expression recognition based on mutual information. In *GCC Conference & Exhibition, 2009 5th IEEE*, pages 1–5. IEEE, 2009.

[118] Shaoqing Ren, Xudong Cao, Yichen Wei, and Jian Sun. Face alignment at 3000 fps via regressing local binary features. In *Proceedings of the IEEE Conference on Computer Vision and Pattern Recognition*, pages 1685–1692, 2014.

[119] Microsoft. Serviços cognitivos. URL: https://azure.microsoft.com/pt-pt/services/cognitive-services/ [last accessed 05.01.2019].

[120] Danielle Mathersul, Leanne M Williams, Patrick J Hopkinson, and Andrew H Kemp. Investigating models of affect: Relationships among eeg alpha asymmetry, depression, and anxiety. *Emotion*, 8(4):560, 2008.

[121] Lisa Feldman Barrett. Discrete emotions or dimensions? the role of valence focus and arousal focus. *Cognition & Emotion*, 12(4):579–599, 1998.

[122] James A Russell. A circumplex model of affect. *Journal of personality and social psychology*, 39(6):1161, 1980.

[123] Georgios Paltoglou and Michael Thelwall. Seeing stars of valence and arousal in blog posts. *IEEE Transactions on Affective Computing*, 4(1):116–123, 2013.

[124] Ron Artstein. Inter-annotator agreement. In *Handbook of linguistic annotation*, pages 297–313. Springer, 2017.

[125] Matthew B Blaschko and Christoph H Lampert. Learning to localize objects with structured output regression. In *European conference on computer vision*, pages 2–15. Springer, 2008.

[126] Mark Everingham, Luc Van Gool, Christopher KI Williams, John Winn, and Andrew Zisserman. The pascal visual object classes (voc) challenge. *International journal of computer vision*, 88(2):303–338, 2010.

[127] F. Pedregosa, G. Varoquaux, A. Gramfort, V. Michel, B. Thirion, O. Grisel, M. Blondel, P. Prettenhofer, R. Weiss, V. Dubourg, J. Vanderplas, A. Passos, D. Cournapeau, M. Brucher, M. Perrot, and E. Duchesnay. Scikit-learn: Machine learning in Python. *Journal of Machine Learning Research*, 12:2825–2830, 2011.

[128] Chih-Chung Chang and Chih-Jen Lin. Libsvm: a library for support vector machines. *ACM transactions on intelligent systems and technology (TIST)*, 2(3):27, 2011.

[129] Scikit learn developers. sklearn.ensemble.randomforestclassifier. URL: https://scikit-learn.org/stable/modules/generated/sklearn.ensemble.RandomForestClassifier.html [last accessed 14.01.2019].

[130] Alexander Kraskov, Harald Stögbauer, and Peter Grassberger. Estimating mutual information. *Physical review E*, 69(6):066138, 2004.

[131] Brian C Ross. Mutual information between discrete and continuous data sets. *PloS one*, 9(2):e87357, 2014.

[132] Ratna Astuti Nugrahaeni and Kusprasapta Mutijarsa. Comparative analysis of machine learning knn, svm, and random forests algorithm for facial expression classification. In *Technology of Information and Communication (ISemantic), International Seminar on Application for*, pages 163–168. IEEE, 2016.

[133] Guoying Zhao and Matti Pietikainen. Dynamic texture recognition using local binary patterns with an application to facial expressions. *IEEE transactions on pattern analysis and machine intelligence*, 29(6):915–928, 2007.

[134] Jingying Chen, Mulan Zhang, Xianglong Xue, Ruyi Xu, and Kun Zhang. An action unit based hierarchical random forest model to facial expression recognition. pages 753–760, 01 2017. doi:10.5220/0006274707530760.

[135] Mostafa K Abd El Meguid and Martin D Levine. Fully automated recognition of spontaneous facial expressions in videos using random forest classifiers. *IEEE Transactions on Affective Computing*, 5(2):141–154, 2014.

[136] Peiyao Li, Son Lam Phung, A Bouzerdom, and Fok Hing Chi Tivive. Feature selection for facial expression recognition. In *Visual Information Processing (EUVIP), 2010 2nd European Workshop on*, pages 35–40. IEEE, 2010.

[137] Jiabei Zeng, Shiguang Shan, and Xilin Chen. Facial expression recognition with inconsistently annotated datasets. In *Proceedings of the European conference on computer vision (ECCV)*, pages 222–237, 2018.